TOPICAL REPORT: CO_2 SEQUESTRATION CAPACITY AND ASSOCIATED ASPECTS OF THE MOST PROMISING GEOLOGIC FORMATIONS IN THE ROCKY MOUNTAIN REGION: LOCAL-SCALE ANALYSES

Type of Report: Topical Report
Reporting Period Start Date: December 8, 2009
Reporting Period End Date: September 30, 2013

Principal Authors of this report:
Denise Laes, University of Utah
Chris Eisinger, Colorado Geological Survey
Craig Morgan, Utah Geological Survey
Steve Rauzi, Arizona Geological Survey
Dana Ulmer-Scholle, NM Bureau of Geology and Mineral Resources
Phyllis Scott, Colorado Geological Survey
Si-Yong Lee, University of Utah
Wade Zaluski, Schlumberger Carbon Services
Richard Esser, University of Utah
Vince Matthews, Colorado Geological Survey
Brian McPherson, University of Utah

Date Report was Issued: December 31, 2013
DOE Award Number DE-FE0001812

Submitting Organization:
University of Utah
Department of Civil and Environmental Engineering
Salt Lake City, Utah 84112 USA

DISCLAIMER

Abstract

The purpose of this report is to provide a summary of individual local-scale CCS site characterization studies conducted in Colorado, New Mexico and Utah. These site-specific characterization analyses were performed as part of the "Characterization of Most Promising Sequestration Formations in the Rocky Mountain Region" (RMCCS) project. The primary objective of these local-scale analyses is to provide a basis for regional-scale characterization efforts within each state. Specifically, limits on time and funding will typically inhibit CCS projects from conducting high-resolution characterization of a state-sized region, but smaller (< 10,000 km^2) site analyses are usually possible, and such can provide insight regarding limiting factors for the regional-scale geology. For the RMCCS project, the outcomes of these local-scale studies provide a starting point for future local-scale site characterization efforts in the Rocky Mountain region.

Table of Contents

List of Abbreviations

AGS	Arizona Geological Survey
ARRA	American recovery and reconstruction act
AZ	Arizona
BOE	Barrels of oil equivalent
CCS	Carbon Capture and Storage
CGS	Colorado Geological Survey
CO	Colorado
CSA	Colorado Study area
DEM	Digital Elevation Model
DF	Drilling Floor
DOE	Department of Energy
EGI	Energy and Geosciences Institute
EPA	Environmental Protection Agency
GHG	Green House Gas
KB	Kelly Bushing
MMT	Million Tonnes
NETL	National Energy Technology Laboratory
NM	New Mexico
NMBGMR	New Mexico Bureau of Geology and Mineral Resources
SGS	Sequential Gaussian Simulation
SRS	San Rafael Swell
TDS	Total Dissolved Solids
THCM	Thermal Mechanical and Chemical Processes
UGS	Utah Geological Survey
USDW	Underground Sources of Drinking Water
UT	Utah

1. Executive summary

The geology of the Colorado Plateau, located in the western United States, contains several deep saline formations that are suitable for carbon sequestration. Three very promising saline storage candidate formations include the Cretaceous Dakota Formation, the Jurassic Entrada Formation and the Permian Weber Formation. The main purpose of this report is to detail results of several local-scale, site-specific analyses within the region. A primary objective of these local-scale analyses is to provide a basis for regional-scale characterization efforts within the broader region. Specifically, high-resolution characterization of a state-sized region would be impractical in most situations, but smaller (< 10,000 km2) site analyses are usually possible and desirable, inasmuch as such can provide insight regarding key attributes of regional-scale geology and hydrology.

Because geologic data availability issues, no site-specific analyses were conducted for Arizona. The RMCCS project conducted two site-specific studies in Utah, one near Woodside and one near Bonanza. Only the Woodside study-site will be included in this report as an example of such a study. In New Mexico, the San Juan Basin was selected for specific assessment, and results of this analysis are included in this report. Finally, the Craig site in NW Colorado became the main focus of the entire RMCCS site Characterization project – the entire project team performed the highest resolution analysis possible, including drilling and utilization of a deep stratigraphic well exclusively for characterization purposes. Much like the site-specific analysis locations in the other states, the geologic conditions at Craig were favorable, including a large nearby power generating station and a willing cooperating partner, Tri-State Generation and Transmission Association Inc.

Geologists of the Geological Surveys of the four states of the Colorado Plateau Region took the lead in characterizing and assessing the carbon sequestration capacities of sites located in their state. Carbon storage capacity was calculated using the volumetric method (Atlas 3). A basic sensitivity study was performed for the Sand Wash basin carbon storage capacity. Because this basin became the main study site of this project, the data were more detailed and more extensive compared to the data for the other site characterization locations. Storage capacity estimates for the Sand Wash Basin vary between 287 and 3,528 million metric tonnes depending on which the geothermal gradient is applied to calculate the CO_2 density at the top of the formation and which efficiency factor is taken into consideration. When these numbers are compared to the 2010 and 2011 CO_2 emissions from the nearby Craig and Hayden coal-fired power plants, the deep saline formations can accommodate between 21 years of emitted CO_2, at the conservative end, and nearly

290 years when applying less restrictive efficiency factors. These numbers do not take technological, political, additional geological constraints or other extraneous factors into account.

The Woodside study results include a potential storage capacity between 3.2 and 34.3 million metric tonnes divided amongst the Mississippian Redwall Limestone, The White Permian Sandstone and the Permian Black Box Dolomite. The three formations that were the focus of the study in the Sand Wash Basin area are too shallow to be considered at the Woodside area. The deep enough formations at the Woodside area could store CO_2 captured at the Huntington and Hunter power plants approximately 60 km to the west and the Carbon power plant nearly 80 km to the northwest. These three coal-fired power plants reported 15.9 million metric tonnes of CO_2 emissions in 2010 and 15.4 million metric tonnes in 2011 to the EPA Greenhouse gas reporting program.

Power generating stations in the New Mexico San Juan basin emitted a combined 15 million metric tons of CO_2 in 2010. Four plants are located on the northern end of the basin near the border with Colorado. The Escalante plant is near the southern end of the San Juan Basin. According to the regional CO_2 storage capacity study, the San Juan Basin can store between 2 billion and 23 billion metric tonnes of CO_2. Of the 3 saline formations that were the focus of the site characterization project, only the Dakota Group and the Entrada Formation are present in the San Juan Basin. The Hermosa Group, the equivalent of the Weber Formation to the north, and Leadville Limestone were included in the study instead.

Narrative

2. Introduction

2.1 Background

The 'Characterization of Most Promising Sequestration Formations in the Rocky Mountain Region', project was one of the ten projects selected by the National Energy and Technology Laboratory (NETL) that received Department of Energy (DOE) funding, provided by the 2009 ARRA act, to characterize promising geologic formations for permanent CO_2 storage. Evaluating geologic formations in terms of assessing available CO_2 storage capacity and their associated uncertainty quantification are important factors in the implementation of geologic Carbon Capture and Storage (CCS). Developing and improving CCS technology has the potential to play a major role in reducing Green House Gas (GHG) emissions (Bachu et al. 2007).

This Topical Report resulted from the work done on a projected that focused on the site characterization of high-potential deep saline storage formations on the Colorado Plateau in the Southwestern US. Deep saline formations are one of the three geologic environments that are suitable to sequester CO_2; the other two types are depleted oil and gas reservoirs and unmineable coal layers. This project assessed not only the target formations but also the seals and underground sources of drinking water (USDWs). The entire project team was made up of the following partners: NETL/DOE, the University of Utah, the Arizona Geological Survey, the Colorado Geological Survey, the New Mexico Bureau of Geology & Mineral Resources, the Utah Geological Survey, Schlumberger Carbon Services, Tri-State Generation and Transmission Inc., and Shell Oil Company. The project started in December of 2009 and ended at the end of September 2013.

The main focus at the Craig, Colorado project site was to study the regionally occurring storage formation candidates: Cretaceous Dakota, Jurassic Entrada and Permian Weber Sandstones. Detailed data were obtained from 131 feet of core recovered from the 9,745 deep single well drilled near the Craig Power station, a coal-fired electric generating station. Less detailed data for the same target formations were compiled across the Uinta, Piceance and Sand wash Basin on the northern Colorado Plateau. Besides the three main target formations, the stratigraphic equivalents of these formations were also studied in the southern part of the Colorado Plateau. The equivalents include the Permian Cedar Mesa and De Chelly Sandstones, and the Pennsylvanian Hermosa Formation in the San Juan,

Paradox and Black Mesa Basins. The Mississippian Leadville Formation of the San Juan Basin was included as well.

2.2 Objectives

The Craig site in Colorado (Figure 2.1) was selected as the project site because of several reasons. Foremost the presence of deep saline formations, capped by seals and having the minimum reservoir storage conditions within the Sand Wash sedimentary basin was well known (reference). They are located within the Colorado plateau at a depth below 2500' (750m) the ground surface. This minimum depth on average is required to maintain CO_2 in its supercritical state. They have a minimum storage capacity of 30 million metric tonnes (Young et al. 2007) and the salinity of the aquifer exceeds 10,000 TDS. Besides favorable geological conditions, the selected site was near 2 coal-fired power-generating stations, Craig and Hayden. Finally, Tri-State Generation and Transmission Association Inc. agreed to participate in the project as an industry partner. The results of the site-specific carbon storage assessments are included in this topical report.

Each of the geological surveys of partnering states with the exception of Colorado, was asked to go through the process of selecting the best sites within their state that met the above criteria. The Navajo Generating Station (Figure 2.1) was the best site for Arizona but because of limited geologic data availability for the area near the power station, no site-specific analysis was completed. For New Mexico, results of a regional analysis of the San Juan Basin are included in this report. For Utah, results of analysis of two local sites, the Woodside and Bonanza sites (Figure 2.1), are summarized in this report.

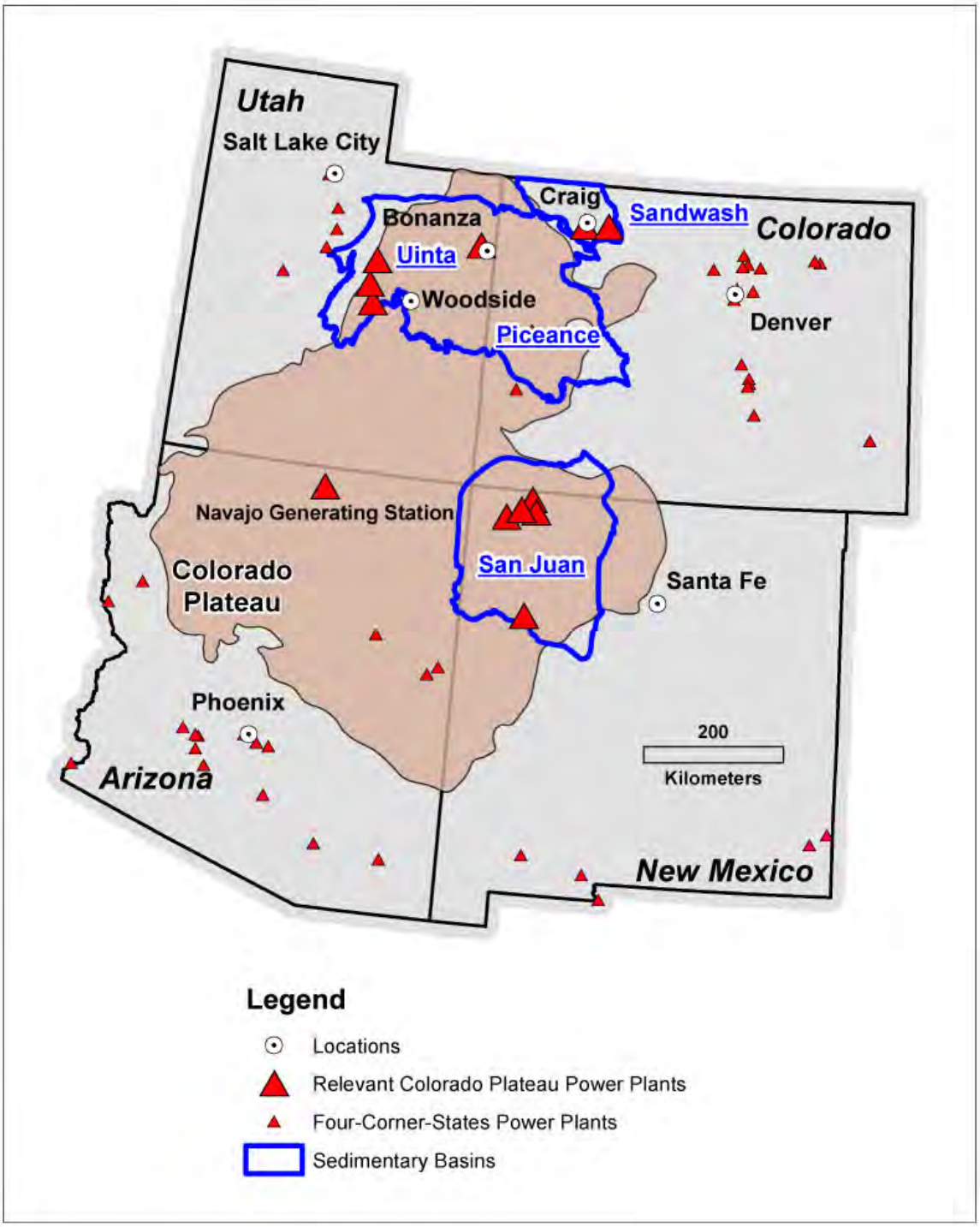

Figure 2.1: Colorado Plateau carbon emission sources in relation and potential site-specific geological sequestration reservoir candidates.

3. Colorado Sand Wash Basin, Site Specific Carbon Storage Capacity Estimations

Denise Laes (University of Utah), Chris Eisinger (Colorado Geological Survey), Phyllis Scott (Colorado Geological Survey) and Wade Zaluski (Schlumberger Carbon Services)

Part 1: Study overview, Geological Framework, Data and Methods (Chris Eisinger and Phyllis Scott)

3.1 Craig Site - Study Overview

The Colorado Plateau covers portions of four states: Colorado, Utah, Arizona and New Mexico. For this report, the Colorado Study Area (CSA) refers to the portion of the Colorado Plateau that lies within the boundaries of western Colorado (Figure 3.1). It includes the western third of the state of Colorado, stretching from Wyoming to New Mexico and eastward nearly 130 miles from the Utah state line (Figure 3.1).

Two key objectives of the RMCCS partnership include:

1. A detailed characterization of saline aquifer and seal forming formations in the vicinity of a stratigraphic test well drilled in February and March of 2012. The well, named RMCCS State #1, was sited in the SW SE of Section 34, Township 6 North, Range 91 West, six miles south of Craig, Colorado.
2. Expanding site and basin characterization to the entire Colorado Plateau incorporating the data acquired from the drilling of the stratigraphic test.

For this topical report, emphasis is on the first key objective.

At the local scale, a very detailed examination has been made of the geology within a single Laramide-age structure called the Yampa Block surrounding the site of the RMCCS State #1 stratigraphic test well. Numerous datasets compiled prior and subsequent to drilling were used to construct a detailed three-dimensional geocellular model of the Sand Wash Basin study area (Figure 3.1).

A primary utility of the geocelluar model was to simulate carbon dioxide injection into the targeted saline aquifer formations surrounding the RMCCS State #1 stratigraphic test well – a site located intentionally adjacent to the Craig Power Station.

An initial characterization of the reservoir quality of the saline aquifers in the Sand Wash Basin was made by mapped the thickness of the net feet of sand and the net feet of porous sand (sand with porosity greater than six percent) within each of the three saline aquifers.

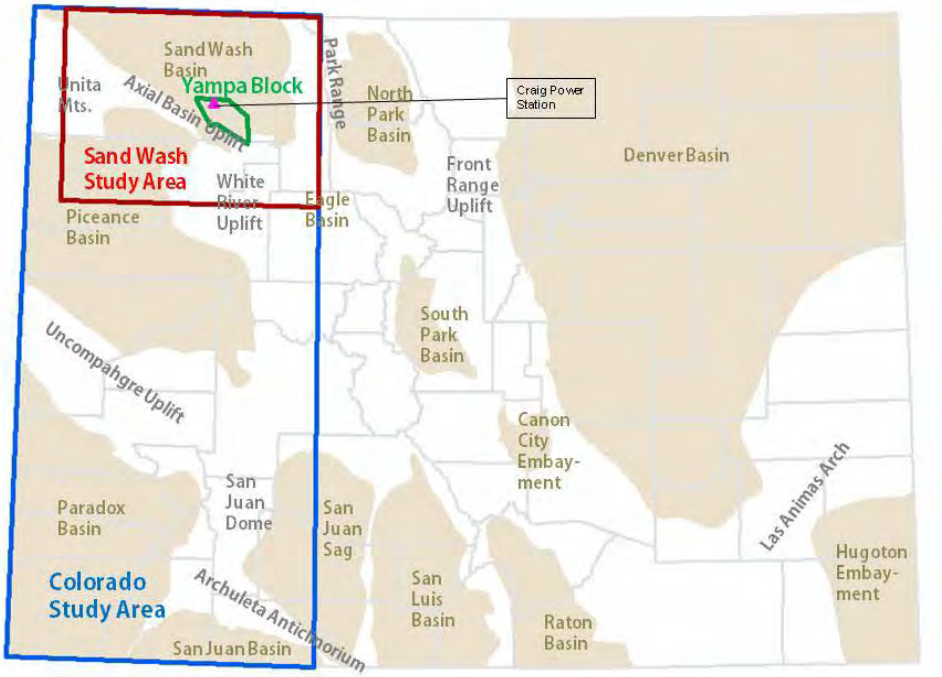

Figure 3.1. Extent of Colorado study areas including Yampa Block (green) and Sand Wash Basin (red).

This topical report chapter is divided into three sections covering (1) the geological framework for the Craig site and the Sand Wash Basin, and (2) the data and methods used in constructing the foundation for the geocellular model.

3.2 Geological Framework, Data and Methods

3.2.1 Geological Framework

3.2.1a Structural Geology

The Colorado Study Area (CSA) contains portions of four major structural basins: the Sand Wash in the north (including the Eagle Basin, its southeastern extension), the Piceance Basin in the west central portion of the state, and the Paradox and San Juan Basins in the south. These basins are separated by uplifted areas that are cored by Precambrian rocks. The locations of these basins and uplifts are shown in Figure 3.1.

These structural elements are the result of four major periods of deformation in the Phanerozoic: (1) the Pennsylvanian Ouachita-Marathon Orogeny that resulted in

the formation of the Ancestral Rocky Mountains (Kluth, 1986); (2) the Jurassic-Cretaceous Sevier Orogeny that formed the Western Interior Cretaceous Seaway; (3) the Cenozoic Laramide Orogeny that resulted in the Rocky Mountain Uplift and the interevening present-day basins; and (4) late Cenozoic extensional faulting. These structural elements were key in controlling sedimentation. Basins provided accommodation space allowing for deposition, while uplifts furnished eroded sediments to fill the basins. Subsequent faulting, both compressional and extensional, created barriers to fluid flow within porous strata.

Pennsylvanian Structures

During the Pennsylvanian Period the collision of the continents of Laurentia (North America) and Gondwana (South America and Africa) created the supercontinent of Pangaea. As a result of this continent-to-continent collision, much of North America was subjected to extreme tectonism. In Colorado the Ancestral Rocky Mountains were formed as broad, block-faulted uplifts rather than intensely folded mountains, with the primary movement focused along Precambrian lineaments (Kluth, 1986). The Uncompahgre and Ancestral Front Range uplifts are components of the Ancestral Rockies. They trend roughly northwest and are within or adjacent to the Colorado study area. These uplifts contributed clastic sediments to the adjacent downfaulted basins. Two major basins were created in the Colorado study area between the uplifts: the Central Colorado Trough and the Paradox Basin (Figure 3.2).

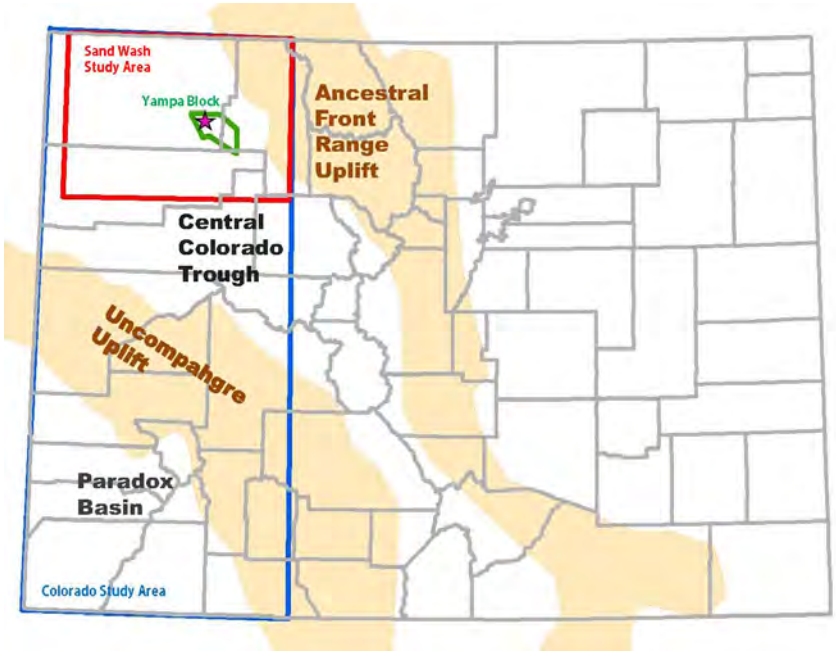

Figure 3.2. Locations of Ancestral Rockies uplifts and basins (Mallory, 1972, p. 132).

The Central Colorado Trough is a northwest-trending basin between the Uncompahgre Uplift and the Ancestral Front Range Uplift. It includes the present-

day Sand Wash, Piceance and Eagle Basins within the CSA, and extends to the South Park and Raton Basins in Colorado outside the study area.

In the Craig area, faults along the southern edge of the present Axial Basin Uplift were active during the Pennsylvanian. Stone (1986) maps them as predominantly northwest trending thrust faults whose planes dip to the northeast under the upthrust blocks; Pennsylvanian displacements of 1,000 to 3,500 feet were mapped by Stone (1986) fault segments south of Craig. The Pennsylvanian section thickens considerably to the south and southeast.

Mesozoic-Cenozoic Structures

The Sevier Orogeny began with Late Jurassic and Early Cretaceous uplift and thrust faulting along the entire western margin of the North American continent as the Farallon Plate subducted under the North American Plate. The thrust belt runs from Canada through western Utah and eastern Nevada to Mexico with thrust fault movement from west to east, becoming progressively younger to the east. As a result of the crustal thickening from the stacked thrust sheets, a foreland basin formed to the east. This crustal downwarping, combined with high eustatic sea levels, allowed marine flooding into the basin creating the Western Interior Cretaceous Seaway. The seaway covered the entire state of Colorado as well as much of the western North American continent from Canada to Mexico, connecting the Arctic Ocean with the Gulf of Mexico at its maximum extent. It was deepest along its western margin adjacent to the Sevier mountain front. Thousands of feet of shales were deposited in the seaway; these form a seal over the underlying saline aquifers.

The Laramide Orogeny began in Late Cretaceous time and extended through the Eocene. The orogeny is thought to be caused by a flattening of the angle at which the Farallon Plate was subducted under the North American Plate. The normal 45 degrees or more subduction angle was changed to a much shallower angle, which caused the Rocky Mountain Uplift to occur almost a thousand miles from the plate boundary (Blakey and Ranney, 2008).

The result of the Laramide Orogeny was the final draining of the Western Interior Seaway and the fragmentation of the foreland into the Rocky Mountain uplifts and intermontane structural basins that are present today. The boundaries between the basins and the uplifts are often dramatic and marked by monoclines or large scale faults. As an example, the Grand Hogback, a nearly one hundred-mile-long rim of nearly vertical beds, bounds the eastern Piceance Basin.

3.2.1b Stratigraphy of the Sand Wash Basin Area

Sedimentary rocks of the Sand Wash Basin, including targeted aquifer formations at the Craig site, range in age from Cambrian through Neogene. Stratigraphic relationships for this area are shown in Figure 3.3.

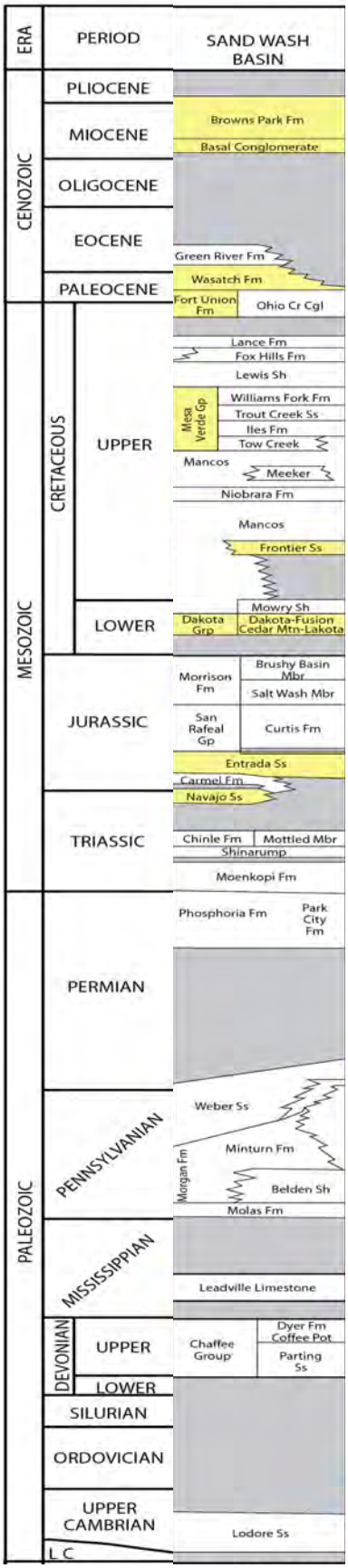

Figure 3.3 Generalized stratigraphic chart for the Sand Wash Basin (Irwin, 1977).

Cambrian through Mississippian Systems

Basal Phanerozoic rocks in the Rocky Mountain region are generally transgressive deposits that overlie the eroded Precambrian surface (Kent, 1972). Cambrian through Mississippian sands and carbonates were deposited on a broad, stable, shallow marine shelf. The uppermost Mississippian formation in the CSA is the Leadville Limestone (which is equivalent to the Madison and Redwall in adjacent states). Uplift and erosion resulted in the formation of a karst surface on the limestone throughout the region, which is called the Molas Formation. (DeVoto, 1980).

The Leadville and its equivalents produce oil and gas throughout the western United States. The Madison is a major CO_2 sequestration target in Wyoming (Thyne, et al, 2010). Therefore, the Leadville Limestone may be considered as a sequestration target in the Colorado Plateau area in the future.

Pennsylvanian and Permian Systems

The Pennsylvanian and Permian Systems are dominated by extensive tectonism and by cyclic sedimentation. During the Pennsylvanian Period a continent-to-continent collision resulted in wide-scale tectonism over much of North America. In the CSA, the Ancestral Rocky Mountains were formed as broad, block-fault uplifts with downfaulted basins between. The uplifts contributed voluminous clastic sediments to the adjacent basins. Because of the high relief of the Pennsylvanian paleogeography and the changing tectonism, the nature and thickness of the Pennsylvanian sedimentation is highly variable over short distances.

At the same time, glaciation in the southern hemisphere caused rhythmic changes in eustatic sea level, which resulted in cyclic patterns of sedimentation that differed greatly between sea level highstands and lowstands.

The uplift of the Ancestral Rockies had a profound effect on the sedimentation in the CSA. The two deep basins that formed on downfaulted blocks in the study area, the Paradox Basin in southwest Colorado (including the San Juan Basin) and the Central Colorado Trough in northwest Colorado (including the present-day Piceance, Sand Wash and Eagle basins), were filled with cyclic deposits formed as sea level changed in response to Gondwana glaciation. During glacial periods, sea level was at a lowstand, the basins were isolated from the open ocean and evaporites in the form of halite, potash and anhydrite were deposited in the basin centers. As sea level rose in response to glacial melting with the onset of an interglacial period, shales were deposited throughout the basin. During marine highstands in interglacial periods the basins were connected with the open ocean and limestones were deposited along the basin margins (Grammer, et. al., 1996). Thick clastic wedges were deposited adjacent to the uplifts. These deposits comprise the Pennsylvanian Paradox Formation of the Hermosa Group in the Paradox Basin and Eagle Valley Evaporites and Minturn Formation in the Central Colorado Trough.

Permian-Pennsylvanian Saline Aquifers in the Central Colorado Trough

In the Central Colorado Trough the cyclic nature of the deposition continued, but the sedimentation was nearly all clastic and formed the interfingering Weber and Maroon formations. The Weber Sandstone is described by Johnson, Chan and Konopka (1992) as massive or cross bedded sands deposited in eolian environments during lowstands or in shallow marine or fluvial environments during highstands. It is described by Masoner and Wackowski (1995) as "a series of interbedded eolian sandstones and fluvial siltstones and shales" in Rangely Field, the largest oil field in the Rocky Mountains.

The Weber Sandstone reaches a maximum of 1,000 feet thick at Dinosaur National Monument (Fryberger and Koelmel, 1986) and is the principal oil producing reservoir in Rangely Field. Therefore, it has been targeted as a regional CO_2 sequestration target. However, the thickness and composition of the Weber vary considerably, thinning to the east and south in the present-day Sand Wash Basin. Therefore, it is only a sequestration target in limited areas, particularly in the southwestern Sand Wash Basin and the northwestern Piceance Basin. An eastern extension of the Weber in the Sand Wash Basin is the Permian Schoolhouse Tongue Sandstone. This unit is 100 to 150 feet thick and extends throughout the southeastern portion of the Sand Wash Basin (Fryberger and Koelmel, 1986). It is indistinguishable from the Weber and the two have been lumped together and called "Weber" in this study.

The Weber interfingers to the south and east with fluvial and eolian sand-sheet deposits of the Maroon Formation (Johnson, Chan and Konopka, 1992) which are described by Whitaker (1975) as arkosic conglomerates and sandstones with red and maroon siltstones and shales associated with alluvial fan deposition. The Maroon Formation is not a sequestration target because of the discontinuous nature of the sandstones and poor reservoir quality. Fryberger and Koelmel (1986) describe the interfingering between the Weber and Maroon in the Rangely Field area as an abrupt transition, with the percentage of Maroon alluvial sedimentation increasing rapidly to the south. They state: "Reservoir quality decreases proportionately with an increase in the percentage of Maroon alluvial sediments."

A marine incursion into northwestern Colorado in the Permian resulted in the deposition of the Phosphoria Formation and its correlative Park City Formation (in this report it is called "Phosphoria") which is comprised of limestone, sandstone, shale and greenish-gray cherty or phosphatic shale (Geldon, 1986). These rocks, along with the overlying Triassic siltstones and mudstones of the Moenkopi and Chinle formations, form a seal over the Weber saline aquifer.

Triassic System

The Triassic rocks in the Sand Wash Basin were deposited along the broad, arid coastal plain of the supercontinent of Pangea. They were deposited in the floodplains of rivers that had their headwaters in the southern Appalachian Mountains far to the east and southeast (Blakey and Ranney, 2008).

The Triassic Moenkopi consists of red and pale reddish brown claystone, siltstone, and sandy siltstone as well as minor very fine-grained, cross-stratified sandstone (Oriel and Craig, 1960). It, and its equivalent State Bridge Formation in central Colorado, is present throughout much of the northern part of the CSA. It is absent in much of the southern portion as mapped by Stewart, Poole and Wilson (1972), although it is identified by operators in many oil and gas wells within the Colorado portion of the Paradox Basin. It is unknown if the well tops are truly Moenkopi or a facies of the overlying Chinle Formation. If it is Moenkopi, it is thin, on the order of 50 to 200 feet.
The Chinle Formation unconformably overlies the Moenkopi and was also deposited by large river systems that originated in the Appalachians. It consists of "predominantly dark-reddish-brown to moderate-reddish-orange fine-grained sandstone, siltstone, and mudstone and lesser amounts of dark-gray to reddish-purple conglomeratic sandstone, limestone-pebble conglomerate, sandstone and gray limestone" (Dubiel, 1992). It reaches a maximum of 1400 feet thick in the southwestern corner of Colorado.

The lowermost member of the Chinle is the Shinarump Conglomerate that consists of coarse-grained sandstone and pebble conglomerate that was deposited in valleys eroded into the Moenkopi. Because it is valley fill, the Shinarump is not present where the Moenkopi formed highlands between valleys (Blakey and Ranney, 2008). The Shinarump produces oil and gas and could be considered a sequestration target. Its maximum net sand thickness in the Sand Wash Basin is 194 feet based on geophysical log measurements from this study.
The Moenkopi and Chinle thin over the salt anticlines in the Paradox Basin and are thicker in the downfolded strata between the anticlines. (Stewart, Poole, and Wilson, 1972).

Jurassic System

The Eolian Wingate, Navajo and Entrada Sandstones

Three great Jurassic sand ergs are represented by the Wingate, Navajo and Entrada Sandstones. The oldest is the Wingate Sandstone, which may be partly Triassic in age. It is a red, cliff-forming unit of cross-bedded sandstone deposited in eolian dunes. It is present in the southwestern part of the study area at least as far north as Grand Junction. The fluvial Kayenta Formation overlies the Wingate and caps its cliffs. Overlying the Kayenta is the Navajo Formation, which may represent the

largest eolian sand deposit on Earth (Blakey and Ranney, 2008). It is composed of mostly buff to pale orange, well-rounded, well-sorted, fine-grained sandstone that was deposited in a coastal dune environment (Molenaar, 1981). Together these three formations, the Wingate, Kayenta, and Navajo, comprise the Glen Canyon Group. In the CSA area they thicken to the west and pinch out to the east along a north-south line.

Unconformably overlying the Glen Canyon Group is the Carmel Formation, a marine formation composed of sandstone, mudstone, gypsum and limestone (Blakey and Ranney, 2008). Conformably overlying the Carmel is the Entrada, the youngest of the three Jurassic eolian sandstones and the only one that is present over almost the entire CSA, although it has been removed by erosion over many of the present-day uplifts. The Curtis Formation, a marine deposit of sandstone and mudstone, caps and seals the Entrada in the northern part of the CSA. In southwestern Colorado, the Entrada is capped by the Summerville, which is comprised of very fine grained sandstone, mudstone and shale that was deposited in a tidal flat or marginal marine environment (Molenaar, 1981).

These predominantly eolian deposits, from the Entrada through the Wingate, thicken dramatically to the west. In the eastern Sand Wash Basin only the Entrada is present and in places it may not be present at all. The intervening Kayenta and Carmel formations are not present everywhere and are difficult to discern on geophysical logs. For the purpose of this study, the entire section of the Entrada through the Wingate has been mapped as one unit that is defined by structure maps on the top of the Entrada and top of the Chinle. (The top of the Chinle correlates to the base of the Wingate or Navajo or Entrada where the lower formations are truncated by erosion or missing because of non-deposition.) The thickness of these units ranges from zero to over 1400 feet in the valleys between the salt diapirs in the Paradox Basin. The sands are porous, permeable and regionally continuous and constitute the largest potential sequestration target on the Colorado Plateau.

Morrison Formation

Beginning in the latest Middle Jurassic time stream drainage patterns changed. They had been flowing toward the northwest, but the Nevadan Orogeny shifted drainage to the northeast. (Blakey and Ranney, 2008). The shales and sands of the Morrison Formation were deposited in this fluvial system.

Four members of the Morrison have been identified: The Salt Wash Member is the lowest and was deposited in fluvial and floodplain environments by braided streams (Berman, Poleschook, and Dimelow, 1980). It is the sandiest of the members in the CSA. In the southwestern corner of the state, eolian dunes of the Bluff and Junction Creek sandstones (called Bluff in this study) were deposited in the lower portion of the Salt Wash Member; these are potential sequestration targets. The Recapture and Westwater Canyon Members overlie the Salt Wash in southwestern Colorado. These were not differentiated in this study. The uppermost member is the Brushy

Basin which is comprised of colorful green, red, purple and gray bentonitic mudstones with interbedded sandstone and limestone beds, (Berman, Poleschook, and Dimelow, 1980) which comprise a seal for deeper saline aquifers.

The Morrison is present over the entire Colorado study area except where it has been removed by erosion on the uplifts. A regional unconformity is present at its top. The top of the Morrison is often difficult to distinguish on geophysical logs, especially if there are channel sands in the upper part of the Morrison. Morrison tops reported by operators were often relied upon in this study because the top should be more easily identified from samples.

Cretaceous System

The Cretaceous System is dominated by the sediments deposited in and along the Western Interior Seaway. The seaway formed as a foreland basin in response to compressional forces to the west of the present-day Colorado Plateau that created the Sevier Orogeny.

Dakota and Lakota/Cedar Mountain/Burro Canyon Saline Aquifers

As lands to the west were uplifted, Early Cretaceous sediments were deposited by rivers as channel sands, gravels, and mudstones onto the Morrison erosional surface. These sediments are known as the Cedar Mountain in the Piceance Basin, the Lakota in the Sand Wash Basin, and the Burro Canyon in the Paradox Basin. Porosity and permeability of these units can be very good at the localized scale.

As the Sevier Orogeny continued, the continental crust to the west of the Colorado Plateau was thickened by stacked thrust sheets. This depressed the crust to the east (including present-day Colorado), creating a foreland basin which filled with a shallow ocean. As the ocean transgressed over the subsiding land, advancing from north to south, marine and fluvial sands, shales and some coals were deposited along the advancing shoreline and coastal plain. These lithologies comprise the Dakota Formation which is present over much of the western United States from the Dakotas to New Mexico.

In this study, the fluvial-deltaic sandstones of the Dakota could not be distinguished from the fluvial sandstones of the Lakota/Cedar Mountain/Burro Canyon because of their discontinuous nature. For this report the Dakota includes the interval from the top of the Dakota to the top of the Morrison.

Mancos Group

As the sea continued to advance, the Dakota shoreline moved farther to the south and east and water depths increased. Conformably overlying the Dakota Formation are the shales and sands of the Mancos Group that were deposited within the Cretaceous Seaway. These vary in thickness throughout the CSA. In general, they

thin to the south, with thicknesses ranging from 2000 feet in the south to almost 6000 feet in the north. The axis of the basin moved east through time along with the thrust faulting of the Sevier Orogeny. The western shoreline of the seaway also moved eastward in conjunction with the advancing mountain front.

The Mancos Group consists of a succession of shales, calcareous shales, and sandstones representing a number of formations. The Mancos Group as a whole represents a definitive seal for the underlying saline aquifers targeted in this study. The Niobrara Formation, a component of the Mancos section, is 1500 feet thick in the Craig area; it contains three calcareous shale benches that are being actively explored for oil and gas, and may be a future target for sequestration in fractured media.

Toward the top of the Mancos Shale, as the western shoreline of the Cretaceous Seaway was advancing eastward, the Mancos section becomes sandier. Tongues of shoreface sandstones were deposited during stillstands; these prograde for many miles into the basin and become thinner and shalier as they extend into the basin until they eventually pinch out. Each of these sandstone tongues was buried by a subsequent pulse of tectonic activity that caused subsidence of the basin and a corresponding transgression of the seaway, thereby creating conditions for another shoreface sandstone tongue to be created. These prograding sandstone layers extend progressively farther to the southeast as they get younger, recording the advance of the western shoreline of the Cretaceous Seaway to the east. Two very extensive prograding shoreface sands in the Piceance and Sand Wash Basins are the Castlegate (which appears to be correlative with the Morapos in the Sand Wash Basin) and the Rollins (which is correlative with the Trout Creek in the Sand Wash Basin); both of these units are potentially good sequestration targets.

Mesaverde Group

With time, the western shoreline finally advanced into the area of study and sedimentation changed from predominantly marine to continental. Marine and fluvial sands, shales and coals were deposited on coastal plains and comprise the Cretaceous Mesaverde Group. The Mesaverde is thicker in the west and thins in the eastern Sand Wash and San Juan basins where the sediments appear to be more marine. A major marine transgression near the middle of the Mesaverde section was recorded in the rock record as an extensive marine shale that can be seen in the eastern part of the Sand Wash Basin. Overlying it is the prograding Trout Creek sand, which is correlative with the Rollins sand in the Piceance Basin.

For this study the top of the Mesaverde was not identified in the Piceance Basin because it was indistiguishable on geophysical logs from the overlying continental deposits of the Ohio Creek, Fort Union and Wasatch formations.

Lewis Shale

In the Sand Wash and San Juan basins a final transgression of the Cretaceous Seaway resulted in the deposition of the Lewis Shale, albeit at different times. In the Sand Wash Basin the Lewis consists of marine shale and sandstones; the sands are fine-grained turbidity deposits (Cain, 1986). The Lewis Shale thins from east to west; it is not present in the Piceance and Paradox basins. Above the Lewis in the Sand Wash Basin is the Cretaceous Fox Hills Formation consisting of shoreline sandstones representing the final regression of the Cretaceous Western Interior Seaway.

Paleogene and Neogene Systems

At the end of the Cretaceous Period, compressive forces from the west initiated the Laramide Orogeny, which continued through the Eocene. This mountain building episode uplifted the western United States, creating the uplifts of the present-day Rocky Mountains which, in Colorado, are in the approximate locations of the Ancestral Rockies. The intervening areas were fragmented into basins into which fluvial and lacustrine deposits accumulated. In Colorado, rocks of the Fort Union, Wasatch, Green River and Uintah Formations were deposited in these basins.

Intense igneous activity occurred in the southwestern part of the state during the Cenozoic. In the Oligocene, laccoliths were intruded in the area of the Elk Mountains and andesitic and ash flows were extruded in the San Juan volcanic field. The eruptions in the San Juan volcanic field became basaltic in the Miocene (Tweto, 1977) as the regional compressional forces of the Laramide Orogeny changed to regional extensional forces that created the Basin and Range (Stern and Constenius, 1997). Igneous sills, dikes, and flows continued in the area through the Pliocene (Tweto, 1979) in response to the extensional forces.

3.2.2 Data and Methods

3.2.2a Data

A goal of this project was to incorporate all existing publicly available data into maps depicting the structural configuration of the saline aquifers and their seals. The data utilized in this mapping included:

- Records from over 30,000 oil and gas wells in western Colorado. These were obtained primarily from the IHS commercial database for the Rocky Mountain region. This database was augmented by data from the Colorado Oil and Gas Conservation Commission's website. The locations of these wells within the Sand Wash Basin are shown in Figure 3.4.

- Images of geophysical logs from over 18,000 oil and gas wells in the CSA. These were purchased from MJ Systems, a company that scans and archives raster logs. Geophysical logs record the physical properties of the rocks and fluids that surrounding the wellbore and were used to determine the depths of the saline aquifers and other formations in the subsurface. The locations of wells with geophysical logs are shown in Figure 3.5.
- One thousand surface measurements of bedding strikes and dips. Nearly 1500 measurements were collected by a team of geologists from the Colorado Geological Survey covering an area of approximately 800 square miles, predominantly in the region of the Yampa Block. 470 of these measurements were deemed unreliable and were not used. Approximately one thousand strike and dip measurements were used to hand modify contours of the Dakota Formation's structure in the subsurface. Figure 3.6 shows the locations of the strike and dip measurements used in this project.
- Approximately 70 miles of existing two-dimensional seismic data in 11 lines. These were purchased through Seismic Exchange, Inc. to help define the structures in the southern part of the Yampa Block, which is updip from the stratigraphic test well, the direction that sequestered CO_2 is expected to migrate. The locations of these lines are shown in Figure 3.7.
- Approximately eight miles of two-dimensional seismic data in two lines that were shot by Schlumberger Carbon Services. These cross the stratigraphic test well location and were shot to define the subsurface structure in the immediate area of the test well. The locations of these lines are shown in Figure 3.7. For work on this portion of the project, these newly acquired lines were used qualitatively to manipulate the shape of the Dakota surface. The precise depth of the Dakota horizon was not picked from the seismic lines because existing shallow data depicting the structural configuration of the Twenty-Mile Sand and the Trout Creek Sand, as well as surface strike and dip measurements, conflicted with the information in the deeper seismic horizons. More work can and should be done with these seismic lines assuming processing and calibration are robust.
- Published geologic maps that depict the rocks and structures at the surface. These include:
    - Outcrop patterns from surface geologic maps, including Tweto (1977).
    - Locations of fold axes from surface geologic maps, including Tweto (1977).
    - Elevations of surface contacts between the Dakota and the overlying Mowry Shale depicted on digital elevation models.

- Geologic publications that contain subsurface maps, cross sections, and/or rock characteristics and properties. Sources of formation tops from published geologic maps are listed in Appendix A.
- Data from relevant well cores and cuttings.
- Data collected from the drilling of the stratigraphic test well RMCCS State #1, including:
    - Geophysical well logs that help determine rock and fluid properties of the penetrated strata.
    - Full-diameter cores and sidewall cores from which direct measurements of rock properties of the saline aquifers and their seals can be obtained.

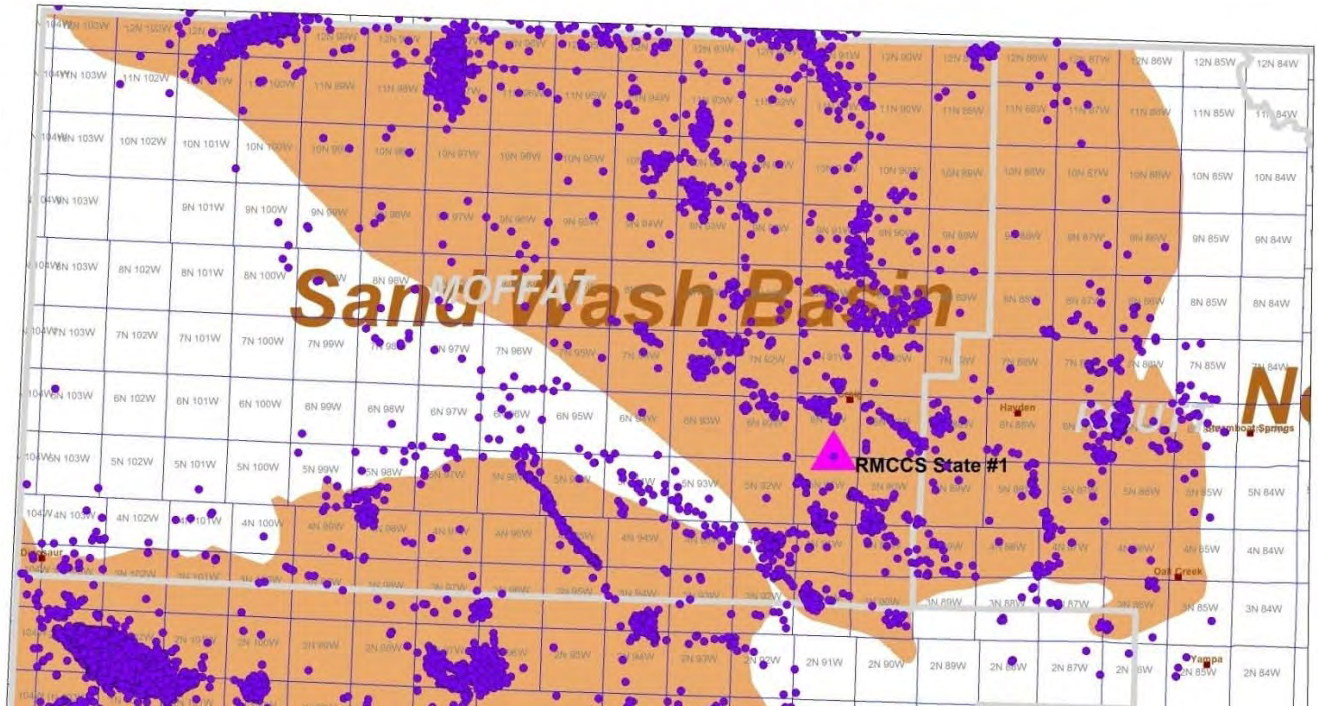

Figure 3.4. Distribution of oil and gas wells (purple) across northwestern Colorado with sedimentary basins (shaded brown areas).

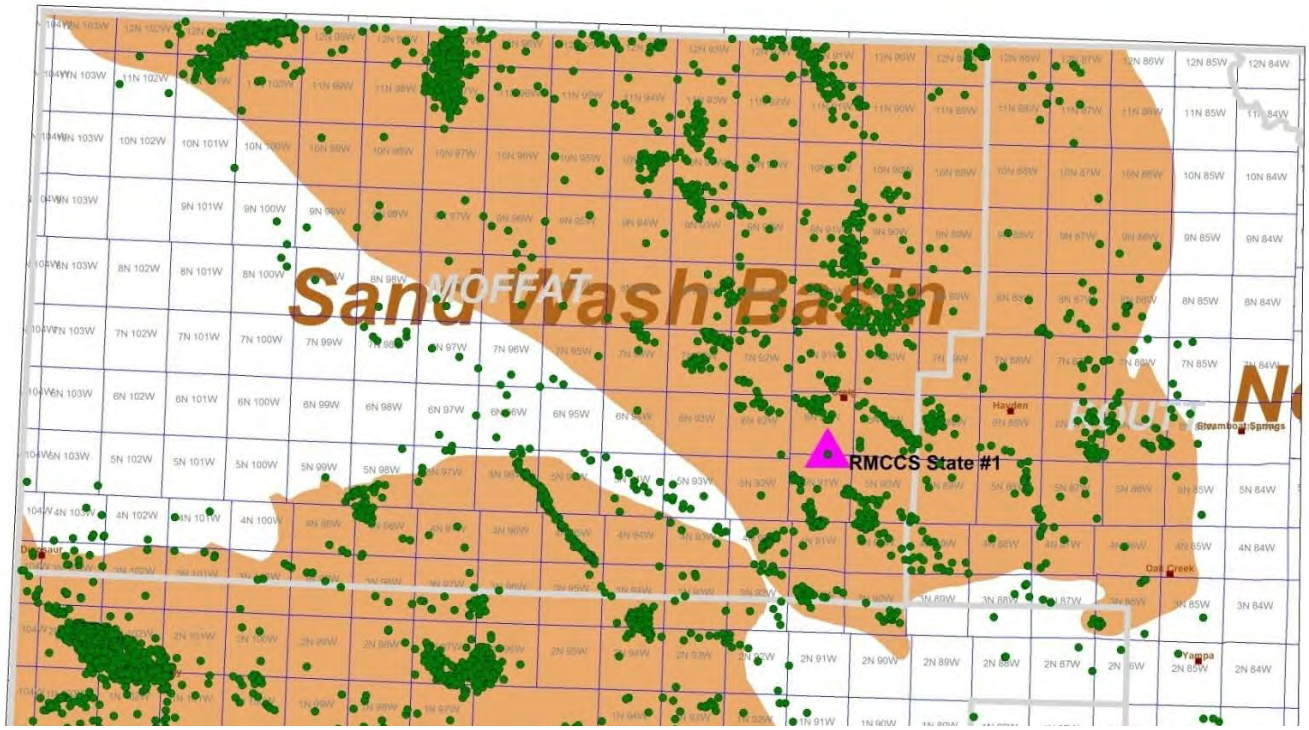

Figure 3.5. Distribution of oil and gas wells with available geophysical wireline logs (green) for northwestern Colorado.

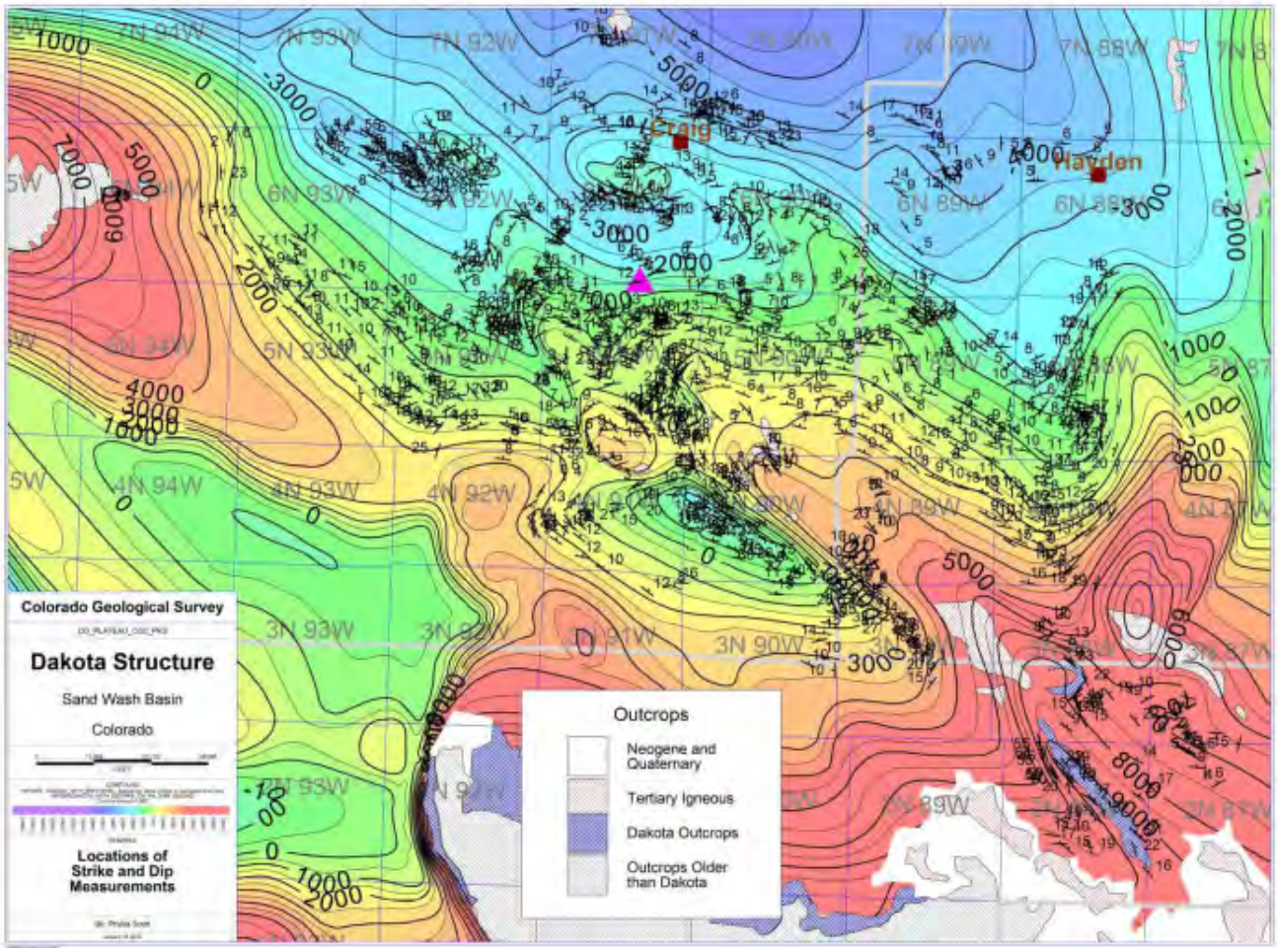

Figure 3.6. Measurements of strike and dip at surface outcrops around the Craig stratigraphic test well site (pink triangle). Data collected by the Colorado Geological Survey during the summer of 2010.

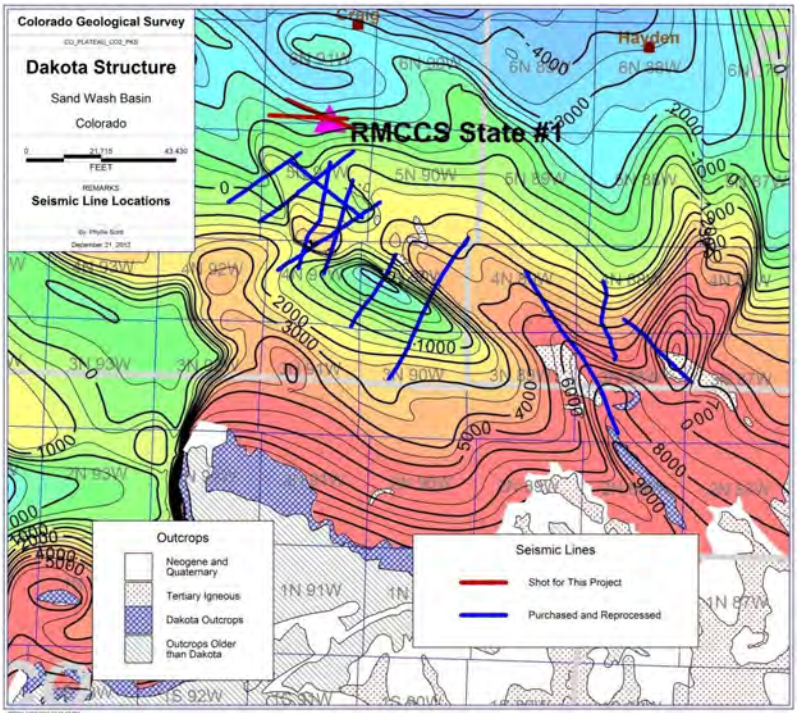

Figure 3.7. Eleven existing seismic lines (blue) and two new seismic lines (red) were utilized for this project.

Extent of Geologic Mapping for Site and Regional Characterization

The sequestration potential of the saline aquifers in Colorado has been examined at two scales (Figure 3.1):

1. Yampa Block: a very detailed analysis of the geology of the Laramide-age Yampa Block south of the town of Craig, Colorado. All of the data types listed above were used in this detailed study component. This block covers approximately 230 square miles and generally dips about 10 degrees to the north. It is bounded on all sides by forced folds.

2. Sand Wash Study Area: a detailed characterization of the three saline aquifers within a 40-mile radius of Craig. This study component augments the Yampa Block mapping with IHS data for oil and gas wells in the expanded area. Also utilized were additional geophysical logs, surface geologic maps and other published data. This characterization included most of the Sand Wash Basin and the adjacent Axial Basin Uplift that separates the Sand Wash and Piceance basins. The final products from this characterization were structure maps of fourteen formation top surfaces that were used for building a geocellular model.

Mapping Software

Three mapping software packages were used to create these maps:

1. Petra: an IHS software package designed for geologic interpretation and mapping based on data from oil and gas wells. Petra was used to correlate formation tops and to create a detailed, hand-contoured structural surface of the Dakota Sandstone.

2. Petrel: a Schlumberger application for geocellular modeling and visualization. Petrel was used to generate multiple, sub-parallel formation surfaces using the Dakota structure map and formation tops interpreted in Petra. A static geologic model was created from this framework that was ultimately used for fluid injection simulations.

3. ArcGIS: a popular ESRI tool for GIS based mapping. ArcGIS has been chosen as the primary RMCCS spatial database format.

Porosity and Permeability

As a part of this study, a cursory examination of existing porosity and permeability measurements was made in an attempt to better estimate the storage capacity of the saline aquifers.

Additionally, core analysis data sheets were downloaded from the Colorado Oil and Gas Conservation Commission's website for wells in the Sand Wash Basin study area. Data from six Dakota cores and three Entrada cores were evaluated.

Data from the Dakota cores (Figure 3.8) shows the average porosity to be 13.72% and the median permeability to be 19 mD. One of the analyzed cores had anomalously high permeability values. The porosity and permeability values are strongly dependent on the position of the core within the section; they vary greatly depending on whether the cores were cut through zones of the highest porosity or through more shaly intervals. Table 3.1 lists the mean and median porosity and permeability values for each core.

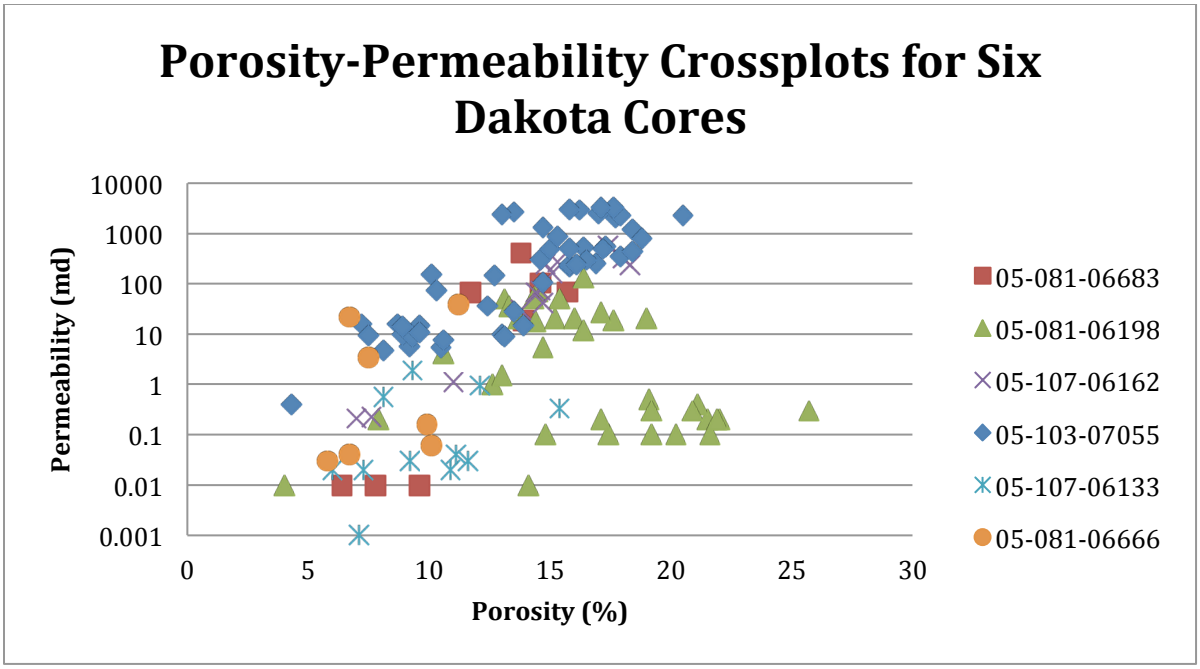

Figure 3.8. Porosity-Permeability crossplots for six Dakota cores.

					Porosity %		Permeability (md)	
API Number	**Location**	**Top of Dakota (MD)**	**Dist. from RMCCS State #1**	**No. of Samples**	**Average**	**Median**	**Average**	**Median**
05-081-06683	SE SW SW 20-5N-90W	4893	6 mi SE	8	11.7	12.8	84	43
05-081-06198	NE SE SW 21-5N-90W	4850	6mi SE	35	16.4	16.4	16	1
05-107-06162	NW SE 29-4N-89W	3183	14 mi SE	13	14.0	14.7	158	72
05-103-07055	NE SE 1-2N-93W	6996	20 mi SSW	51	13.7	14.7	748	240
05-107-06133	NW NE 36-4N-88W	891	22 mi SE	11	9.8	9.3	0.36	0.03
05-081-06666	NE NW 30-5N-93W	2752	16 mi WSW	7	8.3	7.5	9.1	0.16

Table 3.1. Porosity and permeability values for each of the Dakota cores crossplotted in Figure 3.8.

From three available cores datasets, the mean porosity for the Entrada formation was calculated to be 15.01% and the median permeability 23.5 mD (Figure 3.9 and Tabe 3.2) .

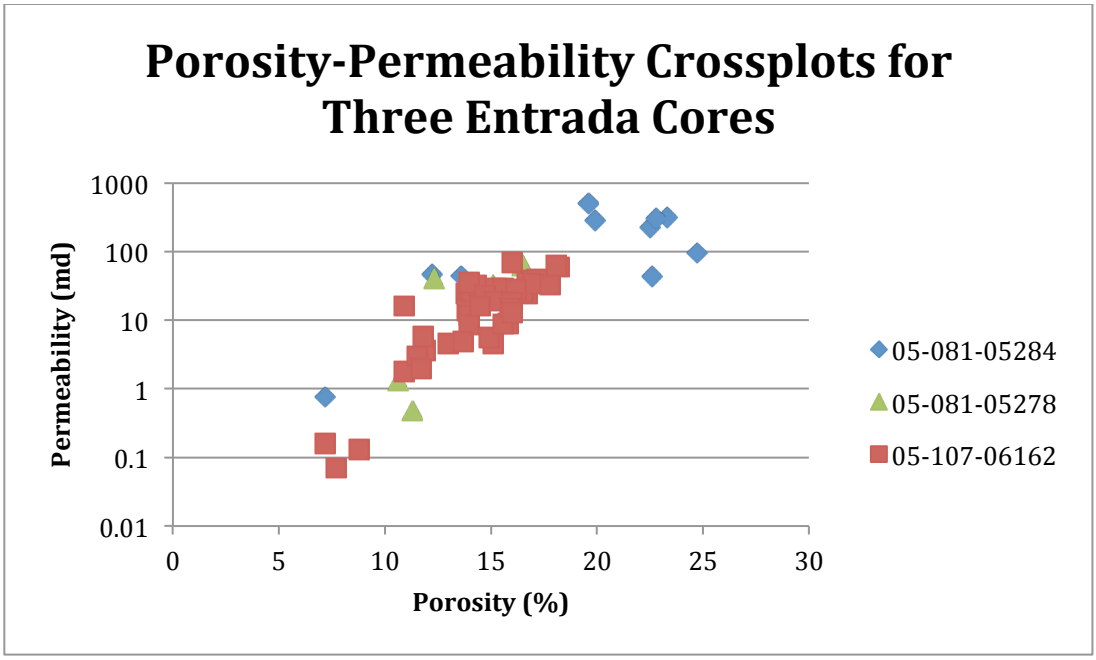

Figure 3.9. Porosity-permeability crossplots for three Entrada cores in the Sand Wash Basin.

Table 3.2. Data for the three individual Entrada cores that are crossplotted in Figure 3.9 above.

					Porosity %		Permeability (md)	
API Number	**Location**	**Top of Entrada (MD)**	**Dist. from RMCCS State #1**	**No. of Samples**	**Average**	**Median**	**Average**	**Median**
05-081-05278	SW SE 20-5N-90W	5421	5.5 mi SE	7	13.7	14.9	26	24
05-081-05284	NW SW 13-5N-96W	5254	28 mi W	10	18.8	21.2	187	161
05-107-06162	NW SE 29-4N-89W	3814	13.7 mi SE	45	14.4	14.7	21	18

3.2.2b Methods

Overview

The general workflow consisted of correlating formation tops in Petra and creating a detailed, hand-contoured, Dakota structure map. The correlated tops and gridded Dakota structure map were transferred to Petrel, which was used to create structure maps of other formations. Finally, the Petrel gridded surfaces were imported into ArcGIS where they will be combined with surfaces created for other portions of the Colorado Plateau in the final report.

Sand Wash Basin – Model Foundation

Petra

Petra was the primary software tool used for analysis and interpretation. Well data from the IHS database and scanned geophysical log images from MJ Systems were central to this interpretation. Formation tops as reported by operators are notoriously unreliable, with inconsistencies common from company to company. Oftentimes, tops do not correlate exactly, creating errors in mapped surfaces. To produce the most accurate maps, formation tops were identified and correlated anew throughout the study area. This detailed correlation process resulted in a high level of consistency throughout the area.

The tops correlated in this project were used to create a detailed structure contour map on the top of the Dakota Sandstone. The Dakota Sandstone was chosen as the key surface because it is regionally extensive and often easy to distinguish on geophysical logs. It is also the shallowest of the regionally targeted saline aquifers.

Initially only the Sand Wash Basin study area (including the Yampa Block and the Axial Basin Uplift) was examined and mapped. On the Axial Basin Uplift, the saline aquifer targets are near the surface, and in some cases have been removed by erosion. In contrast, deeper parts of the basin have thick sections of younger sediments overlying the saline aquifers, with few wells drilled deep enough to penetrate the aquifers. To overcome this problem, depths of the aquifers could be projected from the positions of shallower formations. Many more formation tops not associated with the targeted aquifers were correlated and mapped. From these the tops of the aquifers could be estimated in wells that did not actually penetrate the aquifers.

The Sand Wash study area contained 4924 wells, of which 2708 had at least one geophysical log. Of those, 2000 had either an actual or projected Dakota formation top that was correlated for this project. Altogether, 37 formation tops ranging in age from the Cretaceous Fox Hills Sandstone to the Precambrian erosional surface were correlated for the Sand Wash study area totalling 15,000 individual tops.

The Dakota tops were hand contoured to incorporate the individual data points as well as all the other data sources. The structures were contoured as forced folds overlying the edges of fragmented and differentially uplifted basement blocks.

The Dakota structure map of the Sand Wash Basin study area, shown in Figure 3.10, was then imported into Petrel and subsequently used for generating other modeled surfaces.

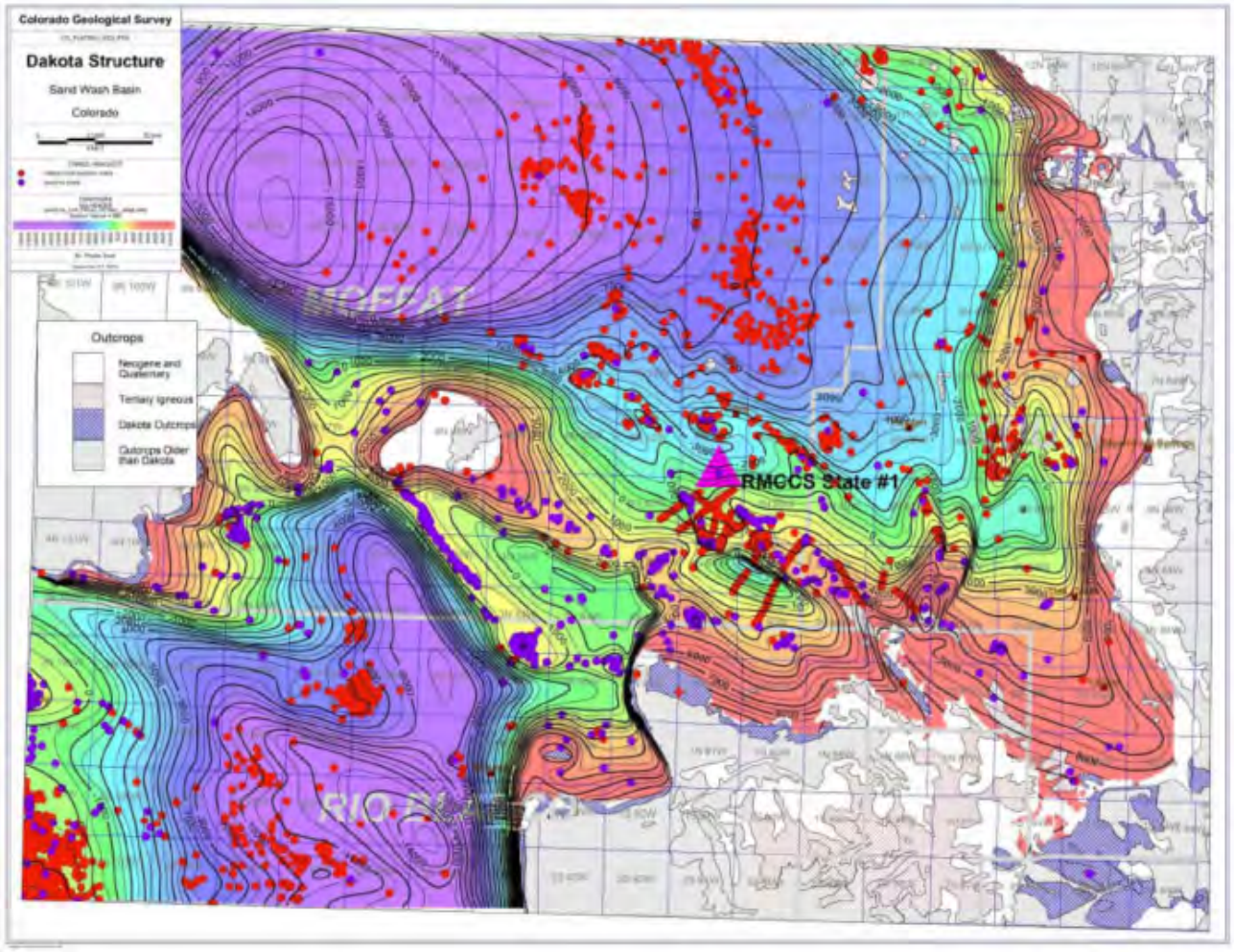

Figure 3.10. Structure map on top of the Dakota Sandstone saline aquifer for the Sand Wash Basin.

Petrel

Petrel is a software package designed by Schlumberger for generating and visualizing static geologic models from a myriad of oil and gas well data. Petrel was used to create a three-dimensional model within the Sand Wash Study area to be used as the structural framework for simulating the injection of CO_2 into the saline aquifers from the RMCCS State #1 well.

The Dakota surface that was generated in the Petra project was imported into Petrel along with the locations of wells within the study area and formation tops for those wells. Petrel used these data to map other surfaces by comparing formation tops for an unmapped surface with an adjacent mapped surface and creating a new, sub-parallel structure map. For example, the top of the Morrison was mapped by using the Dakota

structural surface and Morrison formation tops to create a Morrison structural surface that is sub-parallel with the Dakota surface. The use of both a surface and the formation tops provides much more information for the creation of the secondary surface than tops alone. Relying only on formation tops to create surfaces in this structurally complex area usually resulted in impossible geometries with surfaces that intersected.

Fourteen surfaces were created in Petrel. From shallowest to deepest they are:

Formations Mapped in the Sand Wash Basin Petrel Model

Formation Top	Average Interval Thickness	Description
Mancos	888	The name of the group that comprises all of the formations deposited within the Cretaceous Seaway (including all formations down to the Dakota saline aquifer). The Mancos Group is the ultimate seal overlying the saline aquifers.
Morapos	2311	A prominent sand within the Mancos Group deposited in the Cretaceous Seaway
Niobrara	1528	A calcareous section within the Mancos Group deposited in the Cretaceous Seaway
Carlile	199	A shale within the Mancos Group deposited in the Cretaceous Seaway
Frontier	295	A coarsening-upward shale and sand unit deposited within the Cretaceous Seaway.
Mowry	102	A shale unit directly overlying the Dakota saline aquifer. It is the seal for the Dakota saline aquifer
Dakota	166	A saline aquifer comprised of fluvial and marine sands, silts and shales.
Morrison	415	Fluvial sands and shales. The Morrison top is the base of the Dakota saline aquifer. This unit is a seal for the Entrada saline aquifer, although there are some porous sandstones in the western part of the study area.
Curtis	65	A marine deposit of sand, shale and siltstone that forms the seal for the Entrada saline aquifer.
Entrada	347	A saline aquifer comprised of eolian sandstone. It includes the Navajo Sandstone in the western part of the study area.
Chinle	779	Sands and silts deposited by large river systems. The Chinle is the base of the Entrada/Navajo saline aquifer. This interval includes the Moenkopi, which underlies the Chinle. The entire interval is a seal for the Weber saline aquifer.
Phosphoria	187	Marine limestone, sandstone and shale that acts as a seal for the Weber saline aquifer.

Weber	411	A saline aquifer comprised of eolian sandstone.
Maroon		Alluvial fan redbeds and the base of the Weber saline aquifer.

Figures 3.11 through 3.16 are a series of structure and isopach maps on the top of each of the saline aquifers and the thickness of each saline aquifer over the Colorado Plateau study area. Figure 3.17 is a structure map of the top of the Mancos Shale, the ultimate seal over the saline aquifers. Figure 3.18 is an isopach map of the Mancos Shale.

The digital elevation model was used to create maps showing the depths to the top of each of the targeted saline aquifers. These depth maps were used to outline the area of each aquifer present at depths of more than 3000 feet below the surface (3. 3.19).

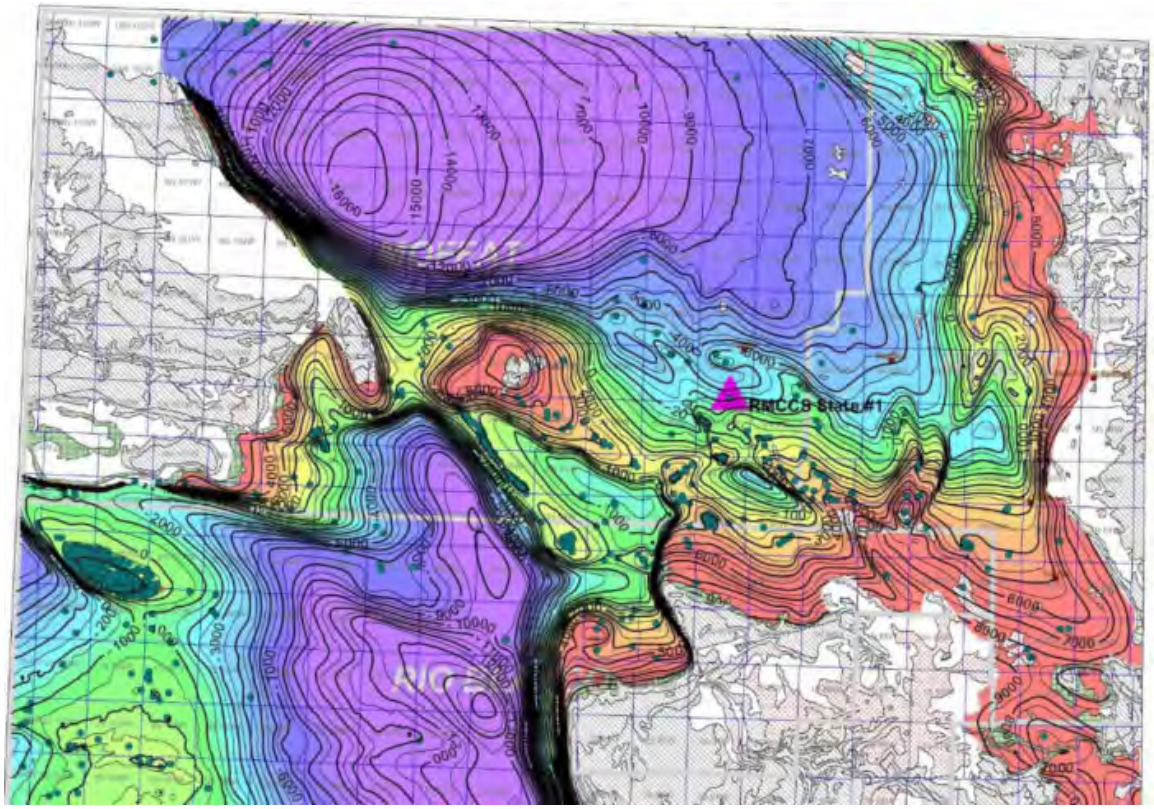

Figure 3.11. Structural top of the Dakota saline aquifer. Contour interval is 500 feet.

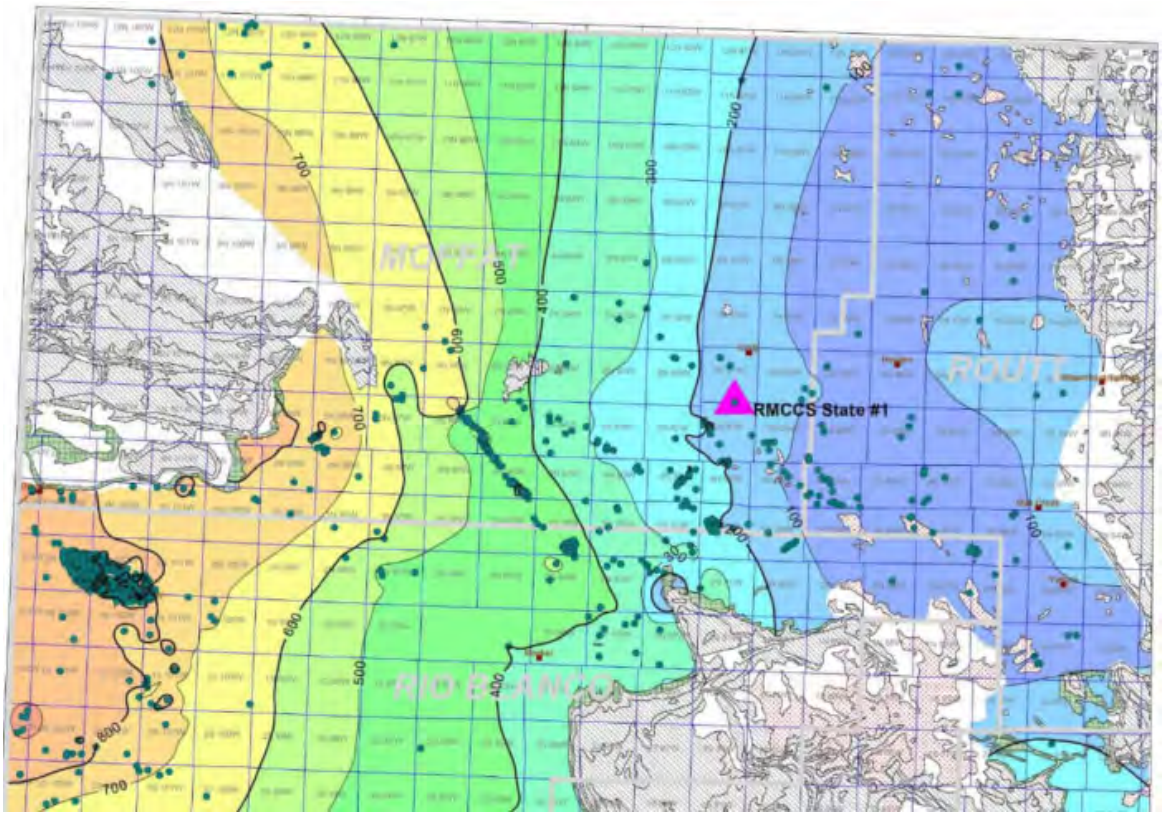

Figure 3.12. Thickness of the Dakota saline aquifer – from the top of the Dakota Formation to the top of the Morrison Formation. Contour interval is 50 feet.

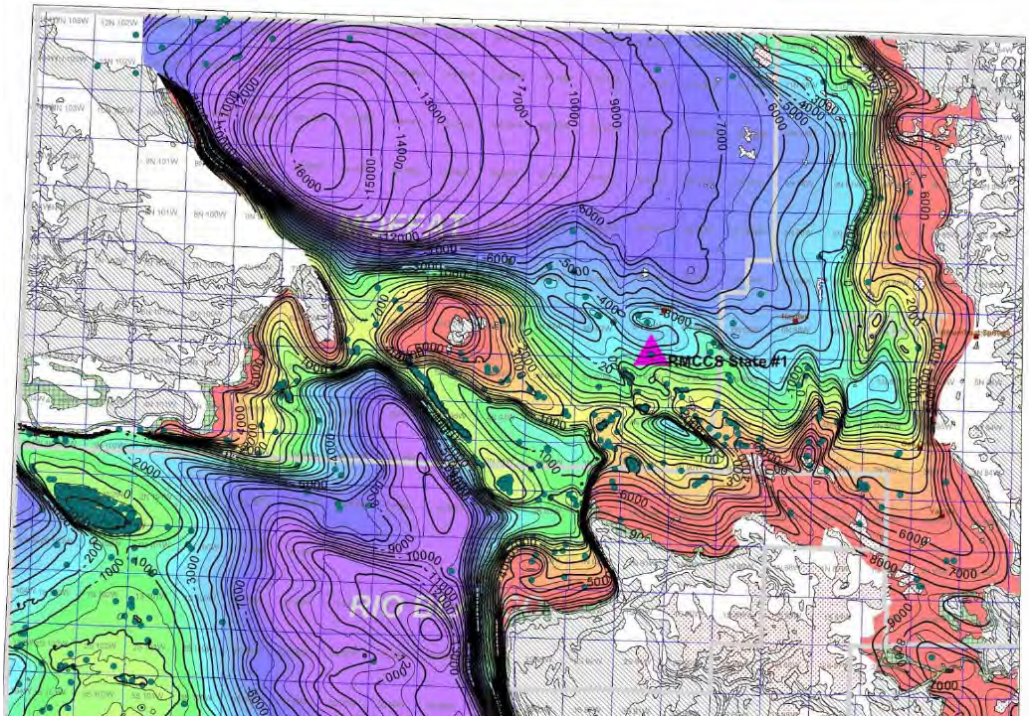

Figure 3.13. Structural top of the Entrada saline aquifer. Contour interval is 500 feet.

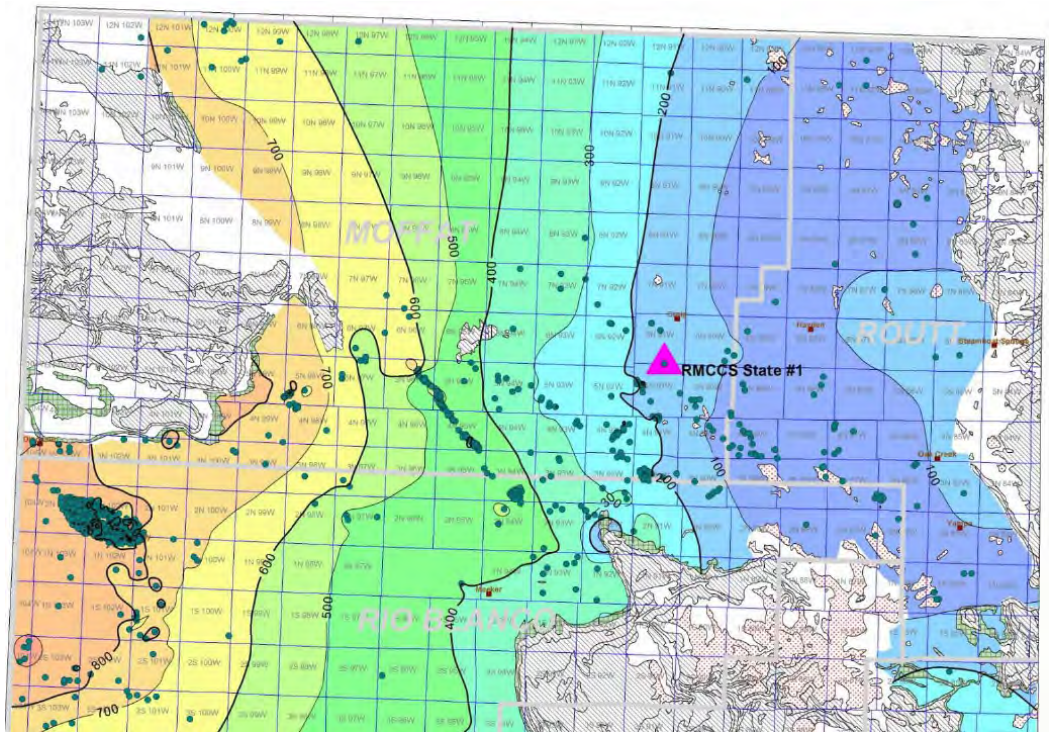

Figure 3.14. Thickness of the Entrada saline aquifer – from the top of the Entrada Formation to the top of the Chinle Formation. Contour interval is 100 feet.

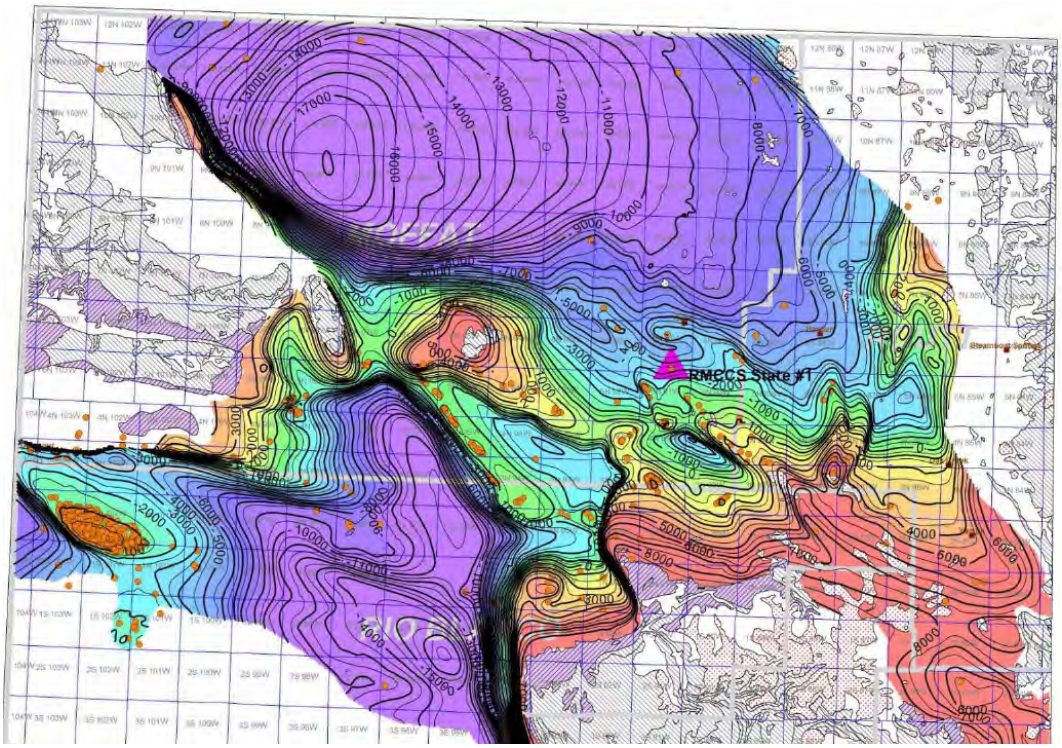

Figure 3.15. Structural top of the Weber saline aquifer. Contour interval is 500 feet.

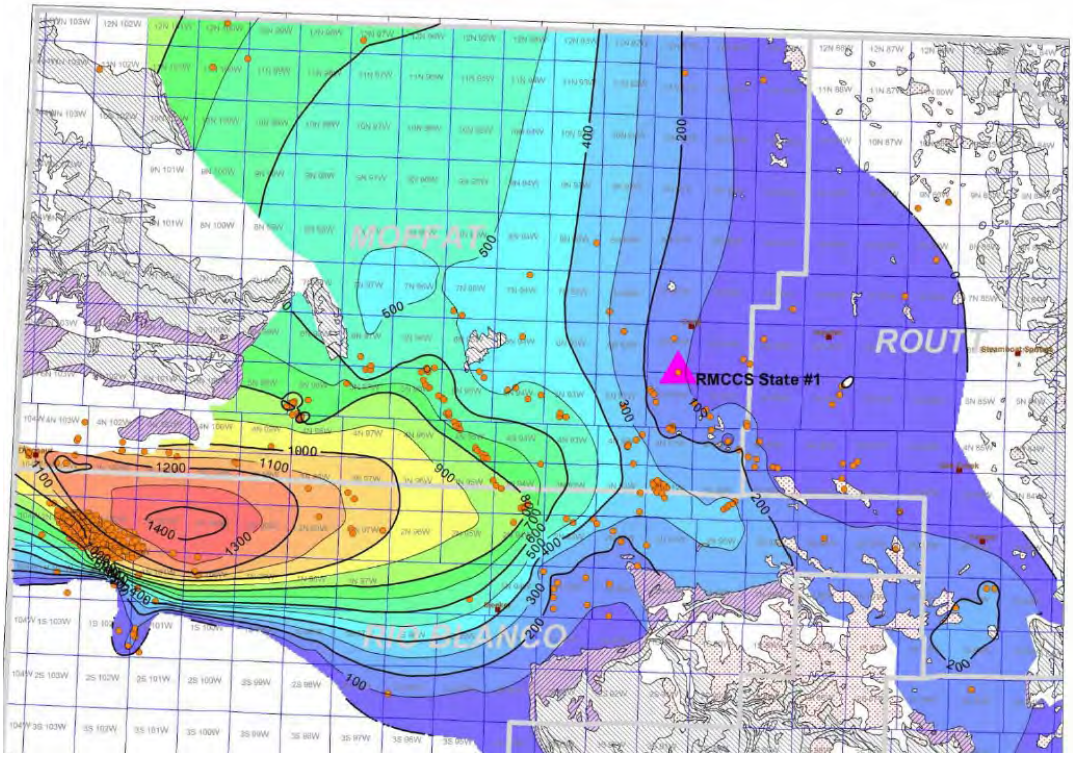

Figure 3.16. Thickness of the Weber saline aquifer – from the top of the Weber Formation to the top of the Maroon Formation. Contour interval is 100 feet.

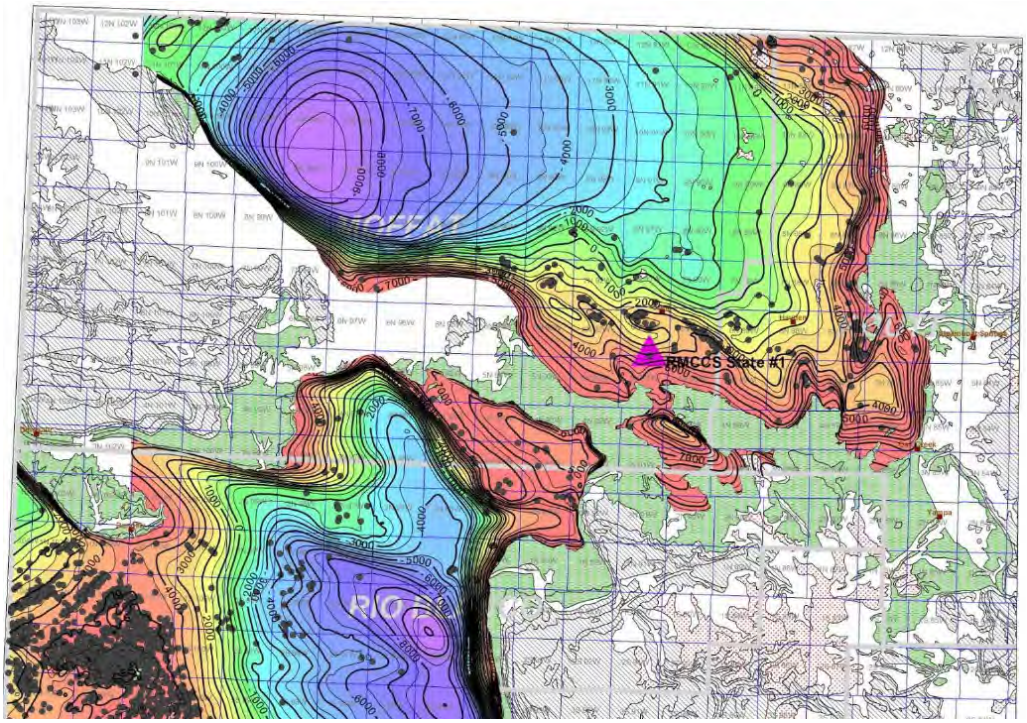

Figure 3.17. Structural top of the Mancos seal. Contour interval is 500 feet.

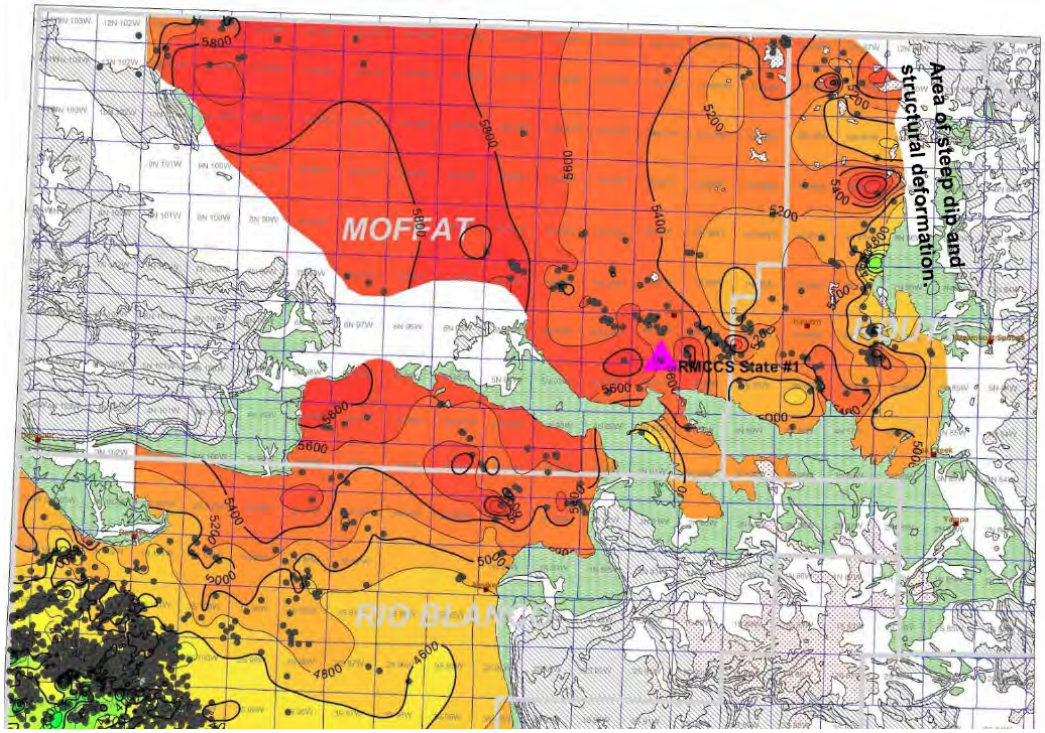

Figure 3.18. Thickness of the Mancos – from the top of the Mancos Formation to the Dakota Formation. Contour interval is 200 feet.

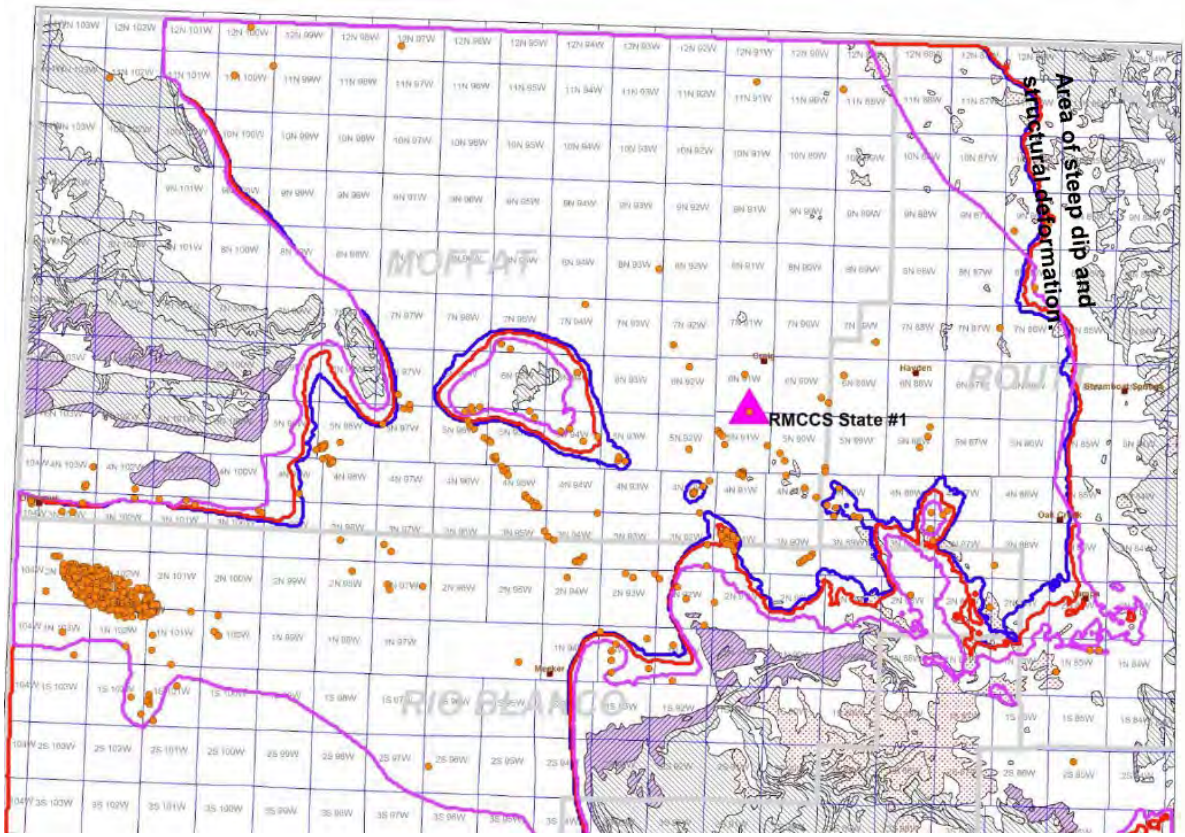

Figure 3.19. Outlines of the extents of each of the saline aquifers at a depth greater than 3000 feet – Dakota (blue); Entrada (red); and Weber (pink).

Geocellular Model

Surfaces for the geocellular model were generated using a minimum curvature algorithm and a grid size of 500 by 500 feet. A digital elevation model was imported into Petrel and used to trim each of the surfaces to prevent projections above the ground surface. Fourteen surfaces and their respective isopach maps were migrated from Petrel into Petra and ArcMap for visualization and database archiving.

Cross sections through the Petrel model are show in Figures 3.20 and 3.21. Figure 3.20 is a north-south cross section while Figure 3.21 is a west-east cross section.

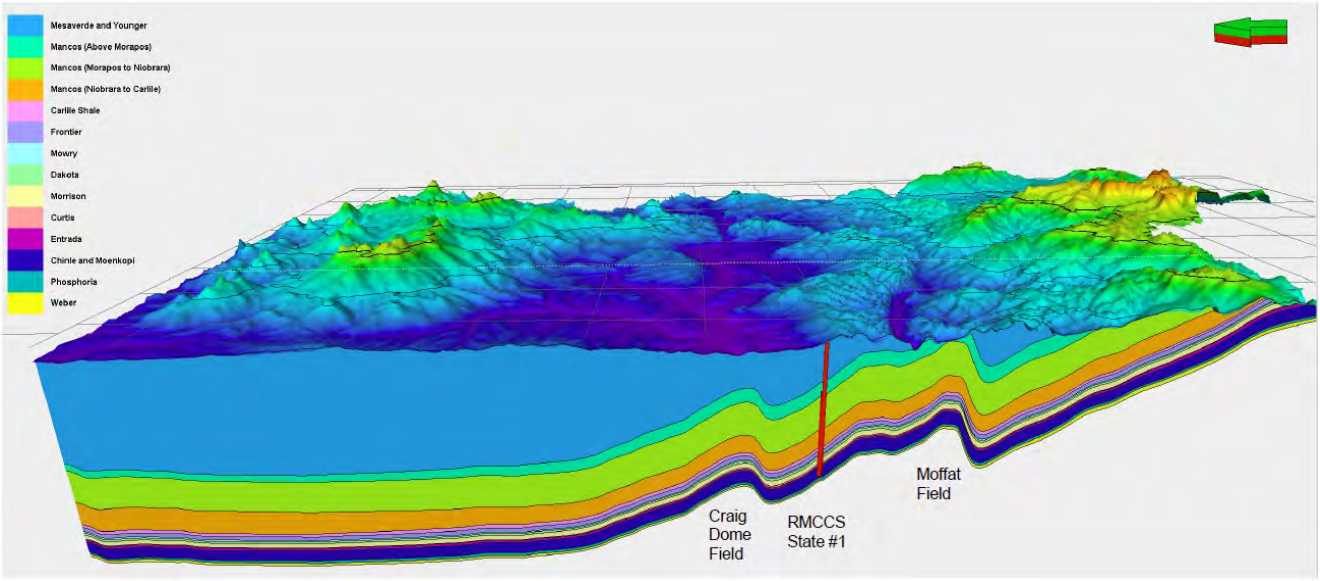

Figure 3.20. North-South cross section through RMCCS State #1 test well site (red vertical line). Linear extent of view is approximately 50 miles, with the Wyoming border shown at left edge and the White River Uplift to the right.

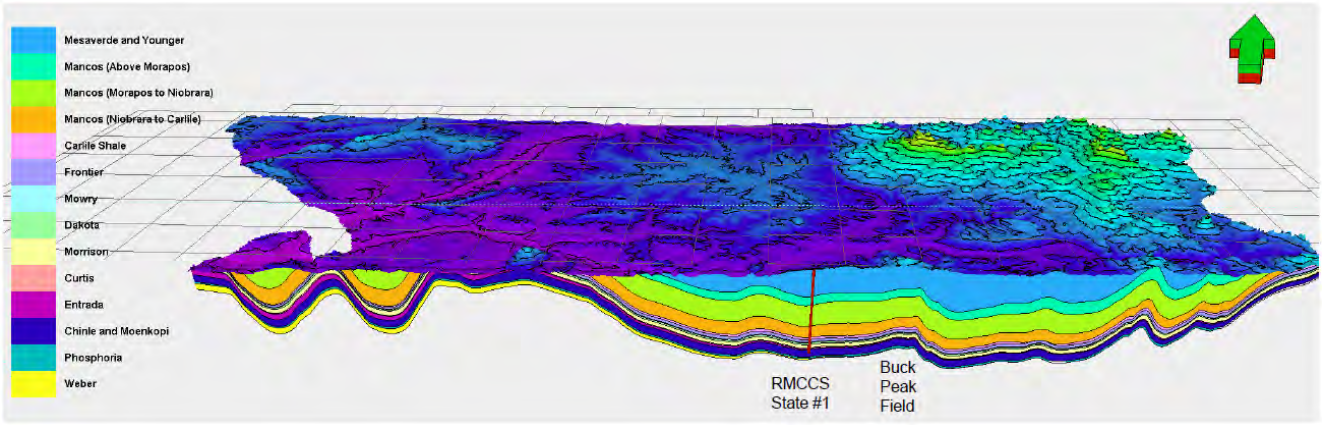

Figure 3.21. West-East cross section through RMCCS State #1 test well site (red vertical line). The Unita Mountains are located at the left edge and the Park Range at Right.

Accuracy of Mapped Surfaces

Potential sources of error in the oil and gas well data and resultant maps include the following (listed in order of significance):

- In areas of sparse well control, the surfaces may be mapped incorrectly. Structural features, both faults and folds, may be completely missed if there is no well control or outcrop patterns that suggest that structures are present.

- The thickness of a formation (or the thickness between two formation tops) may appear to be highly variable. This can be due to:
    - The wellbore cutting a normal fault which has removed part of the section by extension, resulting in an anomalously thin isopach. Anomalous data points were ignored.
    - Incompetent formations such as the Mancos Shale appear to have been deformed and either thickened by compressional forces or thinned by extensional forces.
    - Steeply dipping beds make a section appear thicker than normal because a vertical wellbore does not penetrate the formation at a 90 degree angle. In areas of steep dip, anomalous sections should appear as elongate thick or thin zones that parallel the strike of the section; however, computer gridding algorithms contour these anomalies as bullseyes when there are no other wells nearby for additional control. Because of this, other contoured surfaces that were made from the isopach maps would be in error. However, in areas of steep dip the contour lines are very close together, so a thicker section would result in a very small lateral shift in the contour lines.
- Tops may be miscorrelated because they are difficult to discern, especially on different types of geophysical logs that have been run over the years. Correlations were made above and below the saline aquifer tops in an attempt to insure accurate correlations.
- Formation tops oftentimes are gradational and difficult to pinpoint.
- The datum may have been measured incorrectly. Reported surface elevations were compared with digital elevation model data to gauge the correctness of the surveys.
- Locations may be incorrectly spotted. Data points that did not make sense were checked on the Colorado Oil and Gas Conservation Commission's website. If they could not be rectified, they were ignored.
- Wells may not be vertical. If this is the case, the measured depth of a formation top or an isopach interval may be too great. Anomalous points were ignored.
- Formation tops were picked with the geophysical logs compressed on the screen so that a longer section of the log could be viewed. Because of this,

the top could be off by as much as 10 or 15 feet from where the actual pick would be if the log were enlarged.

Because of the scale of the mapping project, the mapped surfaces are generalized and smoothed.

Discussion

1) Porosity Distributions

Porosity distribution and trends within the saline aquifers were examined by identifying sands and porous sands on raster logs within the Sand Wash Basin study area. The gamma ray curve was used to identify clean sands; sand intervals were picked manually using Petra's pay interval software. Once the sands were identified, porous zones within the sands were identified from a porosity log (density, neutron, or sonic). Occasionally porous sands were estimated from micrologs. A cutoff of six percent was used; the tops and bases of sands with porosities of six percent or greater were picked using Petra's pay interval software. Net feet of sand and net feet of porous sand were summed in each well for each saline aquifer and contoured to illustrate the distributions of those properties.

Figure 3.22 shows the net feet of sand within the Dakota saline aquifer; Figure 3.23 shows the net feet of sand with porosities of six percent or more. These maps show that distribution of both of these properties is highly variable. This is probably due to the fact that much of the Dakota saline aquifer is composed largely of fluvial sandstones which can change character over short distances.

Figures 3.24 and 3.25 show the distribution of net sand and net porous sand within the Entrada saline aquifer. The net sand map shows the steady thinning of the interval to the east as the the Navajo Sandstone is removed from the interval by erosion. Because most of this interval is eolian sand, the porosities are less variable. Figure 3.25 shows a steady increase in net feet of porous sand to the west that corresponds roughly with the increase in net sand to the west.

Figures 3.26 and 3.27 show the distribution of net sand and net porous sand within the Weber saline aquifer. Both of these maps are based on sparse data and are highly interpretive. The Weber eolian sands decrease to the east and interfinger with the alluvial Maroon sands.

Unfortunately, many wells were drilled into the Weber, but only penetrated the top portion of it, so these wells could not be used to characterize the entire Weber interval. Also, the Weber and Maroon cannot be distinguished from each other on geophysical logs, so the base of the Weber was picked using tops reported by operators. Some operators identified the Maroon top; some identified only deeper

formations such as the Morgan or Minturn Formations. Each well that had raster logs and also a deeper top reported by an operator was examined to see how it compared to other nearby wells. The picture that emerged showed thickest net sands and thickest net porous sands in the west. These properties generally decrease to the east. However, there appears to be a band of thicker sand with greater porosities that trends roughly east-west and runs about 15 miles south of the RMCCS State #1 stratigraphic test well. The RMCCS State #1 was not able to drill deep enough to penetrate the Weber, but it is expected that the Weber would have thin sands and very little porosity at that location.

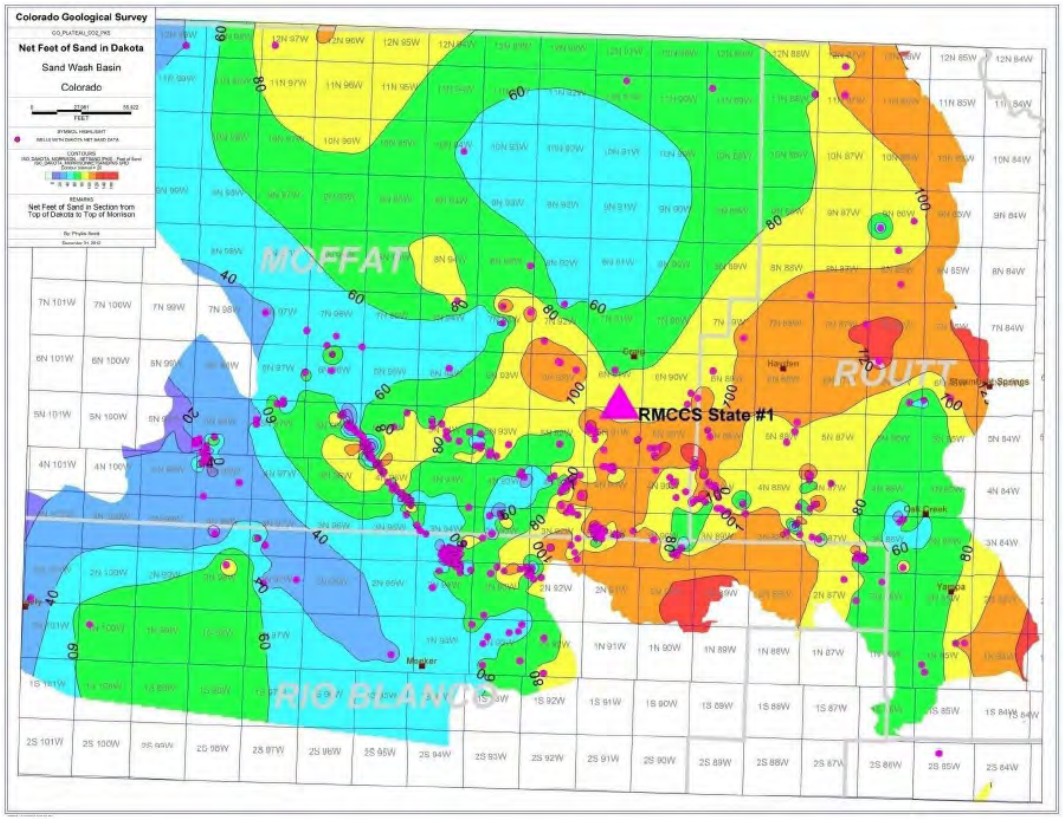

Figure 3.22. Net feet of sand within the Dakota saline aquifer. Contour interval is 20 feet.

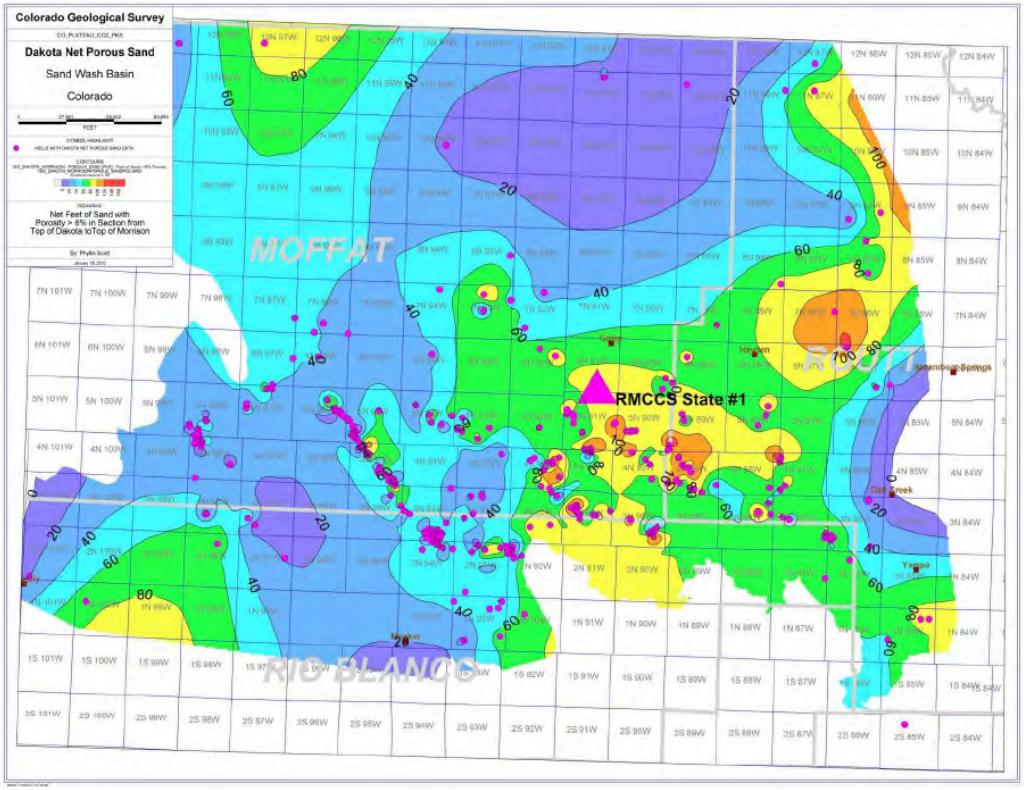

Figure 3.23. Net feet of sand (Φ >6 percent within the Dakota saline aquifer). Contour interval is 20 feet.

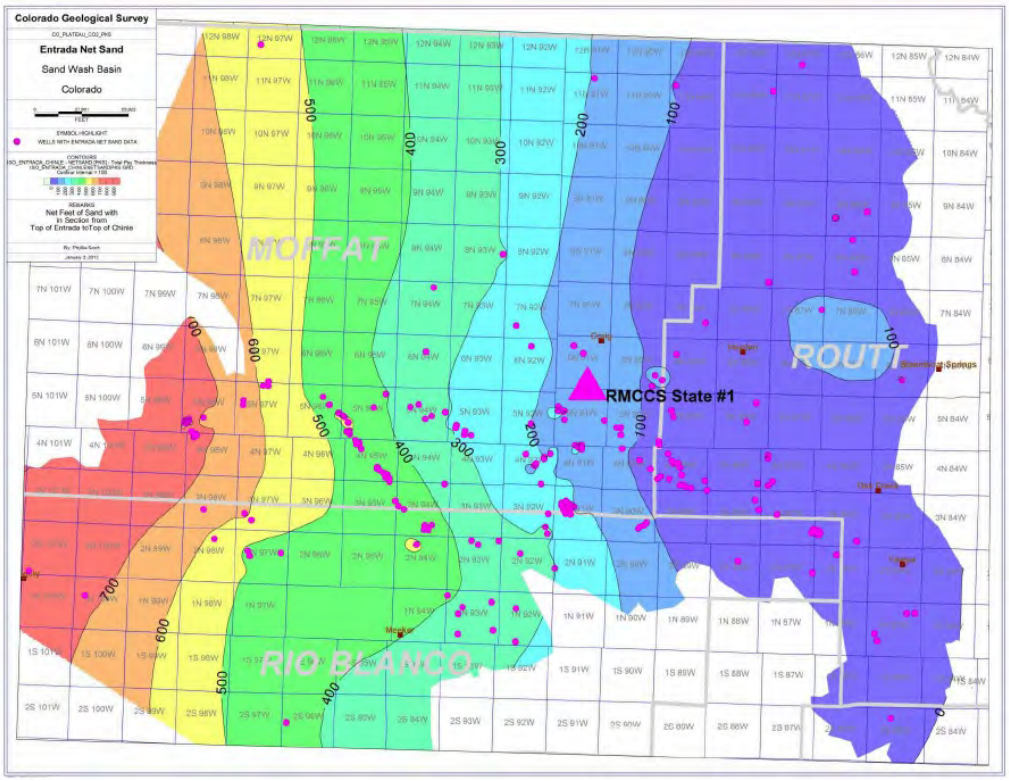

Figure 3.24. Net feet of sand within the Entrada saline aquifer. Contour interval is 100 feet.

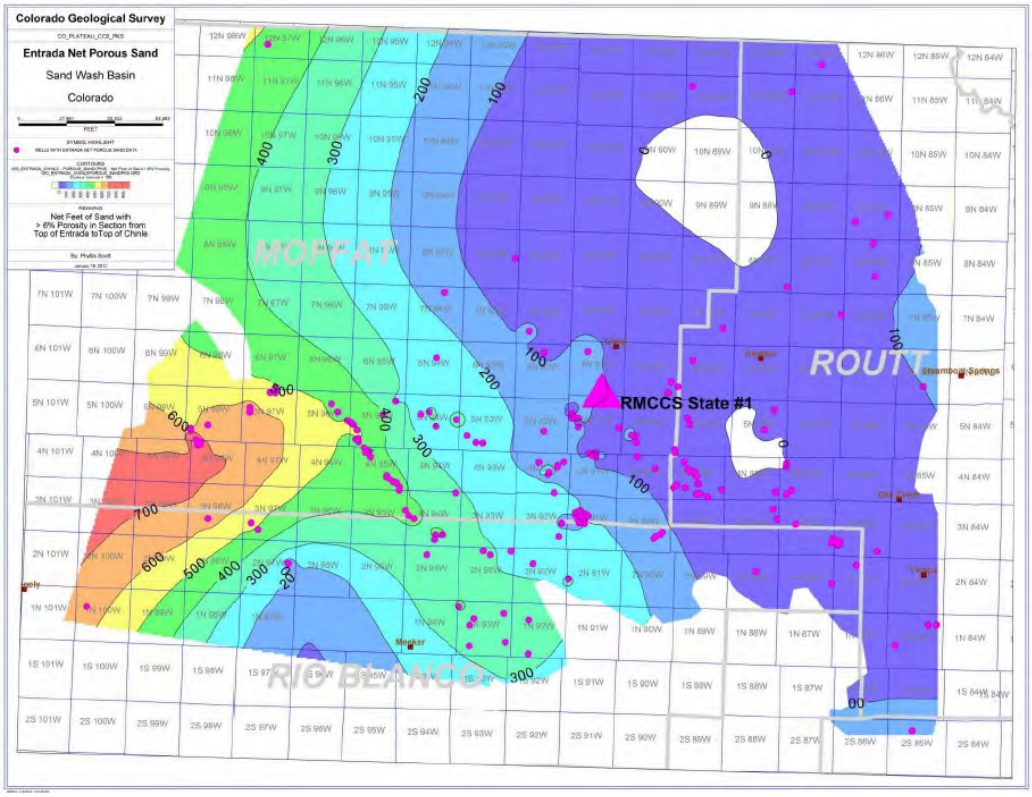

Figure 3.25. Net feet of sand (Φ >6 percent within the Entrada saline aquifer). Contour interval is 100 feet.

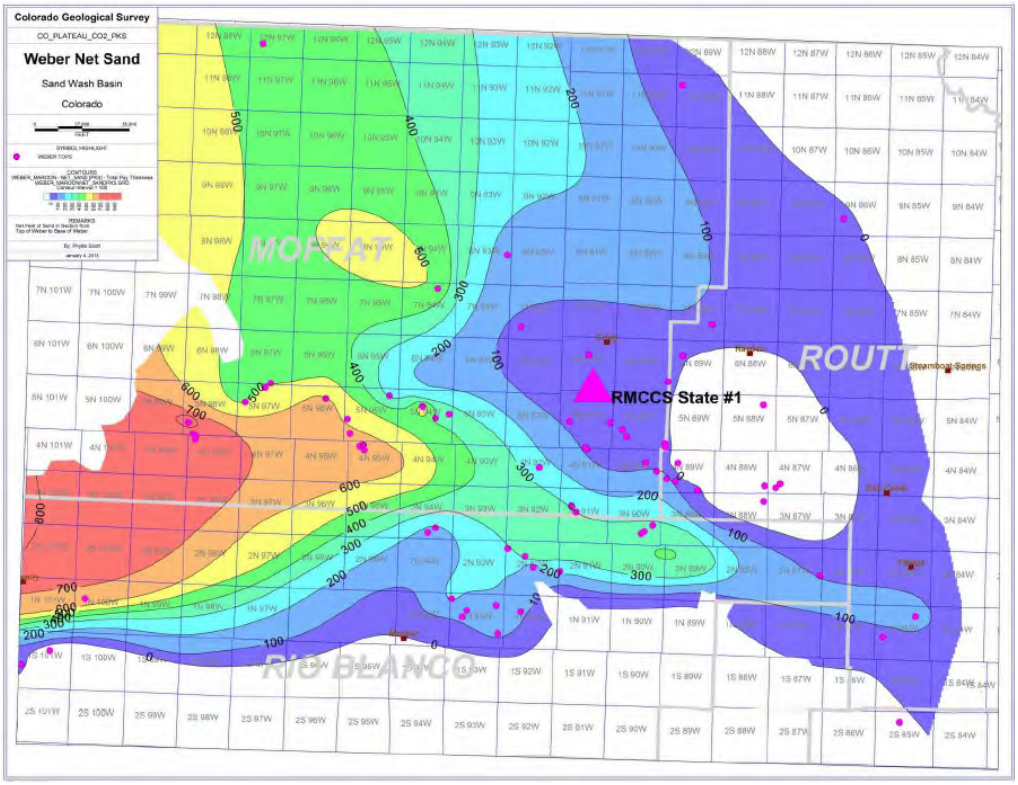

Figure 3.26. Net feet of sand within the Weber saline aquifer. Contour interval is 100 feet.

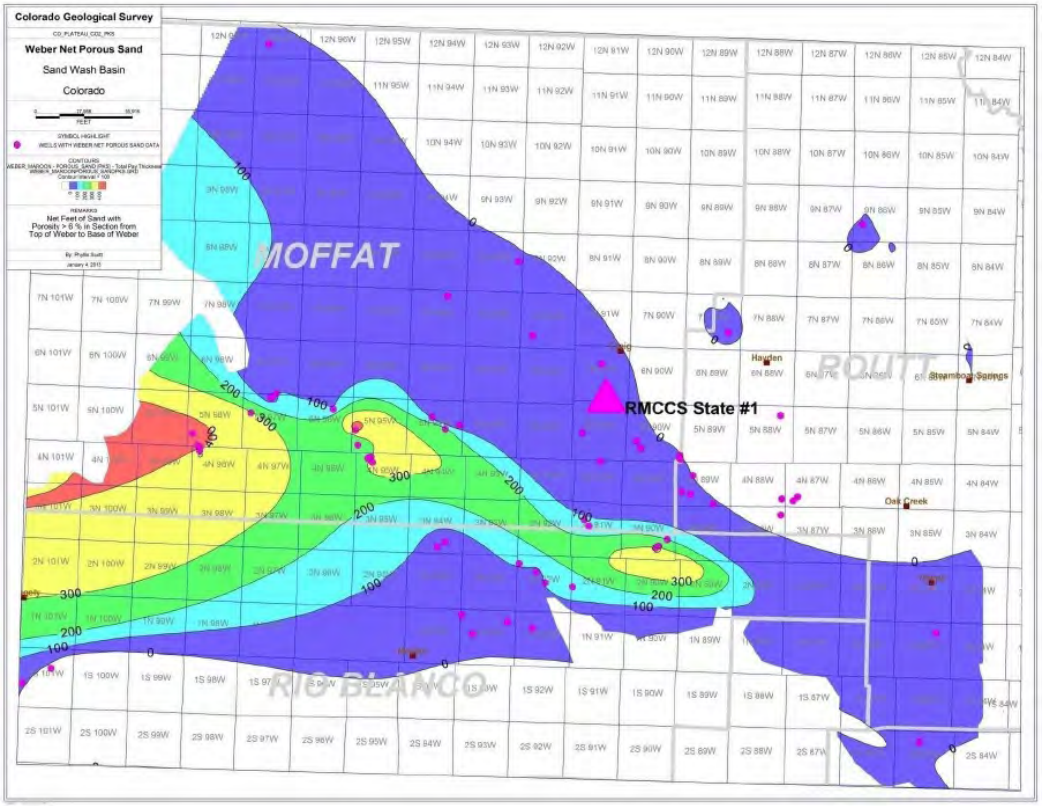

Figure 3.27. Net feet of sand (Φ >6 percent within the Weber saline aquifer). Contour interval is 100 feet.

2) Potential Pathway for Injected CO_2

Detailed mapping suggests:

- There are barriers to the updip migration of sequestered CO_2 to the south, west and east of the RMCCS State #1 well, as shown in Figure 3.28.
- At this scale of mapping there are no clear barriers to the southeast that would prevent injected CO_2 from traveling from the wellbore updip to the Dakota outcrop. Figure 3.29 shows this relationship in a cross sectional view.
- It is very possible that barriers exist either as faults that have not been identified or as permeability barriers. If an injection program is pursued, this potential pathway must be examined in greater detail.

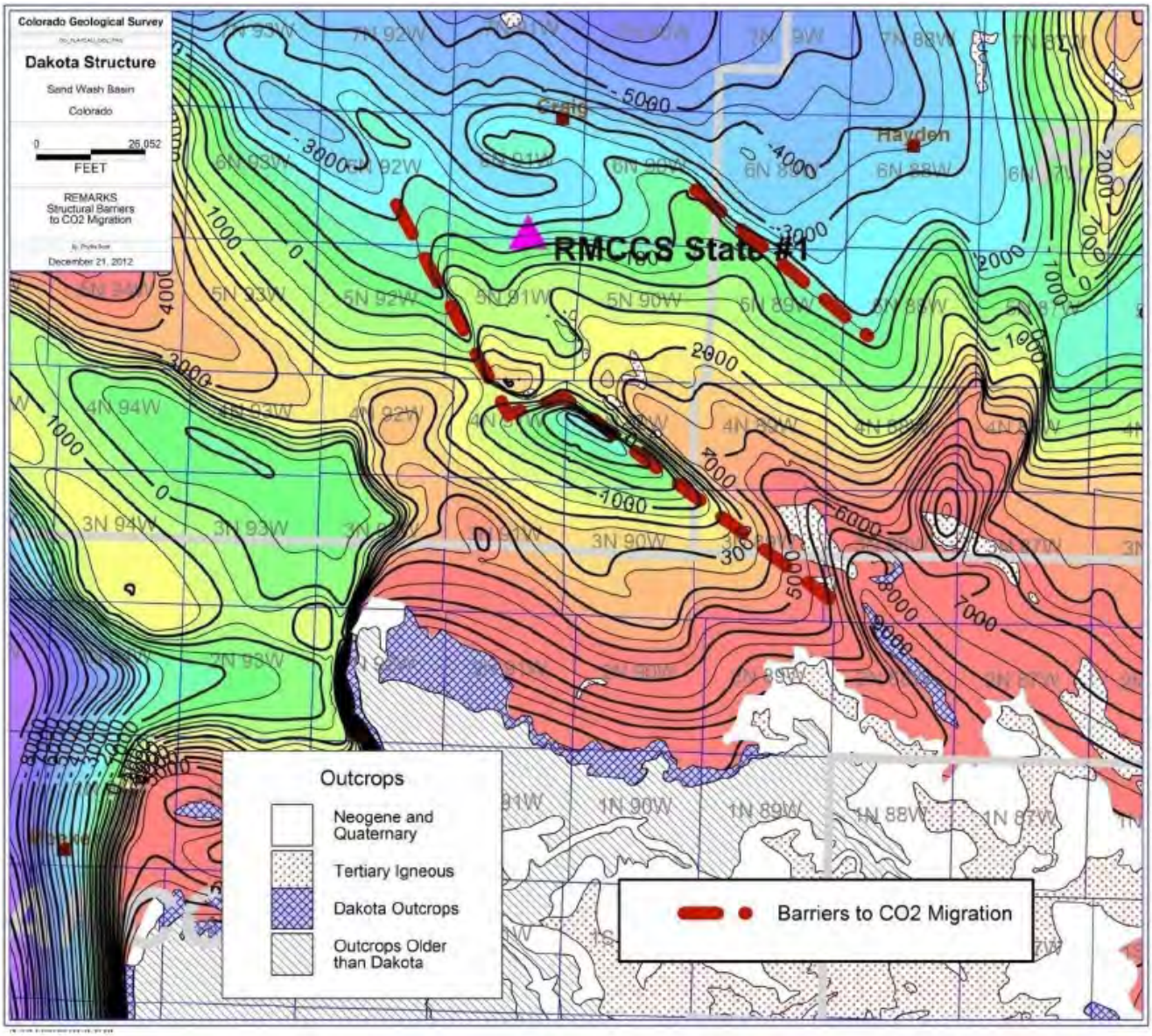

Figure 3.28. Barriers to CO_2 migration superimposed on Dakota structure map.

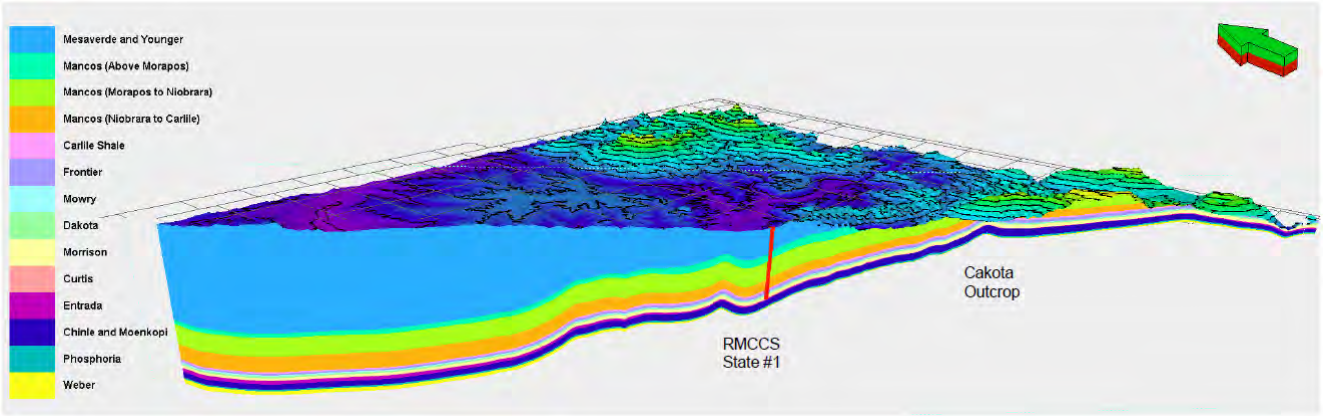

Figure 3.29. Northwest-Southeast cross section through RMCCS State #1 well site (red vertical line) showing possible pathway of migration through the Dakota to the surface. Small undulations in the structure may be sufficient to trap injected CO_2. Unknown fault or permeability barriers may exist.

Summary

Structure contour maps were created to depict the surfaces of fourteen formations in the Sand Wash Basin that will serve as the structural framework in a geocellular model that will be used to simulate sequestration of carbon dioxide into the Dakota, Entrada and Weber saline aquifers. Eight maps were created at that scale, three depicting the structural tops of the saline aquifers and also the Mancos seal, and three depicting thicknesses of the saline aquifers.

Published porosity and permeability data were collected for wells in the Sand Wash Basin. Average data from published field studies were tabulated to be used in estimates of storage capacity for sequestration. In addition, porosity-permeability crossplots were created for six Dakota cores and three Entrada cores. Average Dakota porosity was 13.7 percent and average permeability was 320 md for the six Dakota wells. Average Entrada porosity was 15 percent and average permeability was 47 md for the three wells.

Maps depicting the net feet of sand and the net feet of sand with porosities greater than six percent were created for the Dakota, Entrada and Weber saline aquifers in the Sand Wash Basin study area. These were made by identifying sand and porous sands on raster logs using Petra, then summing those properties for each of the aquifers and contouring the results. The Dakota shows a great deal of variability in the distribution of sand and porous sand because of the fluvial nature of much of the sand. The Entrada shows that both the net sand and net porous sand thickness increases to the west as the Navajo Sandstone (which is considered a part of the Entrada saline aquifer in this report) increases in thickness. The Weber saline aquifer was the most difficult to map because many wells only penetrated the topmost portion of the formation and also because the base of the Weber is hard to distinguish from the underlying Maroon Formation. For these maps, the base of the Weber was estimated from the tops of deeper formations reported by operators.

The thickest Weber sands and thickest porous sands are located to the west and decrease to the east. It is expected that the Weber would have thin sands and very little porosity at the location of the RMCCS State #1 well.

3.3 References Part I

Berman, A. E., Poleschook, D., Jr., Dimelow, T. E., 1980, Jurassic and Cretaceous Systems of Colorado, *in* Kent, H. C., and Porter, K. W., eds., Colorado Geology: Rocky Mountain Association of Geologists—1980 Symposium, p. 111-128.

Cain, Mary Reinarts, 1986, Depositional Environment of Upper Cretaceous Sandstones of the Lewis Shale, Sand Wash Basin, Colorado *in* Stone, D. S., ed., New Interpretations of Northwest Colorado Geology, Rocky Mountain Association of Geologists 1986 Symposium, p. 171-182.

Chapin, E. C., and Cather, S. M., 1983, Eocene Tectonics and Sedimentation in the Colorado Plateau--Rocky Mountain Area *in* Lowell, J. D., ed., Rocky Mountain Foreland Basins and Uplifts: Rocky Mountain Association of Geologists, p. 33-56.
Chronic, Halka, and Williams, Felicie, 2002, Roadside Geology of Colorado: Mountain Press Publishing Company, 398 p.

DeVoto, Richard H., 1980, Pennsylvanian Stratigraphy and History of Colorado, *in* Kent, H. C. and Porter, K. W., eds., Colorado Geology: Rocky Mountain Association of Geologists—1980 Symposium, p. 71-101.

Dubiel, Russell F., 1992, Sedimentology and Depositional History of the Upper Triassic Chinle Formation in the Uinta, Piceance, and Eagle Basins, Northwestern Colorado and Northeastern Utah: U. S. Geological Survey Bulletin 1787, 25p.

Finn, T. M., and Johnson, R. C., 2005, Niobrara Total Petroleum System in the Southwestern Wyoming Province, Chapter 6 of Petroleum Systems and Geologic Assessment of Oil and Gas in the Southwestern Wyoming Province, Wyoming, Colorado, and Utah: U. S. Geological Survey Digital Data Series DDS-69-D, 27 p.

Fryberger, S. G., and Koelmel, M. H., 1986, Rangely Field: Eolian System-Boundary Trap in the Permo-Pennsylvanian Weer Sandstone of Northwest Colorado, *in* Stone, D. S., ed., New Interpretations of Northwest Colorado Geology, Rocky Mountain Association of Geologists, p. 129-149.

Geldon, A. L., 1986, Hydrostratigraphic Characterization of Paleozoic Formations in Northwestern Colorado *in* Stone, D. S., ed., New Interpretations of Northwest Colorado Geology: Rocky Mountain Association of Geologists, p. 265-281.

Grammer, G. M., Eberli, G. P., Van Buchem, F. S. P., Stevenson, G. M., Homewood, P., 1996, Application of High-Resolution Sequence Stratigraphy to Evaluate Lateral Variabilityin Outcrop and Subsurface--Desert Creek and Ismay Intervals, Paradox Basin *in* Longman, M. W., and Sonnenfeld, M. D., Paleozoic Systems of the Rocky Mountain Region: The Rocky Mountain Section SEPM (Society for Sedimentary Geology), p.235-266.

Hasket, G. I., 1959, Niobrara Formation of northwest Colorado, *in* Haun, J. D., and Weimer, R. J., eds., Symposium on Cretaceous Rocks of Colorado and Adjacent Areas: Rocky Mountain Association of Geologists 11th Field Conference, p. 46-49.

Hettinger, R. D., and Kirschbaum, M. A., 2003, Stratigraphy of the Upper Cretaceous Mancos Shale (Upper Part) and Mesaverde Group in the Southern Part of the Uinta and Piceance Basins, Utah and Colorado: Chapter 12 of Petroleum Systems and Geologic Assessment of Oil and Gas in the Uinta-Piceance Province, Utah and Colorado: U. S. Geological Survey Digital Data Series DDS-69-B, Plate 2.

Irwin, Dennis, Chairman of the R.M.A.G. Research Committee, 1977, Subsurface Cross-Sections of Colorado: Rocky Mountain Association of Geologists Special Publication No. 2, 24 cross sections by a number of authors.

Johnson, R. C., 2003, Depositional Framework of the Upper Cretaceous Mancos Shale and the Lower Part of the Upper Cretaceous Mesaverde Group, Western Colorado and Eastern Utah, Chapter 10 of Petroleum Systems and Geologic Assessment of Oil and Gas in the Uinta-Piceance Province, Utah and Colorado: U. S. Geological Survey Digital Data Series DDS-69-B, Plate 1.

Johnson, Samuel Y., Chan, Marjorie A., and Konopka, Edith A., 1992, Pennsylvanian and Early Permian Paleogeography of the Unita-Piceance Basin Region, Northwestern Colorado and Northeastern Utah; U. S. Geological Survey bulletin 1787-CC, 35 p.

Kaiser, W. R., Scott, A. R., Hamilton, D. S., Tyler, Roger, McMurry, R. G., Zhou, N, Tremain, C. M., 1993, Geologic and Hydrologic Controls on Coalbed Methane: Sand Wash Basin, Colorado and Wyoming: Colorado Geological Survey Resource Series 30 and Bureau of Economic Geology Report of Investigations No. 220, 151 p.

Kent, Harry C., 1972 Review of Phanerozoic History, IN Mallory, W. W.; Mudge, M. R.; Swanson, V. E.; Lumb, W. E.; and Stone, D. S., eds., 1972, Geologic Atlas of the Rocky Mountain Region, Rocky Mountain Association of Geologists, 331 pp

Kirschbaum, M. A., 2003, Geologic Assessment of Undiscovered Oil and Gs Resources of the Mancos/Mowry Total Petroleum System, Uinta-Piceance Province, Utah and Colorado: Chapter 6 of Petroleum Systems and Geologic Assessment of Oil and Gas in the Unita-Piceance Province, Utah and Colorado: U. S. Geological Survey Digital Data Series DDS-69-B, Plate 4.

Kluth, C. F., 1986, Plate tectonics of the ancestral Rocky Mountains, *in* Peterson, J. A., ed., Paleotectonics and sedimentation in the Rocky Mountain region, United States: American Association of Petroleum Geologists Memoir 41, p. 353-370.

Kluth, C. F., and DuChene, H. F., 2009, Late Pennsylvanian and Early Permian Structural Geology and Tectonic History of the Paradox Basin and Uncompahgre Uplift, Colorado and Utah, *in* Houston, W. S., Wray, L. L., and Moreland, P. G., eds., The Paradox Basin Revisited--New Developments in Petroleum Systems and Basin Analysis, Rocky Mountain Association of Geologists 2009 Special Publication, p.178-197.

Koelmel, M. H., 1986, Post-Mississippian Paleotectonic, Stratigraphic, and Diagenetic History of the Weber Sandstone in the Rangely Field Area, Colorado *in* Peterson, J. A., ed., Paleotectonics and sedimentation in the Rocky Mountain region, United States: American Association of Petroleum Geologists Memoir 41, p. 371-396.

Molenaar,C. M., 1981, Mesozoic Stratigraphy of the Paradox Basin--An Overview, IN Wiegand, D. L., ed., Geology of the Paradox Basin: Rocky Mountain Association of Geologists, p. 119-127.

Mallory, W. W., 1972, Pennsylvanian Arkose and the Ancestral Rocky Mountains *in* Mallory, W. W.; Mudge, M. R.; Swanson, V. E.; Lumb, W. E.; and Stone, D. S., eds., Geologic Atlas of the Rocky Mountain Region, Rocky Mountain Association of Geologists, 331 pp.

Mallory, W. W.; Mudge, M. R.; Swanson, V. E.; Lumb, W. E.; and Stone, D. S., eds., 1972, Geologic Atlas of the Rocky Mountain Region, Rocky Mountain Association of Geologists, 331 pp.

Masoner, L. O., and Wackowski, R. K., 1995, Rangely Weber Sand Unit CO_2 Project Update; SPE Reservoir Engineering, p. 203-207.

National Energy Technology Laboratory, 2012, The United States 2012 Carbon Utilization and Storage Atlas, 4th Edition, U.S. Department of Energy, 130 p. http://www.netl.doe.gov/technologies/carbon_seq/refshelf/atlasIV/index.html

Oriel, S. S. and Craig, L. C.,1960, Lower Mesozoic Rocks in Colorado *in* Weimer, R. J., and Haun, J. D., eds., Guide to the Geology of Colorado, Geological Society of America, Rocky Mountain Association of Geologists, and Colorado Scientific Society, p. 43-58.

Peterson, J. A., and Hite, R. J., 1969, Pennsylvanian Evaporite-Carbonate Cycles and Their Relation to Petroleum Occurrence, Southern Rocky Mountains: American Association of Petroleum Geologists Bulletin V. 93, No. 4, p. 884-908.

Quigley, M. D., 1959, Correlation of the Dakota-Cedar Mountain-Morrison sequence along the Douglas arch: Rocky Mountain Association of Geologists, Guidebook to 11th Field Conference, pp. 33-36.

Stern, E. J., and Constenius, K. N., 1997, Space-Time Relationships Between Magmatism and Tectonism in the Western United States Between 120 Ma and 10 Ma: a Regional Context for the Front Range of Colorado *in* Bolyard, D. W., and Sonnenberg, S. A., eds., Geologic History of the Colorado Front Range: 1997 RMS-AAPG Field Trip #7, p. 85-100.

Stevenson, G. M., and Baars, D. L., 1988, Overview: Carbonate Reservoirs of the Paradox Basin *in* Goolsby, S. M., and Longman, M. W., eds., Occurrence and Petrophysical Properties of Carbonate Reservoirs in the Rocky Mountain Region: Rocky Mountain Association of Geologists, p. 149-162.

Stewart, J. H., Poole, F. G. and Wilson, R. F., 1972, Stratigraphy and origin of the Triassic Moenkopi Formation and related strata in the Colorado Plateau region: U. S. Geological Survey Professional Paper 691, 336 p.

Stone, D. S., 1986, Seismic and Borehole Evidence for Important Pre-Laramide Faulting Along the Axial Arch in Northwest Colorado, *in* Stone, D. S., ed, New Interpretations of Northwest Colorado Geology: Rocky Mountain Association of Geologists, p. 19-36.

Thyne, Geoffrey D; Tomasso, Mark; Bywater-Reyes, Sharon V; Budd, David A; Reyes, Brian M, Oct. 2010, Characterization of porosity and permeability for CO_2 sequestration models in the Mississippian Madison Group, Moxa Arch-LaBarge Platform, southwestern Wyoming:Contributions to Geology, vol. 45, no. 2, pp.133-150, Oct 2010.

Trudgill, B. D., and Paz, M., 2009, Restoration of Mountain Front and Salt Structures in the Northern Paradox Basin, SE Utah *in* Houston, W. S., Wray, L. L., and Moreland, P. G., The Paradox Basin Revisited--New Developments in Petroleum Systems and Basin Analysis: Rocky Mountain Association of Geologists, p. 132-177.

Tweto, Ogden, 1977, Tectonic History of West-Central Colorado *in* Veal, Harry K., ed., Exploration Frontiers of the Central and Southern Rockies: Rocky Mountain Association of Geologists 1977 Symposium, p. 11-18.

Tweto, Ogden, 1979, Geologic Map of Colorado: U. S. Geological Survey.

Part II: Storage capacity estimates, Sources of CO_2 and Significance (Denise Laes, Si-Yong Lee and Wade Zaluski)

3.4 Storage Capacity Estimation

3.3.4a Methodology

Storage capacity was estimated using the volumetric method (Atlas III; U.S. DOE 2010) using the following formula:

$$GCO_2 = A_t h_g \Phi_{tot} \rho E_{saline}$$

This formula generates the **CO_2 storage resource mass estimates** (GCO_2) based on combining data for the total area (A_t), gross formation thickness (h_g), total porosity (Φ_{tot}), CO_2 density (ρ) and the storage efficiency factor (E_{saline}). The first two input parameters account for the total bulk volume; the CO_2 density converts the reservoir volume of CO_2 to mass while the storage-efficiency factor reflects the fraction of the total pore volume that will be occupied by the injected CO_2.

3.3.4b Workflow

The technical workflow is attached as an appendix to this report. Deriving carbon storage capacity estimates for the Sand Wash Basin area required a few slight modifications to the regional workflow because the input parameters for the EGI storage capacity spreadsheet were not obtained from contour maps but were extracted from the geocellular model created for the basin. This corner point grid model was generated using stratigraphic information from deep wells within the basin and augmented with additional data such as seismic data. The modeling boundary was generated by approximating the 750m contour line below the Weber Formation referenced to the zero-meter elevation datum. This does not take the additional overlaying thickness between the zero meter elevation and the topographic surface elevation into account. Using this criterion to generate the modeling boundary caused a discrepancy on the eastern and southern edge of the basin between the spatial extent of the Sand Wash Basin model as delineated for modeling purposes and the one used for the regional capacity assessment.

From the 3D geocelluar model the cell porosity, volume, IJK cell indices, centroid XYZ coordinates, and distance from the top of the formation of interest to the topographic surface were extracted. Since Petrel uses a corner point grid to

structure the geocellular model, the thickness for each cell does not remain constant across the model. The average thickness for each cell, a parameter not explicitly stored in the geocellular model, was calculated by dividing the volume by the cell area. Unlike the thickness, each cell's footprint of 1000' by 1000' remains constant in the model. The storage capacity spreadsheet was populated with the required values either directly exported from the model or derived from it. The cell index numbers were concatenated to generate a unique cell-ID and the centroid XY coordinates were used to import the data into ArcGIS as a 2D feature class.

Compared to the regional storage capacity estimates for the regional Four-Corner region States, the porosity parameter was handled different for the capacity estimate based on the geocellular model. The regional assessment used a single constant porosity value for each of the three formations. For the geocellular model varying porosity values were assigned to each grid cells of the Dakota, Entrada and Weber Formations. This process involved taking porosity data from 20 existing wells within the simulation model boundary. Available data varied but several wells had density and sonic data available for porosity computation. Variogram analysis was conducted to understand the variation in porosity as a function of separation distance between wells. It was also used as means of determining directions/degree of anisotropy. Using the variogram results, Sequential Gaussian Simulation (SGS) was used to assign porosity values to each cell within the Dakota, Entrada and Weber Formations of the Sand Wash Basin. The minimum, mean and maximum values of the porosity, depth, thickness, pressure and CO_2 density parameters are summarized in Table 3.3. These ranges represent a depth cut-off set at 2500' below the ground surface using a geothermal gradient of 27°C/km.

Table 3.3. Sand Wash Basin geocellular model parameter ranges for the Dakota, Entrada and Weber at the 2500' depth constraint and a geothermal gradient of 27 °C/km)

Formation	Parameter	Min	Mean	Max
Dakota	Depth (ft)	2519	13332	22248
	Thickness (ft)	52	177	243
	Porosity (%)	1.65	6.37	14.34
	Pressure (psi)	1091	5773	9633
	CO2 density (kg/m3)	309	686	699
Entrada	Depth (ft)	2520	14087	23120
	Thickness (ft)	1	321	804
	Porosity (%)	1.63	4.68	13.64
	Pressure (psi)	1091	6100	10011
	CO2 density (kg/m3)	309	689	699
Weber	Depth (ft)	2502	15383	24765
	Thickness (ft)	1	316	836
	Porosity (%)	1.5	2.98	7.22
	Pressure (psi)	1083	6660	10723
	CO2 density (kg/m3)	306	692	700

3.3.4c Capacity Estimates based on geocellular model parameters

The capacity numbers were generated using two different temperature gradients. The lower gradient (27 °C/km) corresponds to the gradient of the grid cell of regional interpolated gradient in which the characterization well drilled was located. The input data for the regional interpolation came from deep well data. The higher gradient of 31 °C/km was obtained from bottom hole temperature measured at the completion of the DOE/NETL funded characterization well drilled in the Sand Wash Basin (169 °F at 9745' deep). Assigning one or the other of these two constant geothermal gradients to all the cells records provided two different carbon storage capacity estimates (Table 3.4). The capacity numbers of the Weber Formation carry a higher degree of uncertainty because the formation is so deep that the basal stratigraphic boundary was not penetrated in several of the wells from which data were extracted for the model. Drilling of the NETL/DOE funded characterization well near Craig was terminated at a depth of 9745' before the top of the Weber was reached. The volumes in the table were calculated at cut-off depths of 2500' and 3000'. The 2500' depth is based on the average depth that is required for CO_2 to stay in supercritical condition. The 3000' is included because it is the cut-off depth used for all the other carbon-storage capacity estimate data generated for the southwest

region. The volumes estimated based on two different cut-off depths do not differ much whether 2500' or a 3000' cut-off is used because most of the formations occur much deeper in the subsurface. The capacity estimates generated by applying the two different geothermal gradients result in a nearly 10% capacity difference.

Table 3.4: Sand Wash Basin CO_2 storage capacity estimates based on the geocellular model parameters with two different constant geothermal gradients

			CO_2 Storage Capacity Estimates (million metric Tonnes)				
Formation	Geothermal gradient (°C/km)	Depth cut-off	Low Efficiency (0.51%)	Medium Efficiency (2%)	High Efficiency (5.4%)	area (km^2)	area (mi^2)
Dakota	27	2500'	98.956	388.063	1,047.770	8,272	3,194
		3000'	98.900	387.845	1,047.180	8,262	3,190
	31	2500'	89.105	349.433	943.469	8,272	3,194
		3000'	89.055	349.235	942.934	8,262	3,190
Entrada	27	2500'	135.858	532.777	1,438.497	8,213	3,171
		3000'	135.825	532.647	1,438.147	8,211	3,170
	31	2500'	123.260	483.373	1,305.107	8,213	3,171
		3000'	123.230	483.254	1,304.786	8,211	3,170
Weber	27	2500'	82.493	323.502	873.456	8,252	3,186
		3000'	82.433	323.266	872.817	8,246	3,184
	31	2500'	75.064	294.370	794.800	8,252	3,186
		3000'	75.009	294.153	794.214	8,246	3,184
Cummulative Totals	27	2500'	317.307	1,244.341	3,359.722		
		3000'	317.158	1,243.757	3,358.144		
	31	2500'	287.430	1,127.177	3,043.376		
		3000'	287.294	1,126.643	3,041.935		

3.3.4d Capacity Estimates of the NATCARB Carbon Sequestration Atlas transformed data

Making the geocellular capacity data compatible with the DOE/NETL carbon sequestration NATCARB Atlas structure required more than a few adjustments to the input parameters. The geocellular model was set up with a different geographic projection than the DOE's NATCARB atlas projection. The model-extracted data were converted from UTM zone 13 to Lambert Azimuthal Equal Area after importing them into ArcGIS. To be able to nest the geocellular derived data into the NATCARB 10 km^2 polygons, the parameters extracted from the model were rasterized to a cell size that could be exactly scaled up to 10-km^2 cells based on the Lambert Azimuth Equal Area projection. After the data were transformed in the GIS

database, the spatial varying geothermal gradient, prepared for the regional carbon storage capacity estimates, could be applied the geocellular model derived data. The interpolated geothermal gradient ranges between 10 °C/km and 50 °C/km within the Sand Wash Basin. The capacity estimates were only calculated at a depth greater than 3000' because these data needed to be integrated with the NATCARB Atlas data for the Southwest region and the Southwest region data represent the storage capacity below 3000'. The scale difference was accounted for by applying an area correction factor calculated based on the total number of data points were available with the larger polygons.

The estimates, shown in Table 3.5, indicate slightly higher numbers compared to the estimates derived from the geocellular model. The less than 1% difference in area between the two estimates can be explained by changing the projection and by summarizing the data at a smaller scale. The differences in capacity estimates are due to applying a geothermal gradient that was location dependent at the smaller scale compared to the two different but constant geothermal gradients applied to the parameters extracted from the geocellular model.

Table 3.5. Sand Wash Basin CO_2 storage capacity estimates calculated for records below 3000' deep after converting the geocellular model derived data to the required NATCARB atlas required Lambert Azimuthal Equal area projection using a spatial dependent geothermal gradient.

			CO_2 Storage Capacity Estimates (million metric Tonnes)			
Formation	# of 1 km cells	# of 250 m points	Low Efficiency (0.51%)	Medium Efficiency (2%)	High Efficiency (5.4%)	Adjusted area (km^2)
Dakota	8446	131860	102.093	400.363	1,080.980	8,241
Entrada	8420	131528	144.380	566.196	1,528.730	8,221
Weber	8462	131865	86.810	340.431	919.163	8,242
		Total Σ:	333.282	1,306.990	3,528.873	

3.5 Local Sources of CO_2

There are two coal-fired power plants located in the Sand Wash Basin, one located in the town of Craig (Moffat County) and the other in Hayden (Routt County), approximately 25 km (22 mi) east of Craig (Figure 2.1). The EPA reported 2010 combined annual CO_2-emissions totaling 13.5 million metric tonnes for the two plants (EPA 2010). Their combined reported CO_2-emissions for 2011 totaled 12.2 million metric tonnes (EPA 2011) (Table 3.6).

Table 3.6. EPA reported CO_2-emmisions of power plants in the Sand Wash Basin

		EPA GHGRP CO_2-emissions (metric tonnes per year)	
Power Plant	County	2010	2011
Craig	Moffat	9,749,564.6	9,149,964.0
Hayden	Routt	3,736,507.7	3,083,527.0
	Total:	**13,486,072.3**	**12,233,491.0**

3.6 Significance

Based on the capacity estimates calculated from the geocellular model parameters, the deep saline formations of the Sand Wash Basin have the potential to store 21 years of the CO_2 emission from both power plants at the lowest efficiency factor (0.51% efficiency with a 31°C/km geothermal gradient storing the CO_2 at depth greater than 3000'). The number of years goes up to nearly 290 years when considering higher 5.4% efficiency factors and the spatial dependent geothermal gradient (Table 3.7).

Table 3.7. Years of potential CO_2-emission storage in the Sand Wash Basin comparing the different carbon storage estimates at the three efficiency factors to two years of total CO_2-emissions.

	CO2 storage capacity estimates (million metric Tonnes)			Years of Capacity @13.5 MMt CO2 emissions			Years of Capacity @ 12.2 MMt CO2 emissions		
gradient	low	medium	high	low	medium	high	low	medium	high
27 °C/km	317.43	1244.82	3361.01	24	92	249	26	102	275
31°C/km	287.55	1127.63	3044.60	21	84	226	24	92	250
Spatial dependent	333.28	1306.99	3528.87	25	97	261	27	107	289

3.7 References Part II

Bachu S., Bonijoly D., Bradshaw J. Burruss R., Holloway S., Christensen N.P., and Mathiassen O.M. 2007, CO_2 storage capacity estimation: methodology and gaps. International Journal of Greenhouse Gas Control. 1, 430-443.

U.S. Department of Energy, National Energy Technology Laboratory, NATCARB, 2012 Carbon Sequestration Atlas of the Unites States and Canada – Third Edition (Atlas III).

U.S. Department of Energy, National Energy Technology Laboratory, NATCARB, 2012 Carbon Sequestration Atlas of the Unites States and Canada – Forth Edition (Atlas IV).
[http://www.netl.doe.gov/technologies/carbon_seq/refshelf/atlasIV/index.html accessed 16 July 2013]

U.S. Environmental Protection Agency 2010 Greenhouse Gas Reporting Program: 2010 data sets [http://epa.gov/ghgreporting/ghgdata/2010data.html accessed 27 September 2013]

U.S. Environmental Protection Agency 2011 Greenhouse Gas Reporting Program: 2011 data sets [http://epa.gov/ghgreporting/ghgdata/2011data.html [accessed 27 September 2013]

Young, G. B. C.; Lintz, V. A.; Widmann, B. L.; Bird, D. A.; and Cappa, J. A., 2007, CO_2 Sequestration Potential of Colorado: Colorado Geological Survey Resource Series 45.

Appendix 3.A: Data Sources for Published Tops

Published cross sections were used to locate as many formation tops as possible. Tops from the published cross sections were manually entered into the Petra project and their sources were noted as "PUB" and used as a framework for the regional correlations. The published cross sections included:

- Irwin (1972) chaired a committee of the Rocky Mountain Association of Geologists that published 22 cross sections in the state of Colorado. Cross Sections 7, 10, 11, 12, 13, 14, 15,16, 17, 20, and 21 covered the Colorado study area. The tops shown on the cross sections extended from the Wasatch to the Precambrian.

- Hasket (1959) correlated the Niobrara in the Sand Wash Basin.

- Finn and Johnson (2005) refined the cross section of Hasket (1959) by correlating the benches of the Niobrara (Buck Peak, Tow Creek and Wolf Mountain).

- The intertonguing relationship between the Mesaverde and Mancos was illustrated by Hettinger and Kirschbaum (2002) in an east-west cross section through the Uinta and Piceance basins.

- Johnson (2002) made a detailed north-south cross section of the Mancos in the Piceance Basin starting from the base of the Mesaverde and extending to the top of the Dakota Sandstone.

- Kirschbaum (2002) made a north-south cross section along the Colorado-Utah state line correlating the basal Mancos through the Mowry, Dakota and Cedar Mountain.

- Quigley (1959) correlated the Dakota and Cedar Mountain along the Douglas Creek Arch.

- Kaiser, et al (1993) included many cross sections through the Lewis and Mesaverde in the deeper portion of the Sand Wash Basin.

In addition, the IHS database that provided well data for this project included tops that had been reported by operators. These were posted on well logs during the correlation process. They were considered, but were often inconsistent and were not used if they disagreed with the published cross sections or my correlations.

4. Utah: Woodside preliminary CO_2 storage site selection (Craig Morgan, UGS)

4.1 Preliminary Site Selection For CO_2 Storage

The Utah Geological Survey (UGS) compiled a list of potential sites with basic reservoir information about the three primary target reservoirs, Cretaceous Dakota Sandstone, Jurassic Entrada Sandstone, and Pennsylvanian Weber Sandstone, along with any other potential saline aquifers in stacked sequence at each site. The area for each site was defined using geologic maps; the depth, thickness, and porosity of the target reservoirs were defined from published reports or from a representative well log. Pressure and temperature, used to calculate CO_2 density, were calculated from standard pressure and geothermal gradients. Storage capacity was calculated using the storage capacity equation: Area (ft^2) * thickness (ft) * porosity * CO_2 density (lbs/ft^3) * 0.04 (efficiency) = lbs/metric ton.

Minimum qualifications for a potential CO_2 storage site are:

1. must have at least one of the primary reservoir targets,
2. potential reservoirs must be at least 2500-foot (750 m) drill depth,
3. must have minimum storage capacity of 30 million metric tonnes (MMT),
4. must be a saline aquifer with 10,000 TDS or more, and
5. must be within the Colorado Plateau.

Eight Utah sites were evaluated; four sites did not meet one or more of the minimum qualifications. The top two sites were the Bonanza site in Uintah County and the Woodside site in Emery County (Figure 4.1). Both sites were selected for more detailed evaluation.

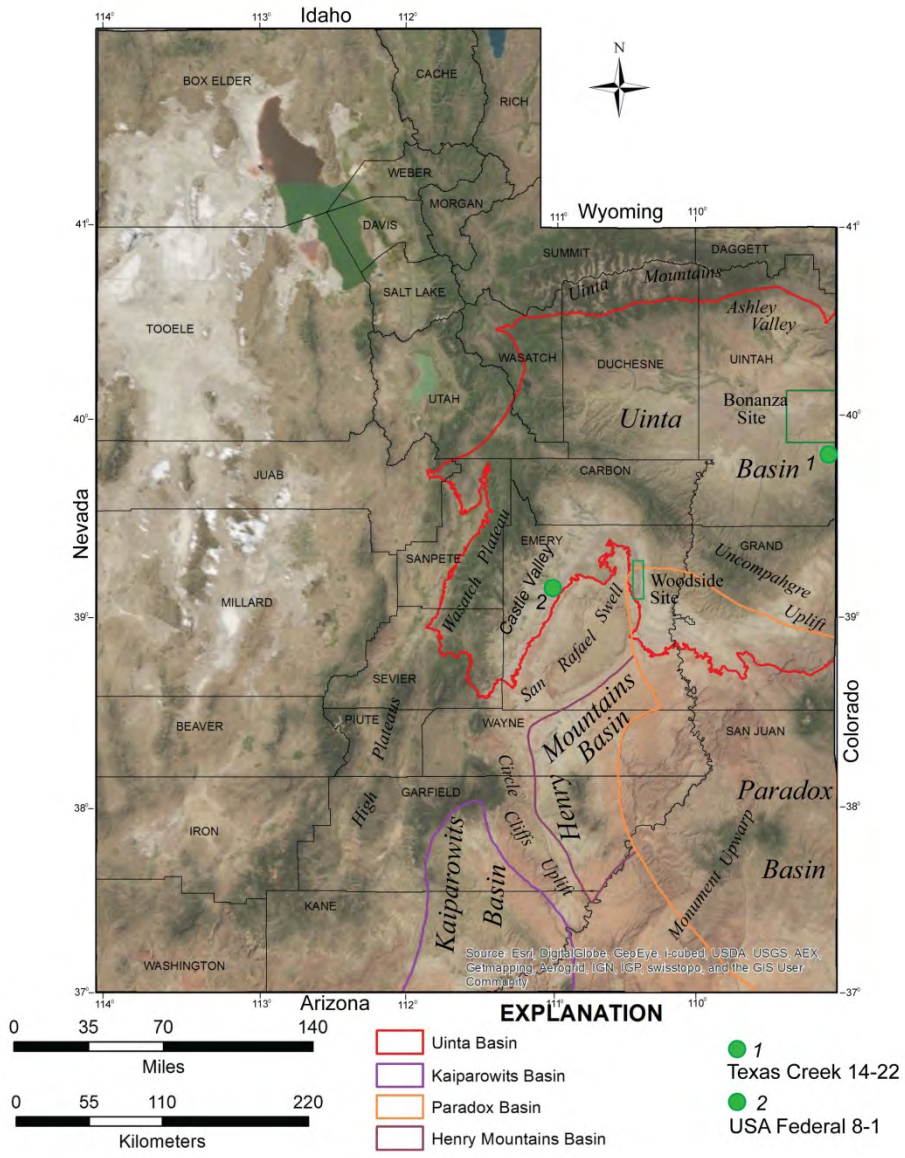

Figure 4.1. Map of Utah showing basins and uplifts of the Colorado Plateau. Bonanza and Woodside areas (rectangular outlines), were evaluated as potential storage sites. Well 1 has a Weber Sandstone (?) core and 2 has a White Rim core.

4.2 Woodside Dome Storage Site

4.2.1 Reason for Selecting the Woodside Site

Woodside Dome was ranked number two during the preliminary site evaluation. The Cretaceous Dakota Sandstone crops out along the flanks of Woodside Dome, the Jurassic Entrada and Navajo Sandstones are too shallow for consideration at this location but have regional significance. The Permian White Rim Sandstone (age equivalent to the upper Weber Sandstone) along with the deeper Mississippian Redwall Limestone combined had sufficient storage capacity to meet the minimum capacity required for consideration as a potential commercial storage site.
The Pennsylvanian Hermosa Group has storage potential but was beyond the scope of this study. Woodside Dome has easy access, is a double plunging anticline (Figure 4.2) with potentially well-defined traps for the reservoirs. A few deep wells have been drilled along the crest of the anticline providing some subsurface reservoir and seal data. Woodside is near undeveloped coal beds and a potential site for a new power plant. It is close enough to the power plants in the Castle Valley area to the west that a CO_2 pipeline could be constructed.

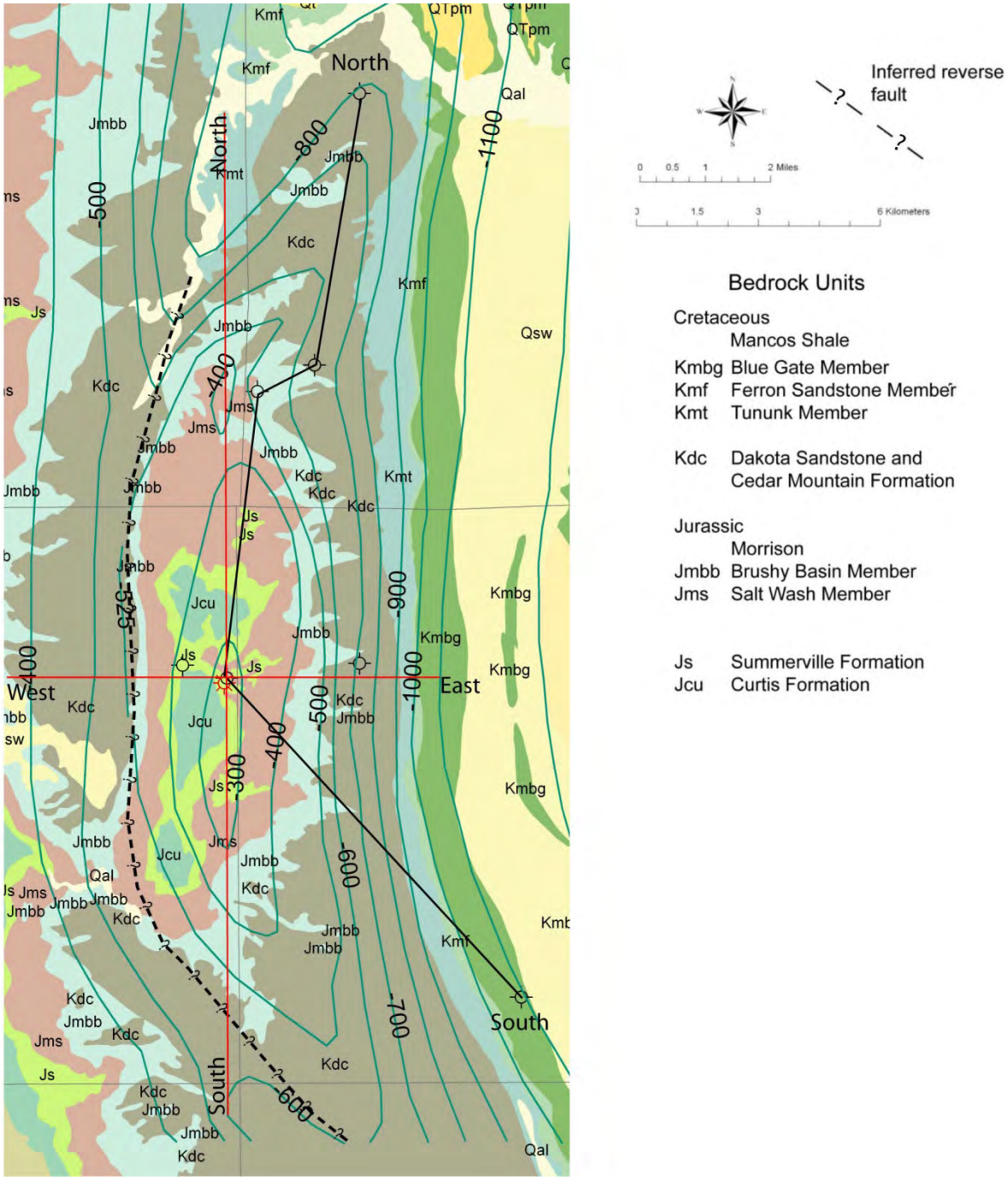

Figure 4.2. Structure contour map on the top of the Mississippian Redwall Limestone. Contour interval is 100 meters, mean sea-level datum. See Figure 1 for location of Woodside Dome. Geologic map of Woodside Dome anticline in Emery County, Utah, was clipped from Witkind (2004). See Witkind (2004) for map details. Oldest formation exposed along the crest of the anticline is the Jurassic Curtis Formation (Jcu). See Figure 3 for west-to-east and south-to-north structural cross sections (red lines), and Figure 4 for Redwall Limestone well log cross section (black line).

4.2.2 Methods

South-to-north and west-to-east cross sections (Figure 4.3) were constructed using formation contacts from the geologic map, formation strikes and dips collected from the outcrop, and well data. Well logs in the Woodside area were digitized in an LAS format so wells could be more easily correlated and reservoir porosity calculated. A well database was developed in Excel® containing well locations, name, unique API number, and drill depths of all formations penetrated. The structural elevations along the cross sections and elevations from the well database were used to construct structure contour maps of the tops of the Redwall Limestone, White Rim Sandstone, and Permian Black Box Dolomite. The structure data were gridded in ArcMap® and subtracted from a digital elevation model (DEM) grid to get overburden maps, or drill depth grids of the top of each reservoir. The structure, overburden, porosity, pressure, and temperature data for each reservoir were imported into the EGI storage capacity spreadsheet and the CO_2 storage capacity was calculated for 0.51%, 2.0%, and 5.4% efficiency.

There are no usable outcrops of the Redwall Limestone near Woodside so only well data were available. Seven wells have been drilled at Woodside but only one penetrated a complete section of the Redwall (Figure 4.4). Porosity logs were digitized and the data were used to determine porosity range, average porosity, and net thickness of the reservoir, defined as having 4% or more porosity.

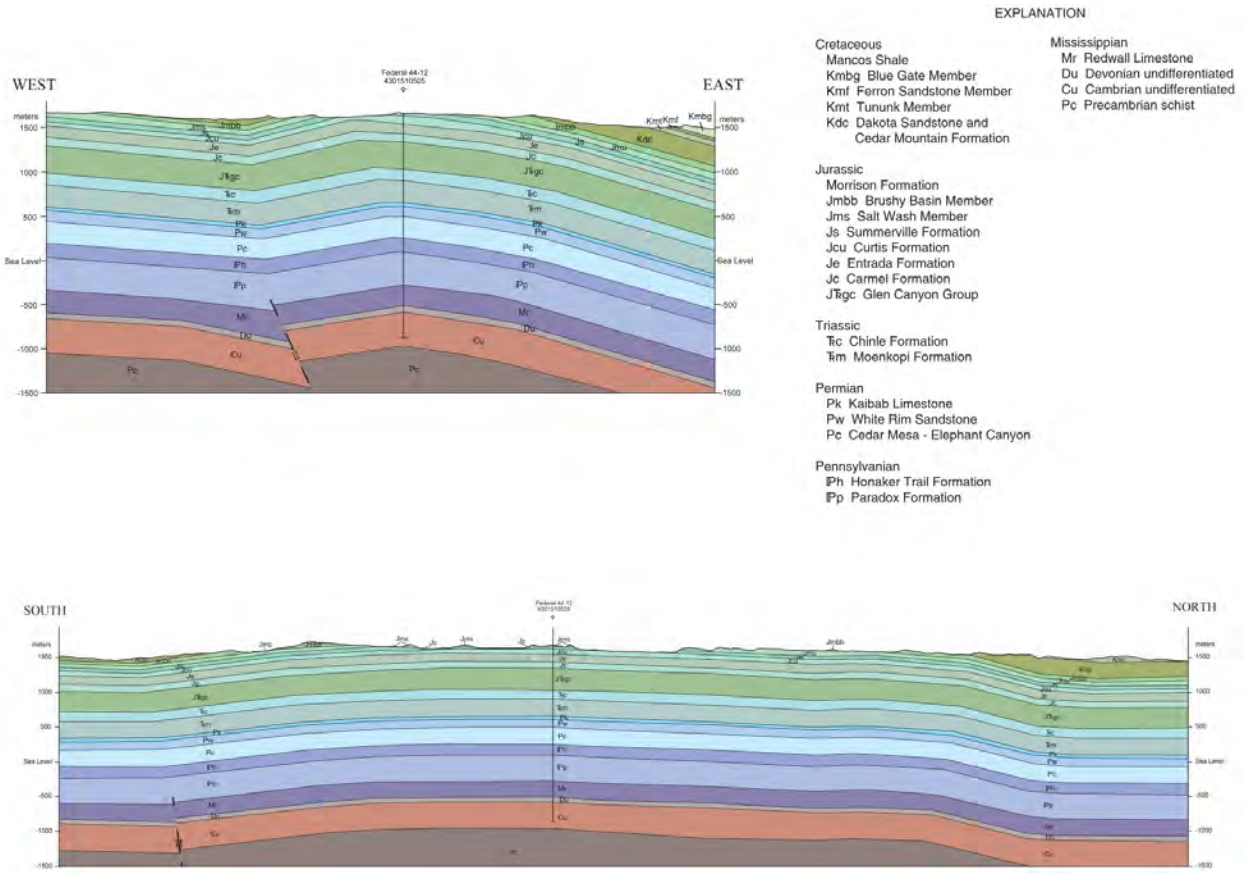

Figure 4.3. West-to-east and south-to-north cross sections of Woodside anticline based on surface geology and limited well control. Depth and horizontal distance are in meters, no vertical exaggeration. See Figure 4.2 for location of cross sections. We used Kaibab Limestone (Pk) on the cross sections for the equivalent Black Box Dolomite. From Morgan and others, 2013.

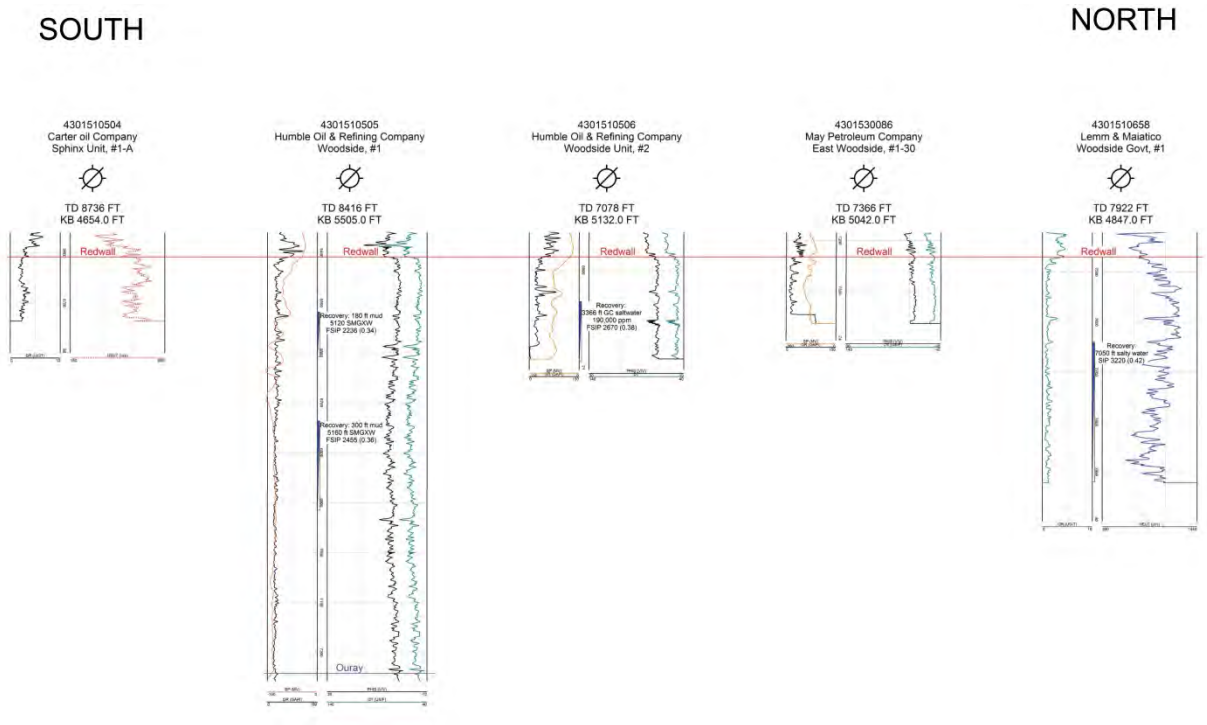

Figure 4.4. South-to-north well log cross section of the Mississippian Redwall Limestone at Woodside Dome. The deepest penetration is the Woodside 1 well which drilled 830 feet (253 m) of Redwall encountering 347 feet (106 m) of 4% or more porosity. See Figure 4.2 for location of cross section.

The Black Box Dolomite (Kaibab Formation) and White Rim Sandstone are exposed in many areas of the San Rafael Swell (SRS) within miles of the Woodside Dome. The UGS contracted with Professor Thomas Morris of Brigham Young University to investigate the Black Box and White Rim reservoirs in outcrop and in the wells at Woodside Dome (Harston and Morris, 2013). Walter Harston a graduate student under Professor Morris measured, described, sampled, and collected gamma-ray data over several exposures of the Black Box and a nearly complete section of White Rim in Black Box Canyon of the San Rafael River. Thin sections were used for detailed petrographic descriptions of the two formations. Plug samples (90) were used to determine porosity and permeability of various facies within the Black Box and White Rim. Gamma-ray data collected every meter from the outcrop were used to generate synthetic log curves that could be correlated to geophysical well logs at Woodside.

4.3 Geologic Characterization

4.3.1 Mississippian Redwall Limestone

Strikes and dips were collected from the outcrops at Woodside and added to the geologic map of Witkind (2004). Using the geologic map and well log correlations, two cross sections were constructed: one north to south, and one west to east (Figure 4.3).

The structural elevations along the cross sections and elevations from the well database were used to construct a structure contour map (Figure 4.2) and overburden map of the top of the Redwall Limestone. The area of structural closure was determined from the mapping, average reservoir thickness, porosity, pressure and temperature, were determined from the well logs and tests (Table 4.1). We used the EGI storage capacity spreadsheet to calculate the CO_2 storage capacity for 0.51%, 2.0%, and 5.4% efficiency (Table 4.2). The calculated storage capacity is significantly less than originally estimated (Table 4.3). We originally calculated an area of 40 miles^2 (100 km^2) based on the surface geologic map of the Woodside anticline but the area of closure at depth may only be 12-17 miles^2 (30-45 km^2). The area of closure is poorly constrained, so we used a very conservative estimation; the area could be much larger.

Table 4.1. Parameters used to calculate the CO_2 storage capacity of the Redwall Limestone, White Rim Sandstone, and Black Box Dolomite at Woodside. Ft = feet, m = meters, km^2 = kilometers squared, F = degrees Fahrenheit, C = degrees Celsius, psi = pounds per square inch, and kpal = kiloPascals.

	Area	Average Depth	Reservoir Thickness	Average Porosity in percent (%)	Temperature	Pressure
Redwall	16.6 miles^2 43 km^2	6749 ft 2058 m	345 ft 105 m	5%	141 F 61 C	2835 psi 19,544 kPal
White Rim	11.9 miles^2 31 km^2	3445 ft 1050 m	420 ft 128 m	15%	98 F 38 C	1447 psi 9977 kPal
Black Box	13.5 miles^2 35 km^2	3422 ft 1043 m	75 ft 23 m	16%	98 F 38 C	1437 psi 9911 kPal

Table 4.2. CO_2 storage capacity of the Redwall Limestone, White Rim Sandstone, and Black Box Dolomite at Woodside using three efficiency factors.

CO_2 Storage Capacity in Million Metric Tonnes			
	Efficiency Factors		
	0.5%	2.0%	5.4%
Redwall	0.8	3.2	8.8
White Rim	2.0	7.9	21.4
Black Box	0.4	1.5	4.1
Total	***3.2***	***12.6***	***34.3***

Table 4.3. Comparison of the preliminary and (final) parameters and resulting storage capacity calculations at an efficiency factor of 5.4%. Black Box Dolomite was not originally evaluated as a potential storage reservoir. The parameter that had the largest change in the final characterization was the area. Diff = difference between preliminary and (final) capacity calculations.

Preliminary (Final) Parameters and Storage Capacity							
	Area ($miles^2$)	Thickness (feet)	Porosity in percent (%)	Temperature (F)	Pressure (psi)	Capacity (MMT) 5.4%	Diff %
Redwall	40 (16.6)	700 (345)	4% (5%)	120 (141)	1300 (2835)	35.3 (8.8)	25%
White Rim	40 (11.9)	450 (420)	7% (15%)	95 (98)	2900 (1447)	36.7 (21.4)	58%
Total						72 (30.2)	42%

4.3.2 Permian Black Box Dolomite and White Rim Sandstone

Outcrops of the Permian White Rim Sandstone and Black Box Dolomite in the northern SRS, Emery County, Utah were studied (Figure 4.5) by Walter Harston and Thomas Morris at Brigham Young University under a contract with UGS (Harston and Morris, 2013). The outcrop data were then applied to interpretation of the well data at Woodside.

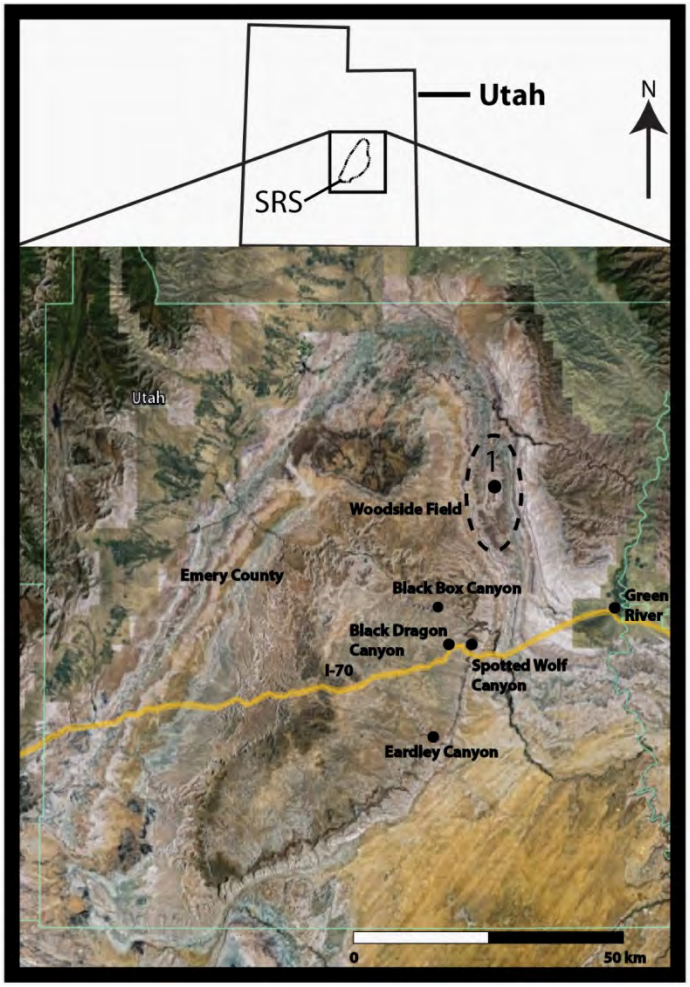

Figure 4.5. Location map of the SRS and Woodside Dome area in central Utah. A stratigraphic section of the White Rim, Black Box, and lower portion of the Moenkopi was measured, described, and sampled at Black Box Canyon (Figure 4.6). Additional stratigraphic sections of the upper portion of the White Rim and Black Box were described from the Spotted Wolf Canyon and Black Dragon Canyon areas (Figures 4.15 and 4.16). Location 1 in the Woodside field is the Bill Barrett Corporation Woodside 1 well. From Hartson and Morris unpublished contract report, Google Earth Pro licensed to Dr. Morris.

Black Box Canyon is the nearest outcrop to the Woodside Dome study site that has a nearly complete section of Permian White Rim Sandstone. More than 490 feet (150 meters) of White Rim were measured and described at Black Box Canyon (Figure 4.6). Three primary facies were identified in the White Rim: a basal sand sheet facies (Figure 4.7), an eolian dune facies (Figure 4.8) that makes up the majority of the formation, and a reworked upper transitional facies (Figure 4.9). Point count analyses of thin sections identified all three facies as quartz arenites from a

continental block provenance (Figures 4.10, 4.11, and 4.12). The eolian dune facies and most samples of the transitional facies exhibit good reservoir quality with porosities generally above 15% and permeabilities above 100 millidarcies (mD) (Figure 4.13). The sand sheet facies generally has porosities from 7% to 12% with permeabilities ranging from 0.1 mD to 20 mD.

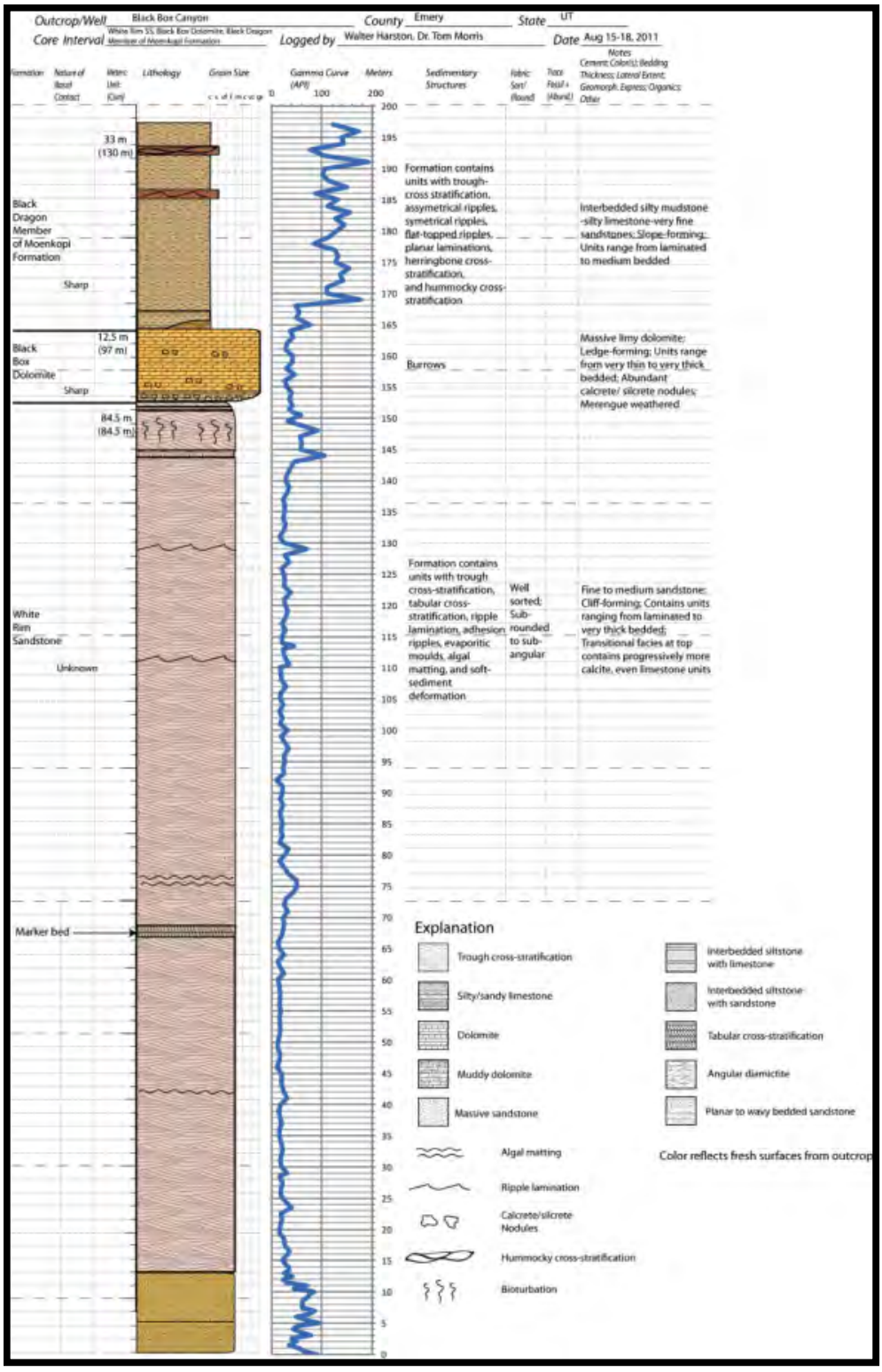

Figure 4.6. Stratigraphic measured section from Black Box Canyon. The base of the White Rim is not exposed but the section is believed to represent a nearly complete section.

A

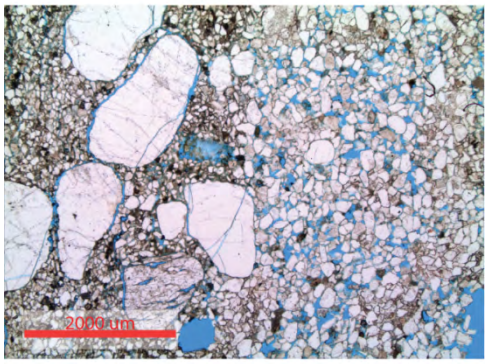

B

Figure 4.7. Basal sand sheet facies of the erg margin: A) Outcrop photograph of low angle foresets terminating into very coarse lags observed at Black Box Canyon. B) Photomicrograph of sand sheet facies at Black Box Canyon.

A

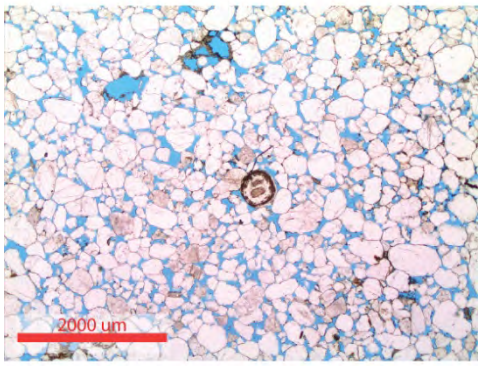

B

Figure 4.8. Trough cross-stratified sandstone beds of the eolian dune facies of the erg proper. A) Outcrop photograph of medium- to high-angle foresets at Black Box Canyon. Foreset angles are highlighted with yellow bars. B) Photomicrograph of trough cross-stratified sandstone from Black Dragon Canyon East. Note the sub-rounded to rounded grains and the chertified ooid in the center.

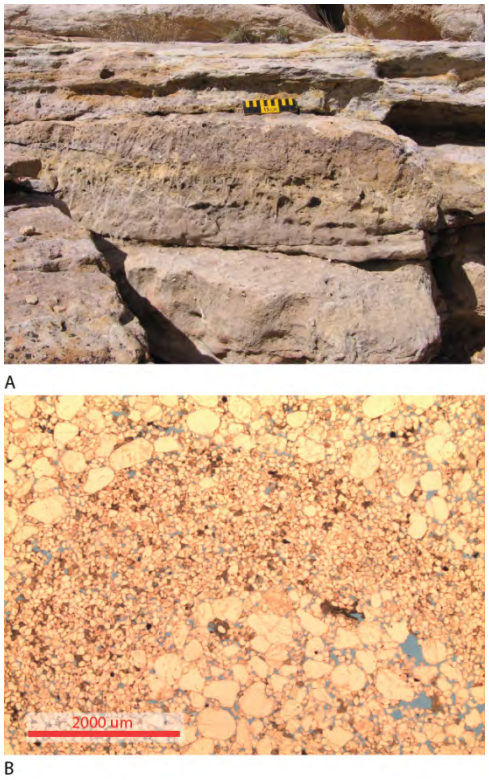

Figure 4.9. Bioturbated bed in the reworked upper transitional facies. A) Outcrop photograph of bioturbated bed at Black Box Canyon. Note faint vertical burrows of the Skolithos trace fossil assemblage. B) Photomicrograph of a bioturbated bed from Black Dragon Canyon West.

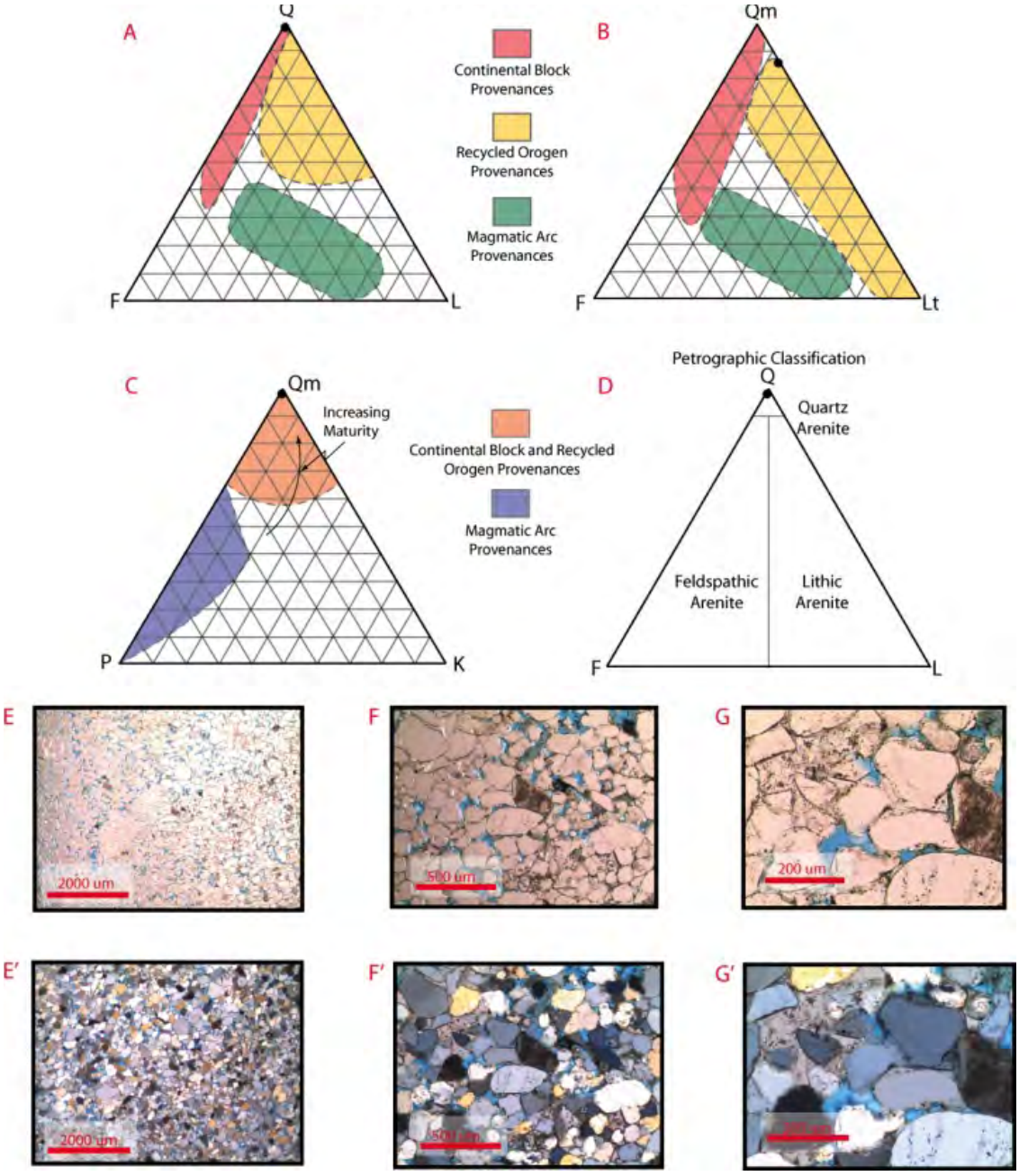

Figure 4.10. Photomicrographs and ternary diagrams of the sand sheet facies of the White Rim Sandstone (WRS). Photomicrographs are of one thin section at different magnification. E, F, and G are in transmitted light and E', F', and G' were taken in cross-polarized light. Q = quartz, F = feldspar, L = lithics, Qm = monocrystalline quartz, K = potassium feldspar, P = plagioclase, Lt = lithics including all forms of quartz other than monocrystalline.

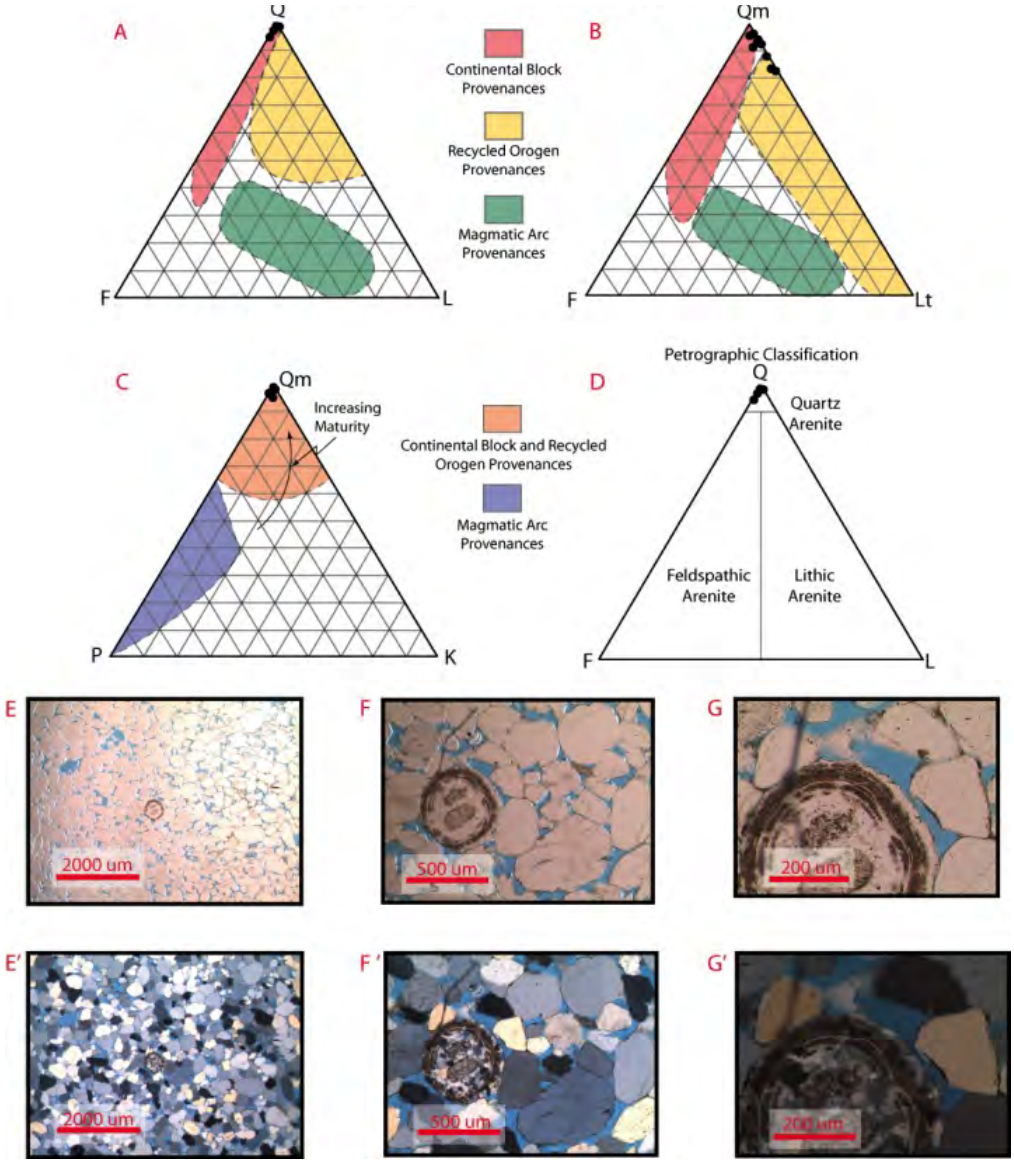

Figure 4.11. Photomicrographs and ternary diagrams of the eolian dune facies of the WRS. Photomicrographs are of one thin section at different magnification. E, F, and G are in transmitted light and E', F', and G' were taken in cross-polarized light. Q = quartz, F = feldspar, L = lithics, Qm = monocrystalline quartz, K = potassium feldspar, P = plagioclase, Lt = lithics including all forms of quartz other than monocrystalline.

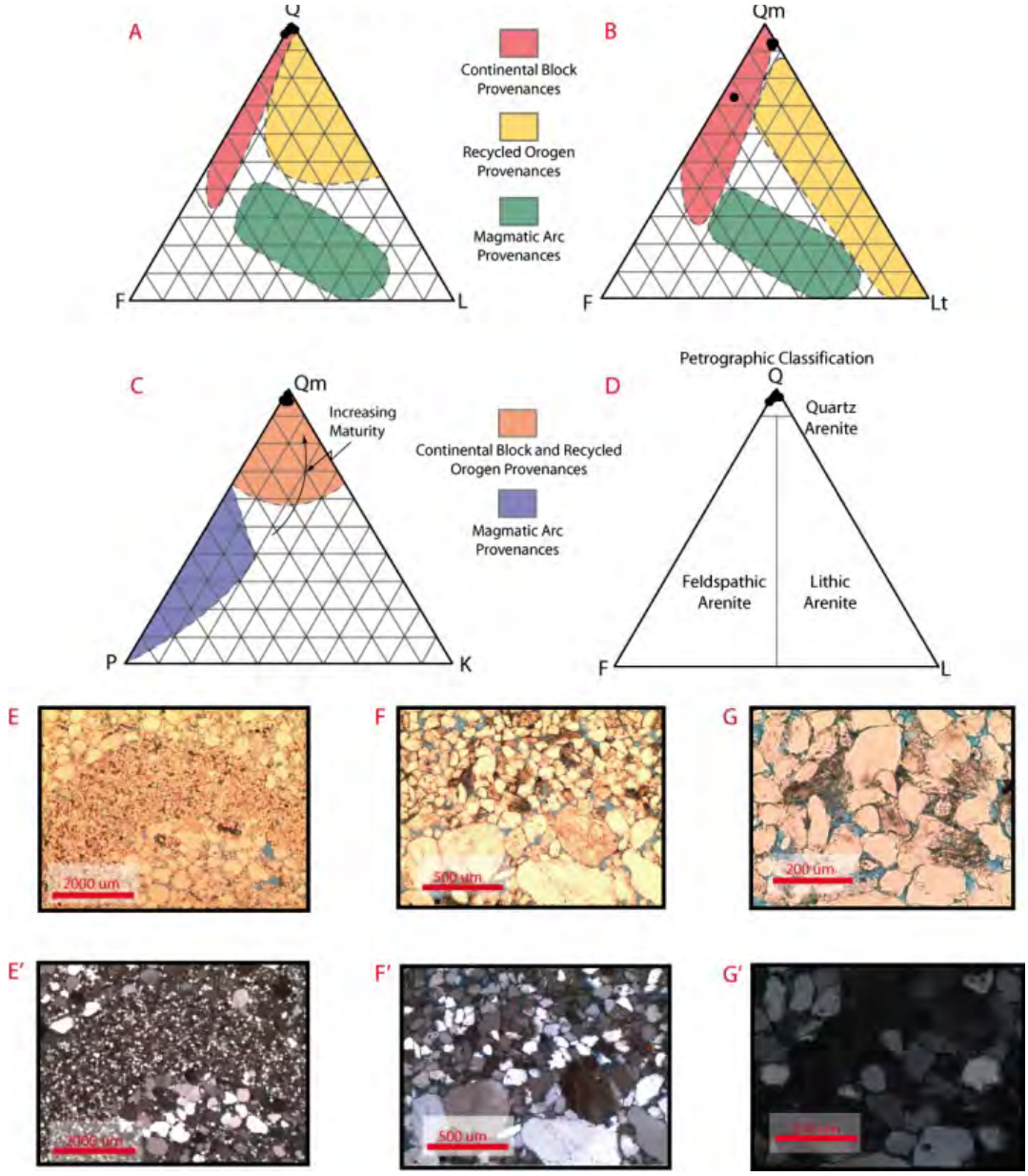

Figure 4.12. Photomicrographs and ternary diagrams of the transitional facies of the WRS. Photomicrographs are of one thin section at different magnification. E, F, and G are in transmitted light and E', F', and G' are taken in cross-polarized light. Q = quartz, F = feldspar, L = lithics, Qm = monocrystalline quartz, K = potassium feldspar, P = plagioclase, Lt = lithics including all forms of quartz other than monocrystalline.

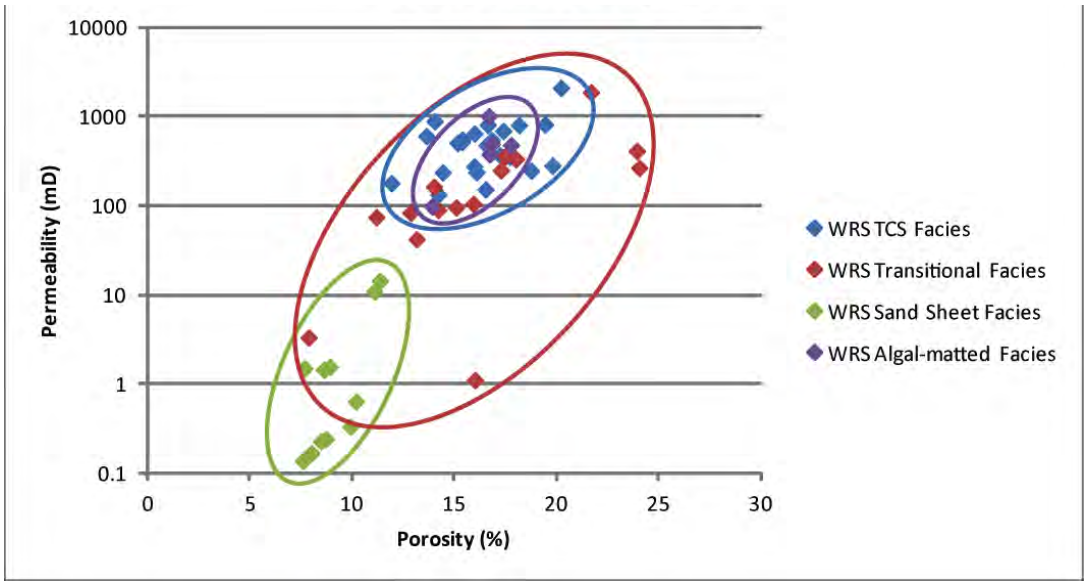

Figure 4.13. Porosity (%) and permeability (mD) cross plot of core plugs collected from the White Rim Sandstone outcrop. TCS is the trough cross-stratified eolian dune facies, and the algal-matted facies are interdunal deposits in the eolian dune facies. The eolian dune facies has the best reservoir properties, the transitional facies has the most heterogeneous reservoir properties, and the sand sheet facies has the lowest quality reservoir properties.

The Black Box Dolomite and overlying lower Moenkopi Formation were described at Black Box Canyon (Figures 4.5 and 4.6). The basal caliche zone (Figure 4.14) of the Black Box is a seal for the White Rim reservoir. The overlying sandy dolomite, massive dolomite, and sandstone facies have good reservoir properties; as a result, the Black Box can be considered both a seal and reservoir. Several stratigraphic sections of the Black Box were described in the Spotted Wolf Canyon and Black Dragon Canyon areas (Figure 4.5) to understand the heterogeneity within the formation (Figures 4.15 and 4.16). The thickness of the Black Box is highly variable and the unit is absent in many parts of the SRS, placing Moenkopi on White Rim. The Black Box is divided into four facies: (1) basal caliche facies, (2) massive dolomite facies comprising most of the formation, (3) sandstone facies, and (4) sandy dolomite facies. The basal caliche is the only facies that does not have good reservoir qualities (Figure 4.17).

Figure 4.14. Black Box caliche facies forms the light-colored receding exposure overlain by the more resistant massive dolomite facies at Black Box Canyon.

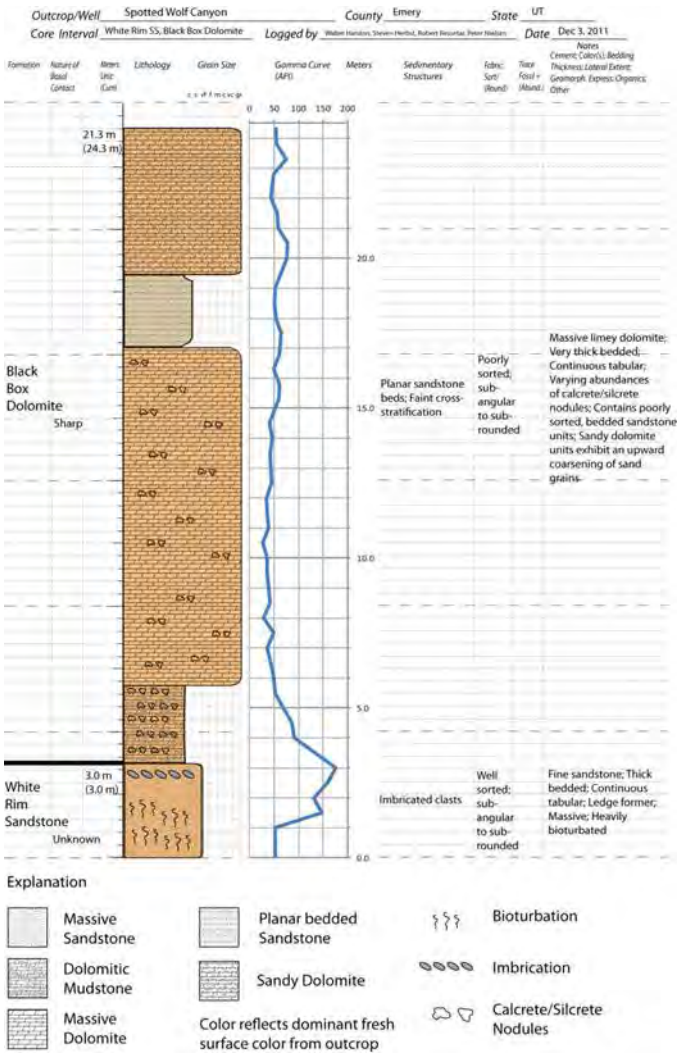

Figure 4.15. Stratigraphic measured section and gamma-ray curve of the Black Box and underlying transitional facies of the White Rim at Spotted Wolf Canyon.

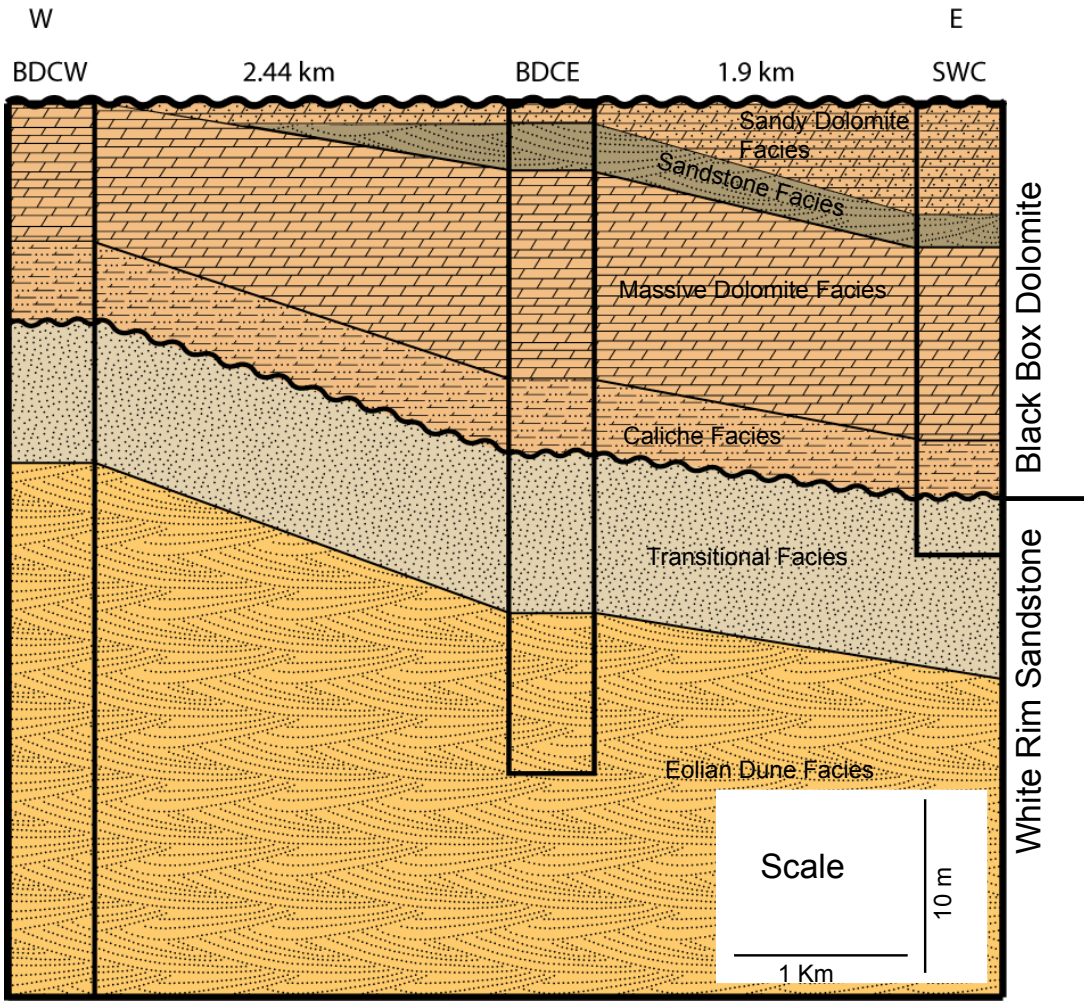

Figure 4.16. West-to-east cross section of the Black Box and upper portion of the White Rim. There is significant heterogeneity within the Black Box and thinning over the White Rim. BDCW = Black Dragon Canyon West, BDCE = Black Dragon Canyon East, and SWC = Spotted Wolf Canyon.

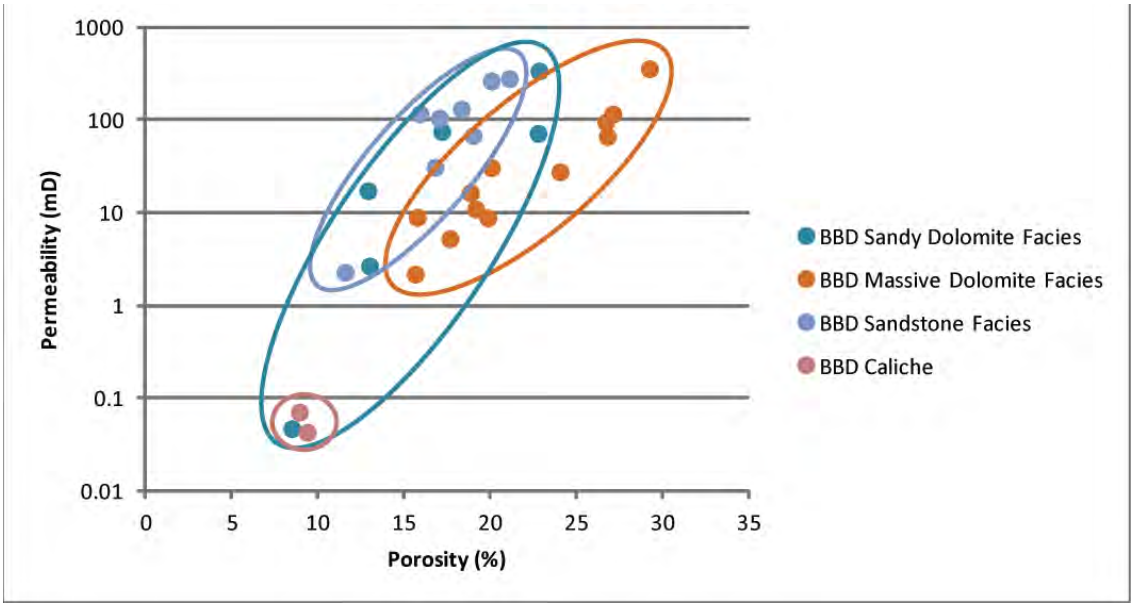

Figure 4.17. Porosity (%) and permeability (mD) cross plot of outcrop core plug samples of the Black Box Dolomite (BBD). The caliche is the only facies with poor reservoir properties.

There is good correlation of the gamma-ray curve from the Black Box Canyon stratigraphic section to the geophysical well log of the most recent well (Bill Barrett Corporation, Woodside 1) drilled at Woodside Dome (Figures 4.5 and 4.18). The surface gamma-ray curve and detailed lithologic descriptions were very helpful in defining formation boundaries in the geophysical well logs.

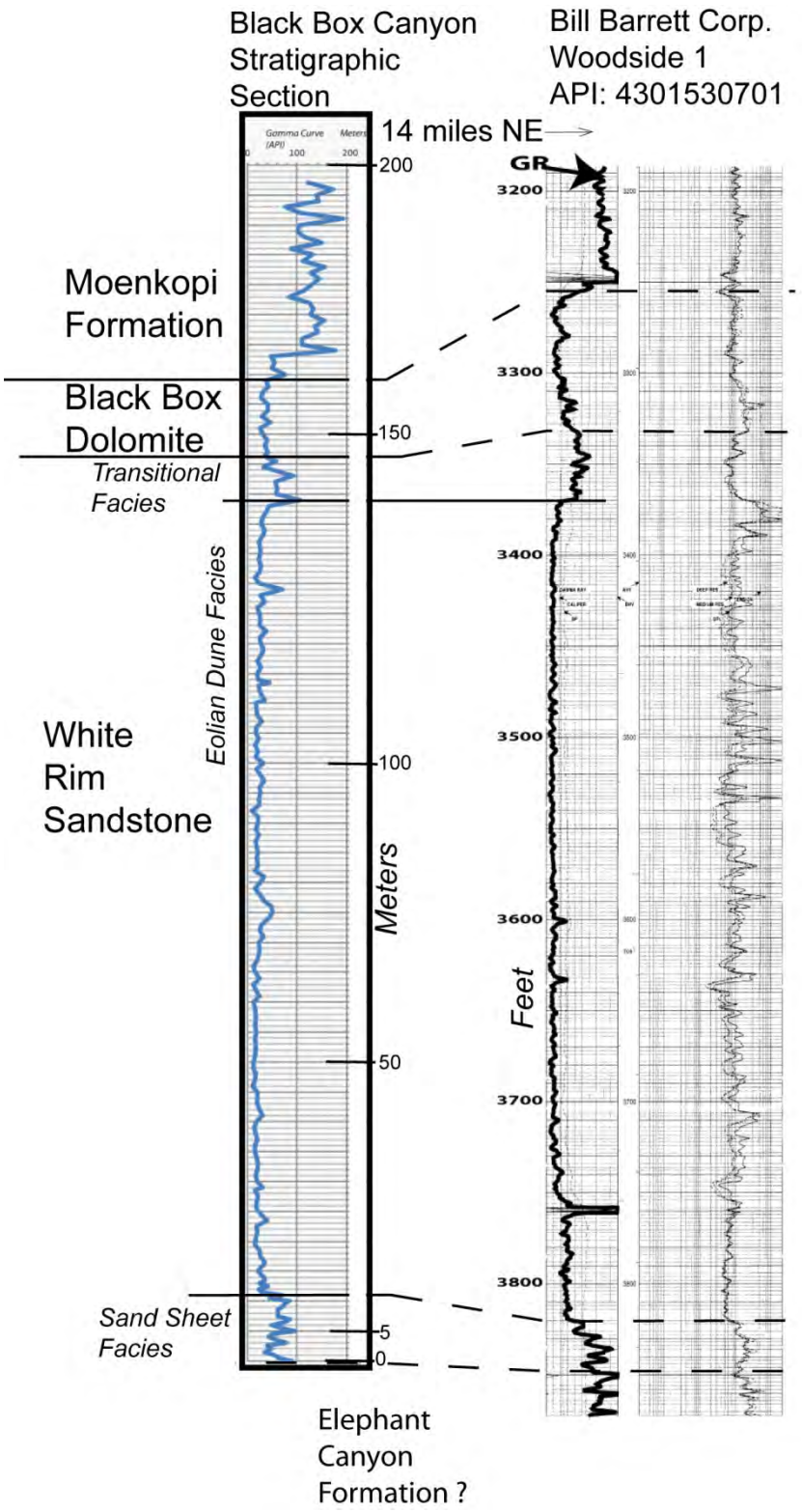

Figure 4.18. Preliminary correlation of gamma-ray curves from the Black Box Canyon measured section and the Woodside 1 well (Figure 4.5) drilled by Bill Barrett Corporation on the crest of the Woodside Dome.

A thickness map of the White Rim Sandstone was constructed from the well data (Figure 4.19). The structural elevations along the cross sections and elevations from the well database were used to construct structure contour maps and overburden maps of the top of the White Rim and Black Box Dolomite (Figure 4.20). The area of structural closure was determined from the mapping; average reservoir thickness, porosity, pressure and temperature, were determined from the well logs and tests (Table 4.1). The White Rim and Black Box data were imported into the EGI storage capacity spreadsheet and the CO_2 storage capacity was calculated for 0.51%, 2.0%, and 5.4% efficiency (Table 4.2).

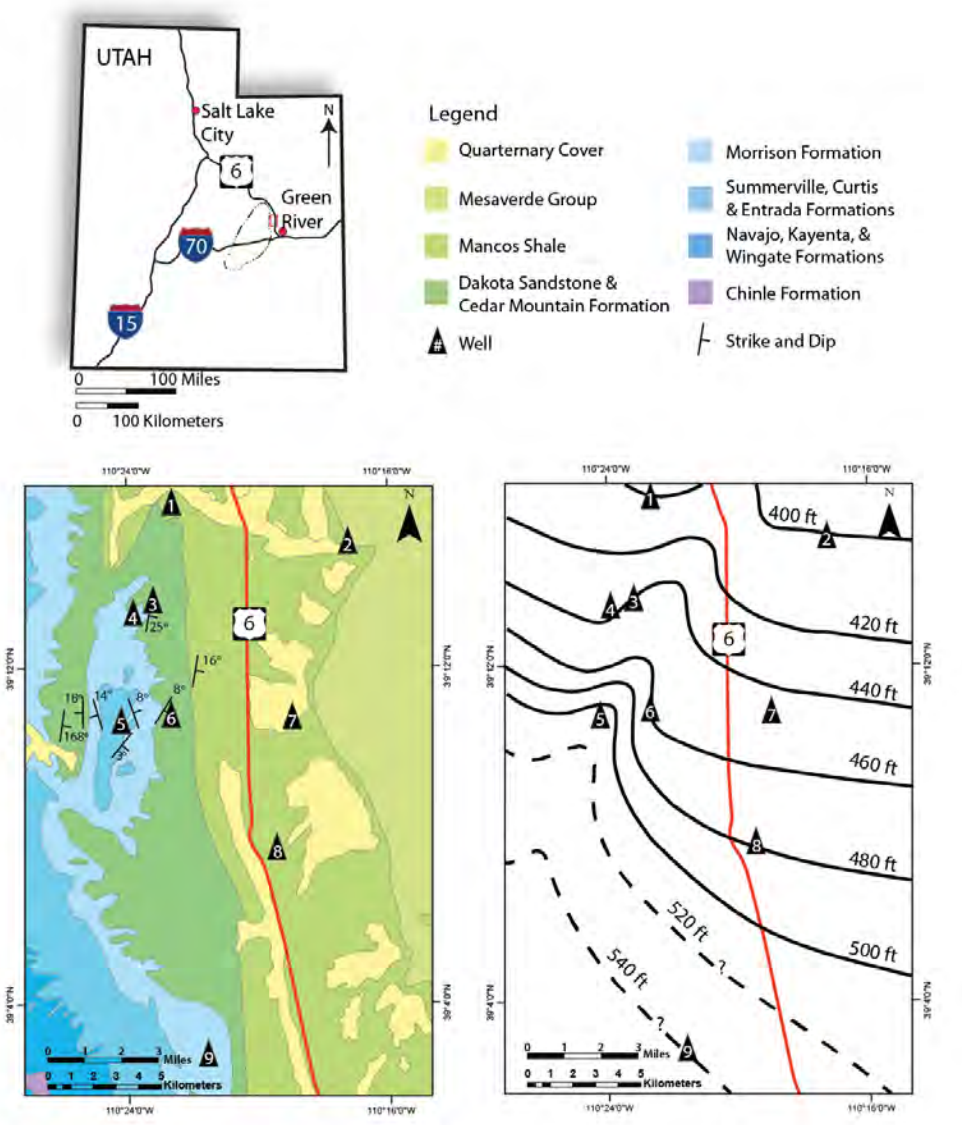

Figure 4.19. Surficial geologic map with strike and dip information and isopach map of the White Rim Sandstone at Woodside Dome. Thicknesses from subsurface well data were corrected according to the dip of the strata. The exact dip of inclined strata is not known at Well #9, but the well appears to be near the crest so we assumed flat lying strata. The White Rim thins to the north and appears to have a northeast-southwest trending paleotopographic high. From Harston and Morris, 2013.

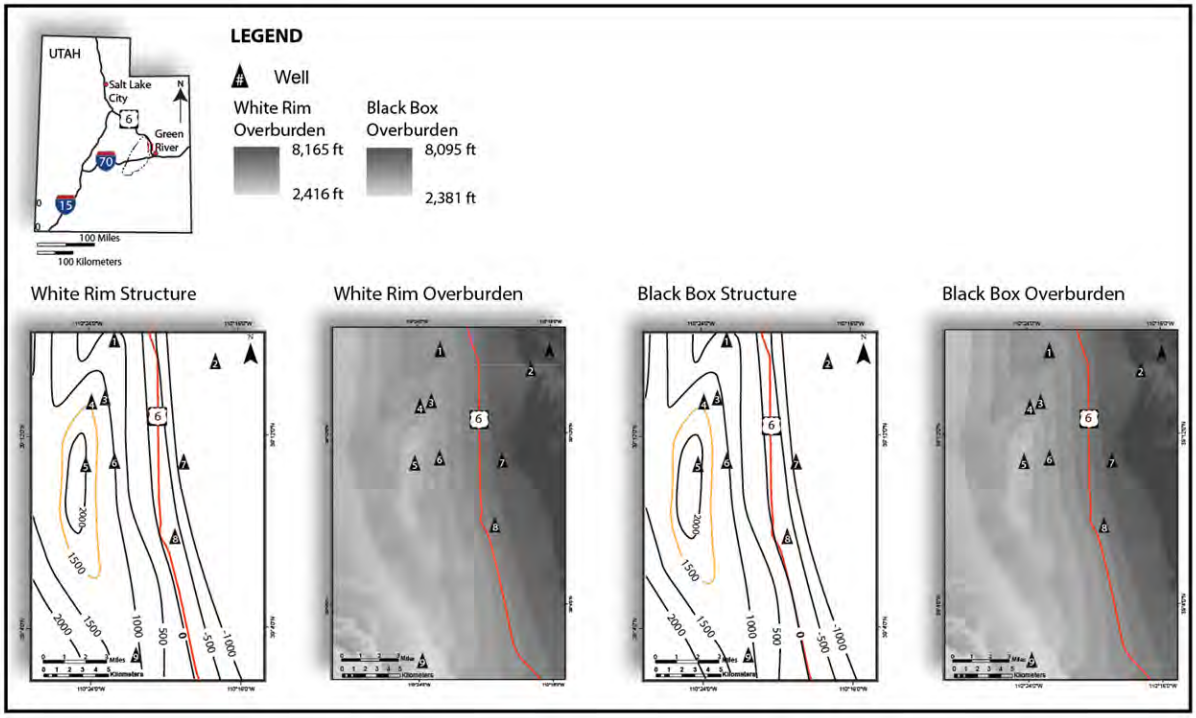

Figure 4.20. Structure and overburden maps for the top of the White Rim Sandstone and Black Box Dolomite. From Harston and Morris, 2013.

4.4 Summary and Recommendations

Woodside is a well-defined anticline (at the surface) on public lands with good access. The Entrada and Navajo Sandstones are very shallow at Woodside but are regionally significant as potential CO_2 storage reservoirs. Potential storage reservoirs at Woodside include Black Box Dolomite, White Rim Sandstone, Redwall Limestone, and numerous beds in the Pennsylvanian Hermosa Group, which were not evaluated.

The Woodside Dome study site has the potential for 3.2 to 34.3 MMT of CO_2 storage capacity in the Redwall Limestone, White Rim Sandstone, and Black Box Dolomite. The White Rim has the most storage capacity. The Redwall has low storage capacity due to the low porosity (5%), which is based on the sonic log from one well that penetrated the entire formation. Coring the Redwall at Woodside would provide much better porosity data and much needed permeability data. If the actual porosity is more than the log indicates, the CO_2 storage capacity would greatly increase.

The calculated CO_2 storage capacity at Woodside is much less than originally estimated. The parameter having the most effect is the area of closure; originally we estimated 40 miles^2 (100 km^2) based on the surficial extent of the anticline but we mapped a more conservative areal extent of the subsurface reservoirs [12-17 miles^2 (30-45 km^2)]. Structural closure of the deeper reservoirs is controlled by a blind reverse fault. Seismic data could show the fault has greater throw and length than we mapped; this would greatly increase the CO_2 storage capacity of all the reservoirs.

The Woodside site should be further evaluated, including acquisition of seismic data, and coring the Entrada, Navajo, Black Box, White Rim, and Redwall reservoirs. The knowledge gained will increase our understanding of the CO_2 storage capacity of Woodside and the regional storage potential of these reservoirs.

4.3 References

Harston, W.A., and Morris, T.H., 2013, Facies analysis of the Permian White Rim Sandstone, Black Box Dolomite, and Black Dragon Member of the Triassic Moenkopi Formation for CO_2 sequestration at Woodside field, San Rafael Swell, Utah, Part I, *in* Morris, T.H., and Ressetar, R., editors, The San Rafael Swell and Henry Mountains basin—geologic centerpiece of Utah: Utah Geological Association Publication 42, in press.

Hintze, L.F., 1974, Geologic map of Utah: modified by Willis, G.C., 2005, scale 1: 2,500,000, pdf map available at http://geology.utah.gov/maps/geomap/statemap/index.htm.

Morgan, C.D., Carney, S., and Nielsen, P., 2013, Recent characterization of Gordon Creek, Farnham Dome, and Woodside fields, Carbon and Emery Counties, Utah, *in* Morris, T.H., and Ressetar, R., editors, The San Rafael Swell and Henry Mountains basin—geologic centerpiece of Utah: Utah Geological Association Publication 42, in press.

Witkind, I.J., 2004, Geologic map of the Huntington 30' X 60' quadrangle, Carbon, Emery, Grand, and Uintah Counties, Utah: Utah Geological Survey Open-File Report 440 DM, Scale 1:100,000.

5. New Mexico: San Juan Basin Site Specific Carbon Storage Capacity Estimations (Dana Ulmer-Scholle – NMBGMR)

5.1 Introduction

The search for reservoirs with accompanying tight seals that occur between 3,000 and 13,000 feet, have total dissolved solids of greater that 10,000 μg/l and a capacity in excess of 500K BOEs is particularly attractive in New Mexico because of its long history of oil and gas production in the San Juan Basins. The size of many of the fields in this basin makes them prospective sequestration targets. In addition, there is the potential for deep saline aquifers to provide additional sequestration opportunities. In addition, there are several large power plants that could take advantage of identified sequestration reservoirs.

Within the San Juan Basin, several horizons were selected as possible sequestration targets: Dakota Group, Entrada Formation, Hermosa Group (equivalent to the Weber) and the Leadville Limestone. They are locally thick, porous and deep enough to be possible CO_2 sequestration targets. Associated seals for each of the units exist, but ultimately, the thick sequence of shales and siltstones of the Mancos Shale is an excellent upper seal for all the units in the basin.

5.2 CO_2 Sources for injection within the San Juan Basin

Within the San Juan Basin area, possible sources of CO_2 emissions were identified. They were the San Juan Generating Plant, Four Corners Generating Plant, Escalante Generating Plant, San Juan Gas Plant, Lybrook Gas Plant and the Giant Refinery. Of these sites, the San Juan and Four Corners Generating Plants were considered the most likely candidates for CO_2 sequestration project because the formations of interest were deep enough and thick enough to meet all of the criteria for injection.

5.3 Geology

5.3.1 Stratigraphy:

The northwestern corner of New Mexico is dominated by the broad, asymmetric San Juan Basin. It covers roughly 26,000 mi^2 (Brister and Hoffman, 2002) and is a structural and a depositional basin. The San Juan Basin is located north of Zuni Mountains, Lucero Uplift and Ignacio monocline, west of the Nacimiento Mountains and Gallina-Archuleta Arch, south of the San Juan and La Plata Mountains and Sleeping Ute Mountain in Colorado, and east of Defiance uplift and Chuska and Carrizo Mountains and (Craigg, 2001; Figs. 5.1). The San Juan Basin center is filled by nearly 15,000 ft of Precambrian to Eocene rocks. Along the flanks of the basin, older sediments are turned up and exposed providing an opportunity to study the older, deeper horizons (Figs. 5.2 – 5.4). The basin is deepest on the northern and southeastern sides of this asymmetric basin.

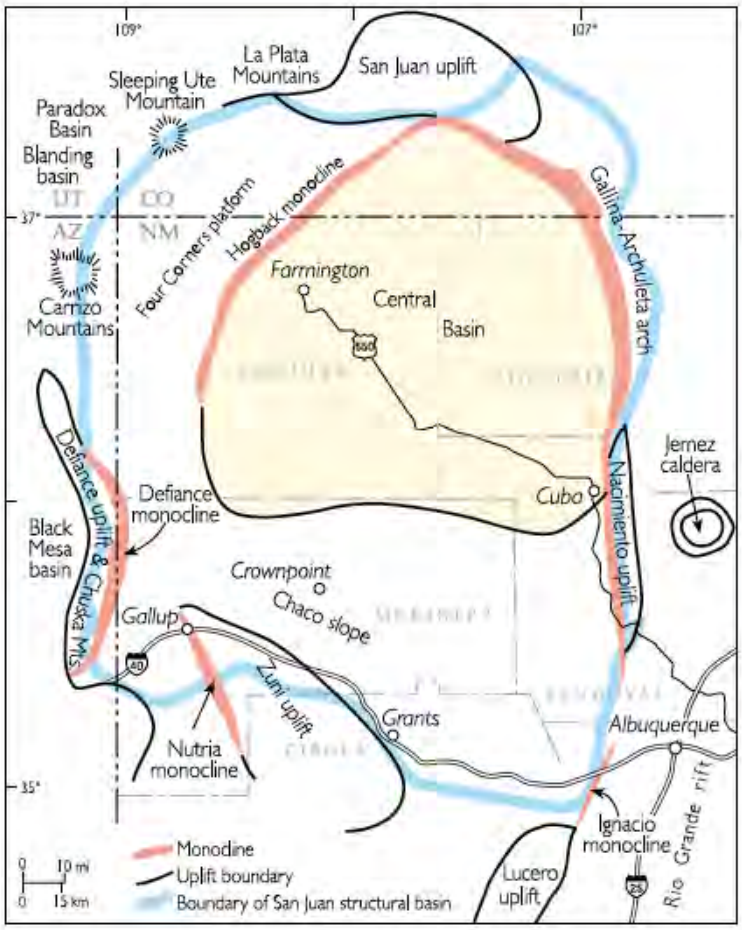

Figure 5.1. San Juan Basin (modified from Craigg, 2001).

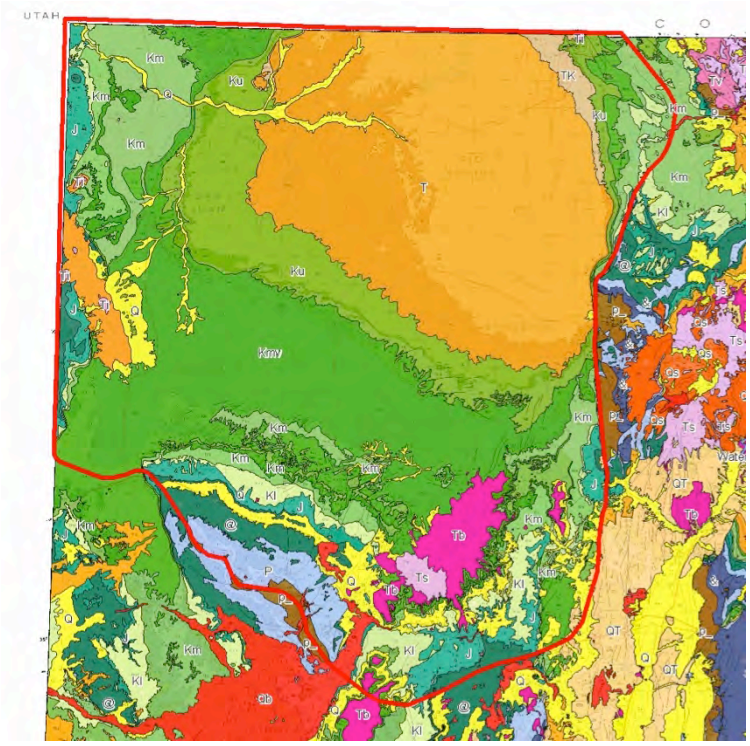

Figure 5.2. Generalized geologic map of the San Juan Basin and the basin outline (from NMBGMR).

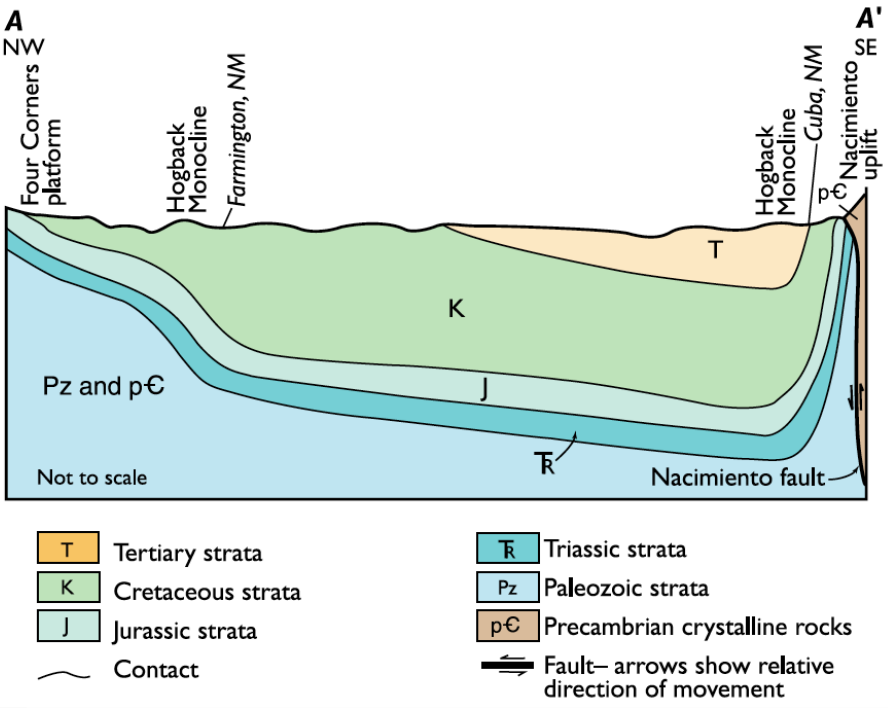

Figure 5.3. A northwest-southeast cross section across the San Juan Basin (from Craigg, 2001).

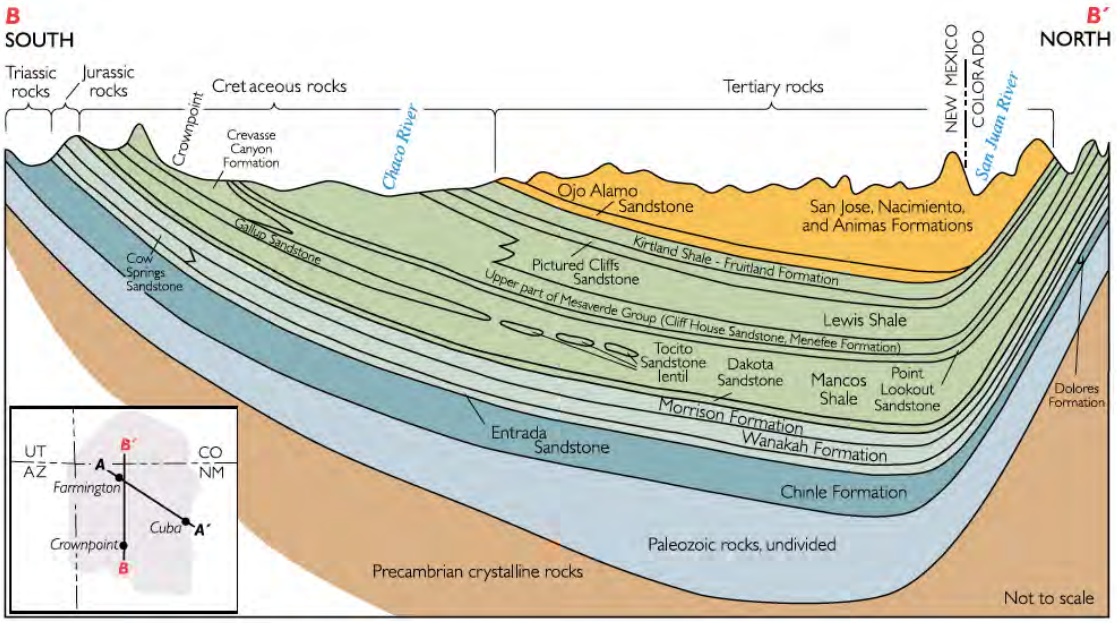

Figure 5.4. A north-south cross section through the San Juan Basin (from Craigg, 2001).

The stratigraphy of the basin starts with Precambrian units (Fig. 5.5). Precambrian rocks in the area are granites and quartzites (meta-sandstones). An unconformity exists between the Precambrian and Cambrian Ignacio Formation. The Ignacio Formation is a marine transgressive sandstone that is quartz-rich, well cemented and contains shale lenses (McLemore et al., 1986a, 1986b). The maximum thickness is approximately 100 feet, and it occurs in block-faulted erosional remnants (McLemore et al., 1986a, 1986b).

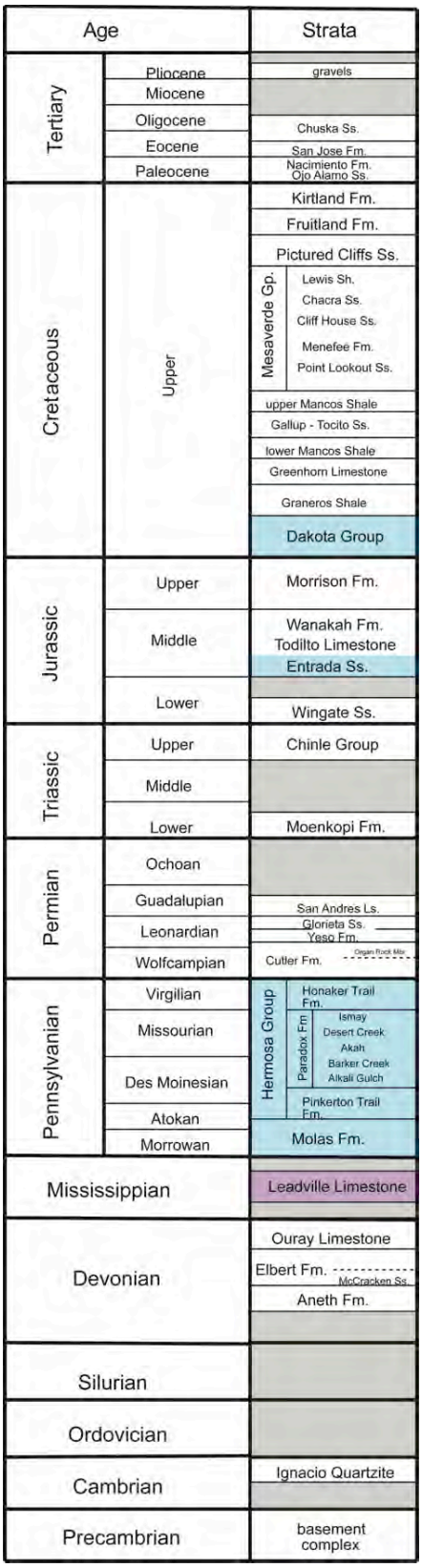

Figure 5.5. Idealized stratigraphic section for the San Juan Basin including the specific resources found in units.

An unconformity on top of the Ignacio Formation lasted until mid-Devonian time. The first Devonian deposit is the Aneth Formation. In places, the Aneth Formation lies directly on Precambrian surface where the Ignacio sediments were removed by erosion (McLemore et al., 1986a, 1986b). The Aneth Formation consists of dark, organic-rich, argillaceous limestones, dolomites, shales and siltstones. These units were deposited in euxinic basin (Stevenson and Baars, 1977) and are approximately 75 feet thick within the basin. The Elbert Formation is conformable with the underlying Aneth Formation. The Elbert Formation is subdivided into the McCracken Sandstone Member and an upper carbonate member.

The McCracken Sandstone Member is approximately 175 feet thick (Stevenson and Baars, 1977) and consists of fine to medium-grained, glauconitic, marine sandstones. The upper unit has a maximum thickness of 200 feet and thins across the basin to east (McLemore et al., 1986a, 1986b). It contains shallow marine limestones, shales and glauconitic sandstones.

The Ouray Formation conformably overlies the Elbert Formation and contains organic-rich, shallow marine limestones and dolomites. It varies across the San Juan Basin from over 90 feet thick to not being present due to erosion (McLemore et al., 1986a, 1986b).

The Mississippian Leadville Limestone unconformably overlies the Ouray Formation and ranges in thickness from 0 to 200 feet thick (McLemore et al., 1986a, 1986b) due to erosion or non- deposition prior to Pennsylvanian sedimentation. The shallow marine carbonates of the Leadville have been brecciated during the exposure event that followed deposition.

Mississippian strata are unconformably overlain by sediments of Pennsylvanian Molas Formation and Hermosa Group. The Molas Formation is up to 150 feet thick and is made up of red-bed terra rossa soil deposits and calcareous sandstones, siltstones and shale with minor limestones (Wengard and Matheny, 1959). Conformably overlying the Molas Formation, the Hermosa Group is a series of mostly marine deposits. They are shallow marine calcarenites and biohermal limestones and dolomites, sandstones, siltstones and shales. The upper part of Hermosa Group is a regressive sequence that grades into the overlying Permian Cutler Formation.

The Permian Cutler Formation (also referred to as the Abo Formation in early literature) is up to 1,600 feet thick, but it thins southward around the Zuni and

Defiance uplifts (McLemore et al., 1986a). It is a non-marine red-bed sequence that consists fluvial and lacustrine conglomerates, sandstones and shales.

The conformable Yeso Formation ranges from fine-grained cross-bedded aeolian sandstones to marginal marine shales, limestones and evaporites (McLemore et al., 1986a, 1986b). The Glorieta Sandstone is well-sorted, quartz-rich shallow-marine sandstone. Due to its almost pure quartz content of this unit, it is a key marker horizon here in the San Juan Basin and elsewhere in New Mexico.

The San Andres Formation interfingers with the underlying Glorieta Sandstone. It is thins from 100 feet in the southern areas to being absent in the northern areas of the San Juan Basin (McLemore et al., 1986a, 1986b). It ranges from shallow marine limestones and dolomites to non-marine red beds. An unconformity overlies the Permian strata, and in areas with carbonates, karst topography formed.

Triassic time in the San Juan Basin was a time of non-marine deposition. From a thick section in Arizona, the Moenkopi Formation wedges out in the far western parts of the San Juan Basin (Akers et al., 1958). In New Mexico, the continental deposits consist of shales to sandstones (Repenning et al., 1969).

The Chinle Formation unconformably overlies the Moenkopi Formation (and Permian). The Chinle floodplain and fluvial deposits are up to 1,700 feet thick in the Colorado Plateau (Repenning et al., 1969). The Jurassic Wingate Sandstone is conformable with the Chinle Formation and formed as part of aeolian dune fields in the southwestern part of the San Juan Basin and get up to 600 feet thick.

The Jurassic Entrada Sandstone unconformably overlies the Wingate Sandstone. The Entrada Sandstones were deposited as part of large aeolian dune fields interspersed with playa lake deposits (Tanner, 1976). The Todilto Limestone conformably overlies the Entrada Sandstones.

The Todilto Limestone Member and the Summerville Member are currently assigned to the Wanakah Formation. The Todilto Limestone is composed of bedded gypsum and organic-rich, algally-laminated limestones and dolomites that were deposited in either a marginal marine or lacustrine environment. Currently, a lacustrine environment is the favored interpretation (see discussion in Ulmer-Scholle, 2005). In places, Todilto deposits fill the relief on the Entrada depositional surface.

The Todilto Limestone Member is overlain by the Summerville Member. The Summerville deposits consist of sandstones, siltstones, mudstones, minor conglomerates and gypsiferous sandstones and siltstones. In the San Juan Basin, it varies in thickness from 90 to 150 feet, and it may represent deposition on a arid coastal plain to sabkha (Anderson and Lucas, 1006)

Jurassic Morrison Formation (Salt Wash, Recapture, Westwater Canyon and Brushy Basin members) was deposited in fluvial, aeolian, sabkha to lacustrine environments and consists of sandstones, siltstones and shales.

The incursion of Cretaceous Seaway into the San Juan Basin during Upper Cretaceous time resulted in the deposition of over 6,500 ft of marine, coastal to non-marine sediments. Between Morrison and Upper Cretaceous sediments, there is an unconformity. During Upper Cretaceous sedimentation, at least 5 episodes of transgression/regression within the seaway occurred (Molenaar, 1983) resulting in deep marine, deltaic, coastal swamps, beach, alluvial and fluvial deposits.

The Dakota Sandstones represents the first transgressive cycle and is composed of sandstones, shales and coals. These sediments were deposited in fluvial environments in the northwestern part of the basin and coastal swamps to marine environments in the southeastern part of the San Juan Basin (Grant and Owen, 1974). It can exceed 200 feet in thickness.

Conformably overlying the Dakota Sandstone is the Mancos Shale. It is a complex sequence of siltstones and shales and minor sandstones representing deep marine environments to shallower marine environments. It exceeds 2,000 feet in thickness.

The Mesaverde Group is subdivided into the Point Lookout Sandstone, Menefee Formation, Cliff House Sandstone and Lewis Shale. The Point Lookout Sandstones (~200 feet) consist of regressive coastal barrier system sandstones. The Menefee Formation (~400 feet) was deposited in coastal swamps to alluvial plains and is composed of sandstones, shales and coals. The Cliff House Sandstone consists of marine, cross-bedded sandstones with shales that are up to 800 feet thick. The contact with the overlying Lewis Shale is gradational. The Lewis Shale, a marine shale, is over 500 feet and contains numerous bentonite beds (McLemore et al., 1986a, 1986b).

Pictured Cliffs Sandstone is a quartz arenite that were deposited as part of a regressive coastal barrier island/bar system (McLemore et al., 1986b)

The Fruitland Formation sediments are non-marine coastal plain deposits formed after the last regression of the Cretaceous Seaway from the San Juan Basin area. The sandstones, shale and coals are over 300 feet thick. The Kirtland Shale is a non-marine coastal plain to alluvial sediments and thins to the southeast. At its maximum, it is over 2, 00 feet thick (Molenaar, 1977)
The Paleocene Ojo Alamo Sandstone lies unconformably on Cretaceous sediments. It is composed of sandstones with minor conglomerates and shales, followed by the Nacimiento Formation, shales with minor sandstone lenses. Nacimiento deposits were followed by sediments of the Eocene San Jose Formation. The San Jose Formation consists of conglomerates, sandstones and shales. The Pliocene Chuska Sandstone unconformably overlies the San Jose Formation, and the rocks are aeolian and fluvial deposits.

5.3.2 Structural History:

From Cambrian to early Pennsylvanian time, the area covered by the present-day San Juan Basin was a broad shelf adjacent to the Cordilleran passive margin (Wengard, 1959). Local uplifts during Pennsylvanian sedimentation resulted in a supply coarse-grained siliciclastics to the area. The area remained relatively flat, and slowly subsiding. Minor tilting (westward during the Permian, northeastward during the Cretaceous) was extent of the tectonic activity in the basin until the Laramide (Wengard, 1959).

The formation of the present-day San Juan Basin began during the Laramide (late Cretaceous/Early Tertiary to Eocene) with downwarping of the area (Stone et al., 1983, Tweto, 1975).

Igneous activity started approximately the same time as the Laramide Orogeny, around 70 Ma and continued until 63 Ma. During Oligocene time (35 to 26 Ma), the San Juan volcanic field produced 60,000 km^3 of volcanic material (Lipman et al., 1978). The San Juan Mountains saw renewed volcanism during Miocene to Pliocene time (Lipman et al., 1978). Most of the volcanics have been removed by subsequent erosion, but intrusives feeding the activity are still preserved.

5.3.3 Geothermal History:

Within the San Juan Basin, heat flow increases toward the San Juan Volcanic Field. In the area of the basin near the San Juan Volcanic field, heat flow averages 127mWm^{-2} (Clarkson and Reiter, 1988). Elsewhere in the basin, the heat flow is

considered to too high to be caused only by the volcanic activities in the San Juan Mountains (Reiter and Clarkson, 1983). The thickness of sediments in the basin do not account for the anomalously high temperatures or the heating event associated with Oligocene San Juan Batholith emplacement. It is thought a large plume-like anomaly at 100 to 35 km depth (Clarkson and Reiter, 1988) is the likely source of the extra heat.

5.4 Project Deliverables

5.4.1 Database

The initial goals of the project was to:

- Collect and review public data from the region including well logs and previous studies, and
- Create a relational geodatabase that could be integrated GIS software to produce derivative products.

The New Bureau of Geology and Mineral Resources (NMBGMR) team created a relational geodatabase in Microsoft Access to collect all the pertinent information for the 50,000 plus wells in the San Juan Basin as well as the 100 to 200 thousand of wells elsewhere in New Mexico. The database was created for this project, but the NMBGMR designed the database in such a way that it can be expanded and upgraded as needed for future projects. To date, in addition to this project, the database has been utilized for a USGS Carbon Capture and Sequestration study and two geothermal projects.

Where available, the data collected geodatabase includes:

- All formation tops available,
- Location and elevation information,
- Core and plug data —
    - Porosity and permeability data,
    - Oil/Gas/Water ratios.
    - Lithologic information,
    - Water chemistry,
- Well site tests —
    - Bottom hole temperatures,
    - Geothermal gradient data,
    - Produced water salinity and
    - Flow rates.

5.4.2 Update NATCARB Database with Regional Data

NMBGMR contributed relevant data and derivative structural and isopachous maps to the RMCCS team to develop databases for the region, using all available existing data. This required the creation of several generations of maps (structure and isopachous) to refine the New Mexico dataset as well as the input of over 70,000 porosity and permeability values derived from core analyses.

5.4.3 Units of Interest for CO_2 Sequestration

The San Juan Basin has the second largest gas accumulations in North America, and it has a long history of production (since 1911) with more than 50,000 well penetrations in the basin (Fig. 5.6). The majority of oil and gas production is shallow units from the Dakota Group and younger strata (Gallup Sandstone, Mesaverde Group and Pictured Cliffs Sandstones) along anticlinal folds within the basin, but there is production from deeper horizons. Most of this deeper production is from the Pennsylvanian Hermosa Formation, but Jurassic Entrada Sandstone, the Leadville Limestone and Devonian units also have had productive fields.

Hydrocarbon maturation patterns mimic heat flow trends within the San Juan Basin and increased to the north; gas is common in the northern and central areas of the basin. The thickness of the sediment package in the deepest parts of the basin also increases the formation temperatures to the north. The San Juan Volcanic Field was also a possible heat source to produce the anomalously high temperatures found in the region. Oil is common in the western, southern and southeastern areas of the basin (Clarkson and Reiter, 1988).

This history of production (Table 5.1) makes the San Juan Basin both an excellent basin for CO_2 sequestration as well as utilization for enhanced oil recovery techniques. Most of the main producing reservoirs within the basin are too shallow to be possible CO_2 sequestration sites, but Dakota Group and older reservoirs are deep enough. If the CO_2 is being used for gas flooding and other enhanced oil recovery technologies, then the shallower horizons may have potential.

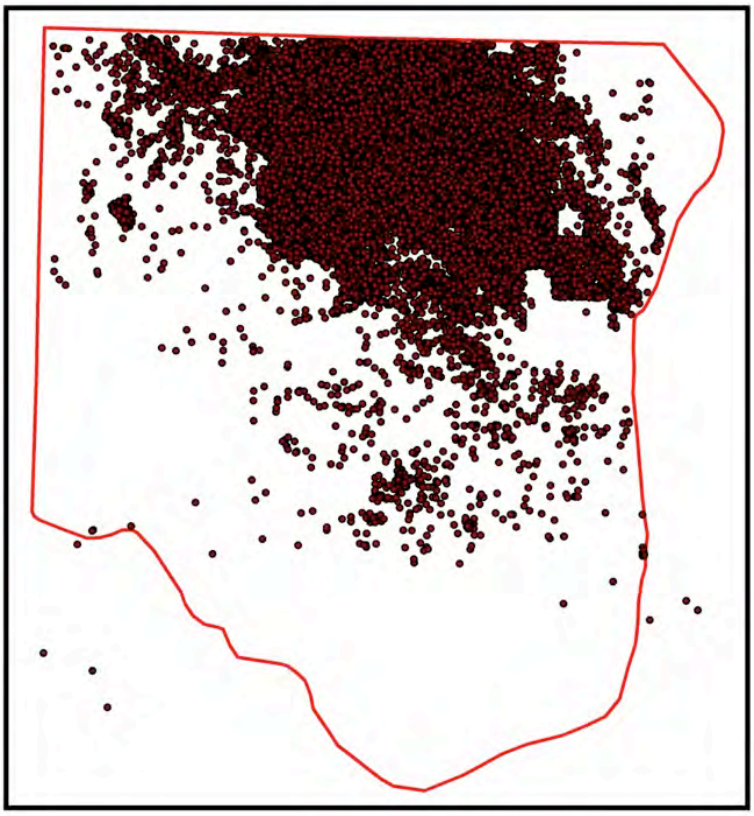

Figure 5.6. Distribution of wells drilled within the San Juan Basin.

Table 5.1: Summary of oil and gas production within the San Juan Basin. The blue areas are from Engler et al. (2001), the orange areas are from Fassett (1993) and the rest of the values are from Fassett (2010).

Formation/Period	Play		Cumulative Production	
	Oil	Gas	Oil (10^3 bbls)	Gas (Tcf)
Tertiary				
San Jose		λ	0	0.0019
Nacimiento		λ	0.7	0.0006
Ojo Alamo		λ	0	0.0003
Cretaceous				
Farmington		λ	–	–
Fruitland Sand		λ	34.6	0.0570
Fruitland Coal		λ	367.1	15.7
Fruitland/Pictured Cliffs		λ	–	–
Pictured Cliffs		λ	1,200	4.5
Lewis Shale		λ	–	–
Chacra		λ	47.6	0.3
Mesaverde		λ	47,300	12.9
Gallup	λ		59,663.2	0.552
Tocito	λ		150,000	–
Sanastee	λ		–	–
Mancos Shale	λ		41,000	–
Greenhorn	λ		–	–
Graneros	λ		–	–
Gallup-Dakota	λ		–	–
Mancos-Dakota	λ		–	–
Dakota	λ	λ	49,600	7.0
Jurassic				
Entrada	λ		6,000	–
Pennsylvanian	λ	λ	14,000	35,481
Mississippian	λ	λ	90.1	3,723
Devonian	λ		18.8	0.0141

To better understand the geology, the distribution and provide information for the CO_2 capacity spreadsheets for the selected units within the San Juan Basin, a series of maps were created in ARC-GIS. Structure maps on top of each of the units of interest and the underlying formation were constructed. The underlying formations were also mapped since they were needed later for the isopachous maps.

To create the structure maps, a surface topographic map was created (Figs. 5.7 - 5.8) to make certain that the elevations were consistent with the regional topography. The surface elevations, used for the digital elevation model (DEM), were the datums provided by the drillers. This is the point that the loggers would measure to the each of formation tops. These elevations range from the actual land surface to the

Kelly bushing (KB) or drilling floor (DF). If values were not in the expected range, then the values were checked on Goggle Earth. Many of the drilling pads are still visible on aerial photographs.

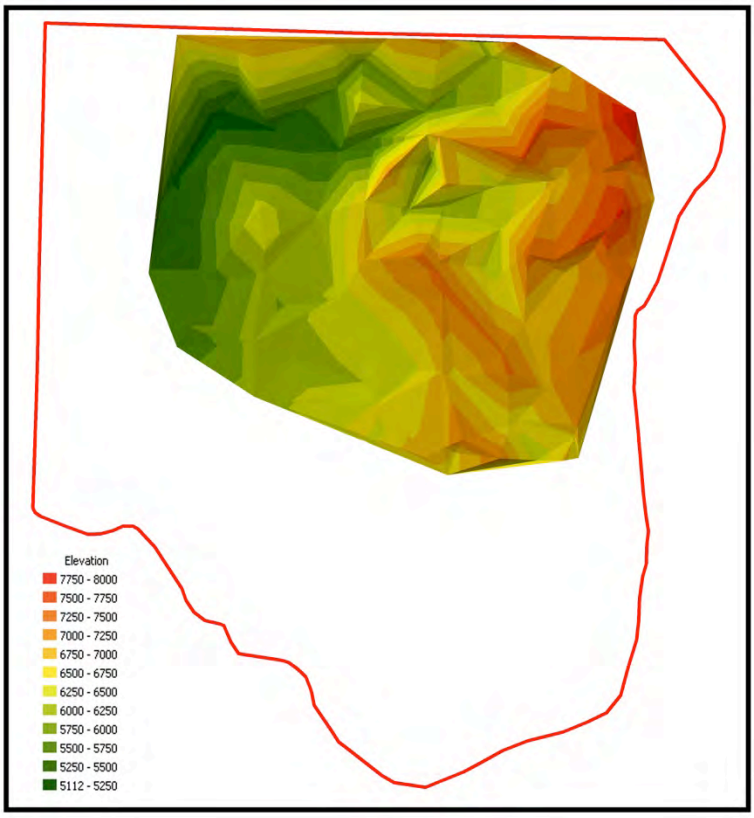

Figure 5.7. Structure contour map of the surface topography (ft). It lacks the fine details of the rasterized version generated from this map (Fig.5.8).

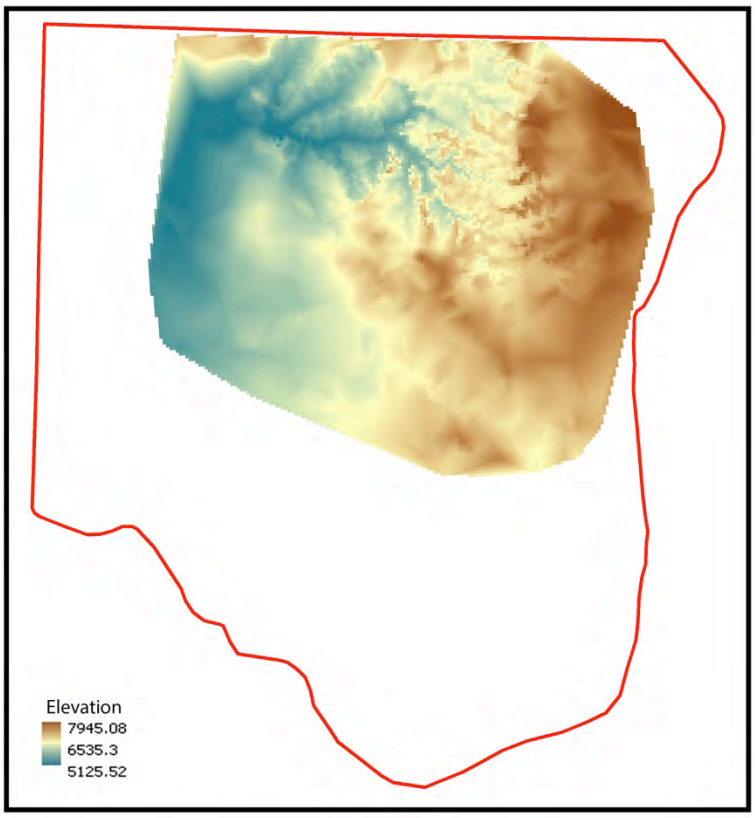

Figure 5.8. The rasterized version of topographic map has more detail.

After the surface topography was checked, a query was created in Microsoft Access to subtract each of the formation tops from the surface elevation to get the formation top with respect to sea level. The formation tops include the Mancos Shale, Dakota Group, Morrison Formation, Entrada Formation, Chinle Group, Hermosa Group, Molas Formation, Leadville Limestone and Ouray Limestone. Structure maps were created for each of the formations. Tops were checked, and wells that were not consistent with surrounding data, the well logs were checked or, if the logs were not available, they were omitted from the map. This was an iterative process until the maps were realistic.

To create the isopachous maps for each of the target units, for example the Mancos Shale, the structural contour map for the top of the Mancos Shale was subtracted Dakota Group to come up with a isopachous (thickness) map of the Mancos Shale. To create overburden isopachous maps for each of the target formations, the surface DEM map was subtracted from the formation's structural map.

5.4.3a Mancos Shale

Geologic Characterization:

The Mancos Shale is thick sequence occurring throughout the San Juan Basin that conformably overlies the Dakota Group and grades into the overlying Pictured Cliffs Sandstone. While there are productive sandstones near the top of the Mancos, the majority of unit is composed of well-compacted, deep marine shales and siltstones that have extremely low porosities and permeabilities. This makes it a potential regional seal for CO_2 sequestration projects. Currently, companies operating in the San Juan Basin are predicting that with horizontal drilling technologies and hydraulic fracturing of the shales, the Mancos shale may be the next Bakken or Barnett play (Fig. 5.9). If this does happen, the sealing capabilities of the unit may be diminished.

The bottom-hole temperatures (Fig. 5.10) support the prospective areas of gas deposits surrounded by shallower oil reservoirs.

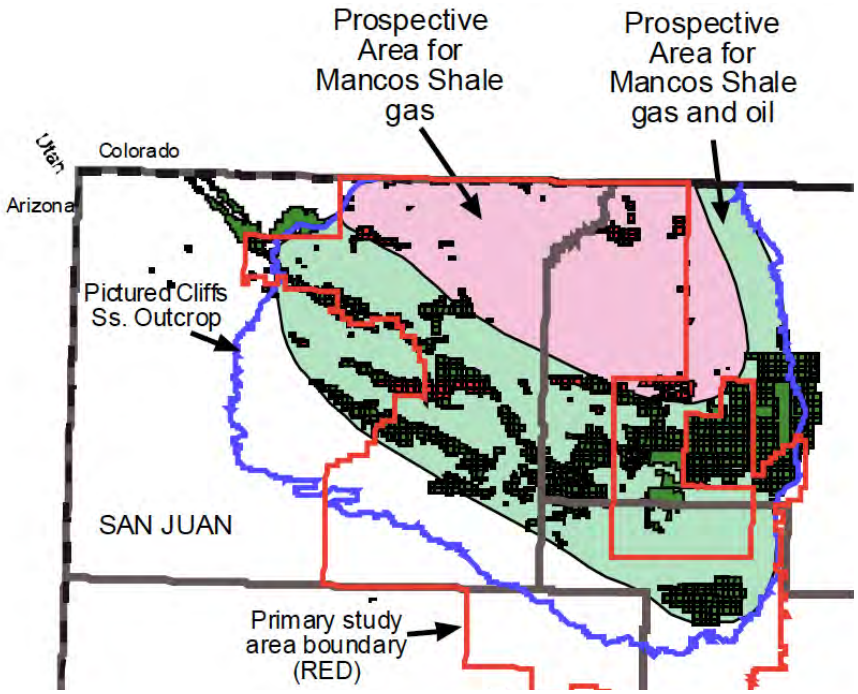

Figure 5.9. Areas that may see exploration growth in the Mancos Shale (from a BLM Report by Engler et al., 2001).

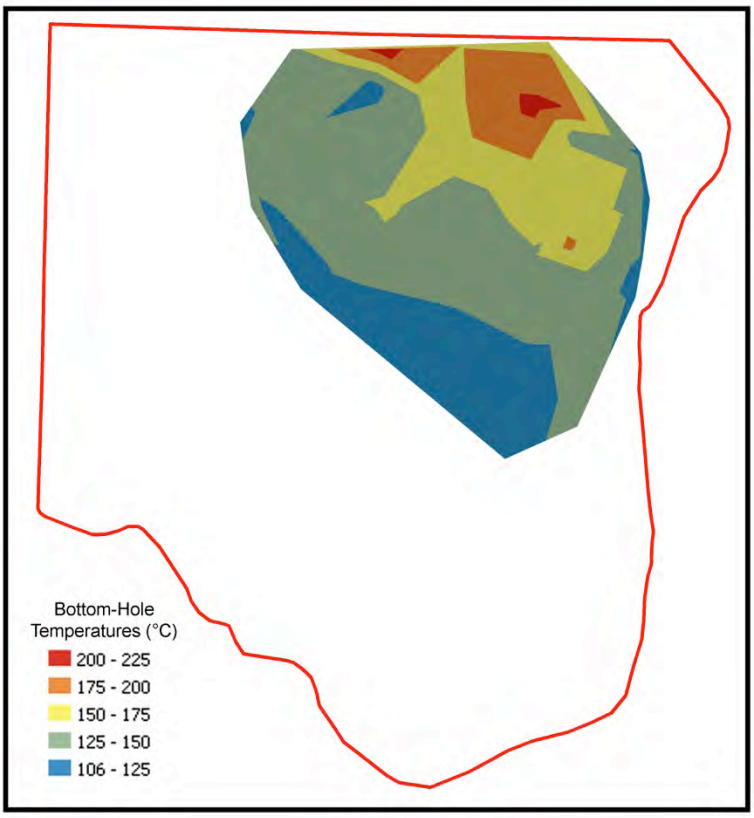

Figure 5.10. Bottom-hole temperatures within the Mancos Shale. The highest temperatures are in the deepest part of the basin and closer to the San Juan Volcanic field.

The stratigraphy of the Mancos Shale is complex due to the conflicting terminologies used by industry and geological surveys. The Mancos Shale (Fig. 5.11) can be subdivided into upper Mancos, Carlile, Lower Mancos, Greenhorn Limestone and Graneros Shale (Nummedal and Molenaar, 1995; Engler et al., 2001). In addition, the Juana Lopez, Gallup Sandstone, Tocito, El Vado, Crevasse Canyon Shale and the Niobrara Shale, all have been used by previous workers to describe members of the Mancos Shale (Engler et al., 2001; McLemore et al., 1986a, 1986b). Many times, this terminology is used incorrectly. For example, the Gallup Sandstone is part of the Carlile member, and in numerous reports, papers and production data, the Gallup Sandstone stands alone and the Tocito Sandstone is a member of the Gallup; however, the Tocito appears to be equivalent to upper Mancos, not the Gallup or Carlile (Nummedal and Molenaar, 1995).

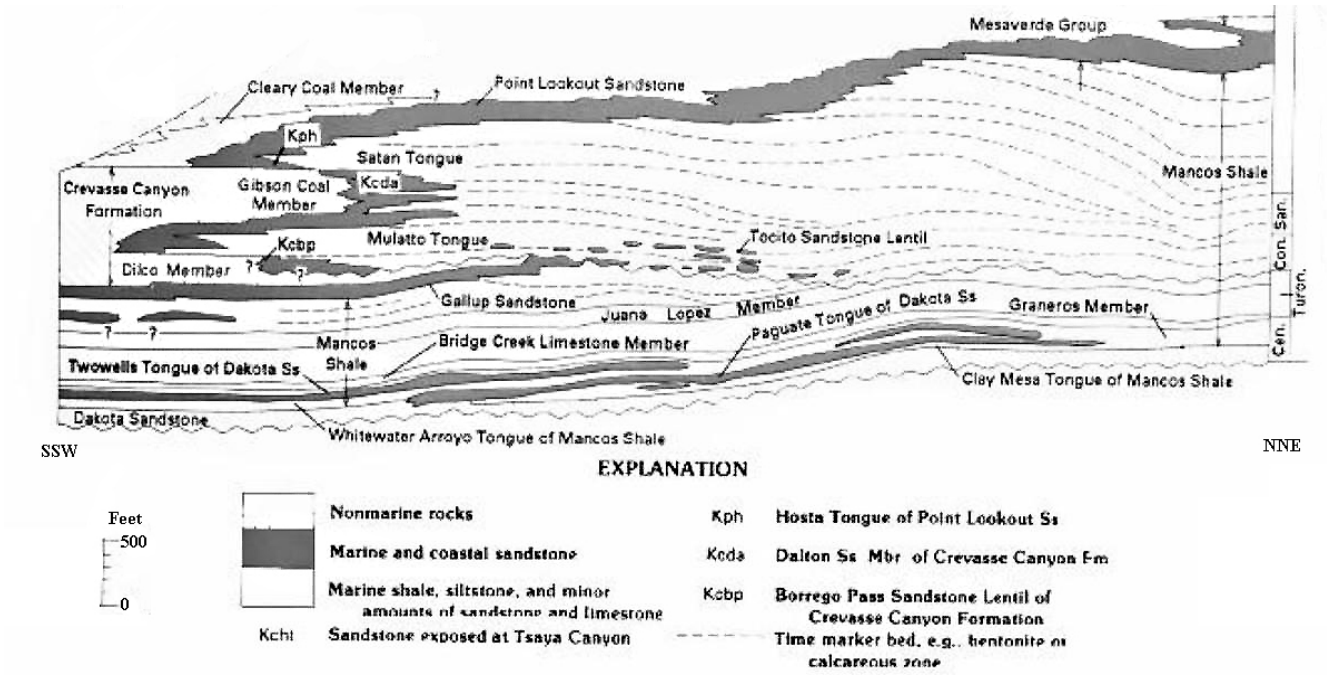

Figure 5.11. An idealized diagram of Mancos stratigraphy from south/southwest to north/northeast (modified from Nummedal and Molenaar, 1995).

Due to asymmetrical nature of the basin, the deepest sections of the Mancos Shale are in the northeastern part of the basin (Figs. 5.12 and 5.13). This area has been more extensively drilled than the edges, because the sediments have been buried deep enough to reach the oil and gas window. The lower Mancos is approximately 850 feet thick; and the upper Mancos Shale is approximately 1,000 to 1,400 feet thick (McLemore et al., 1986a) (Fig. 5.14).

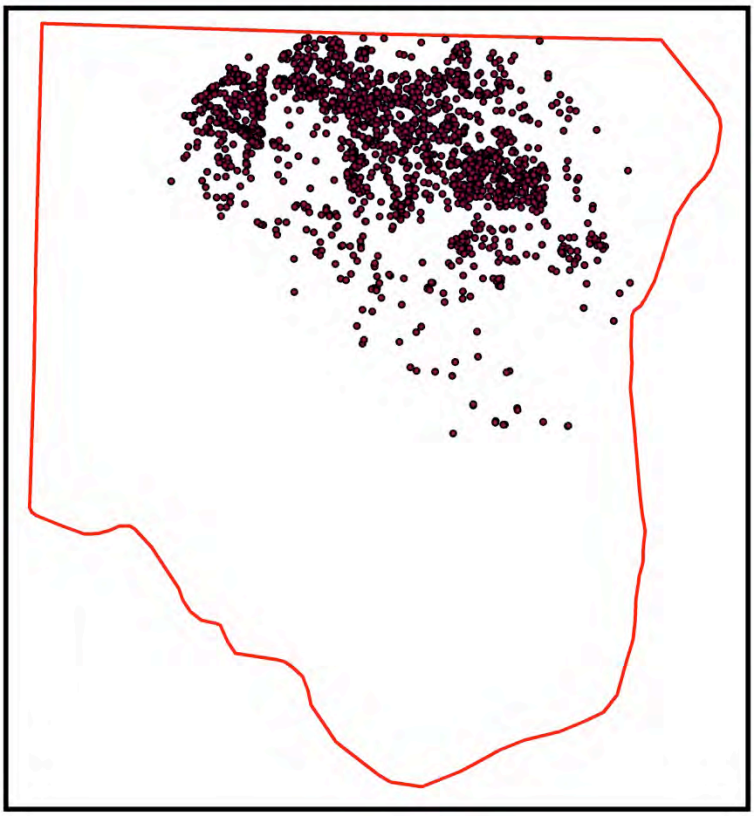

Figure 5.12. Distribution of wells used for mapping that penetrates the Mancos Shale.

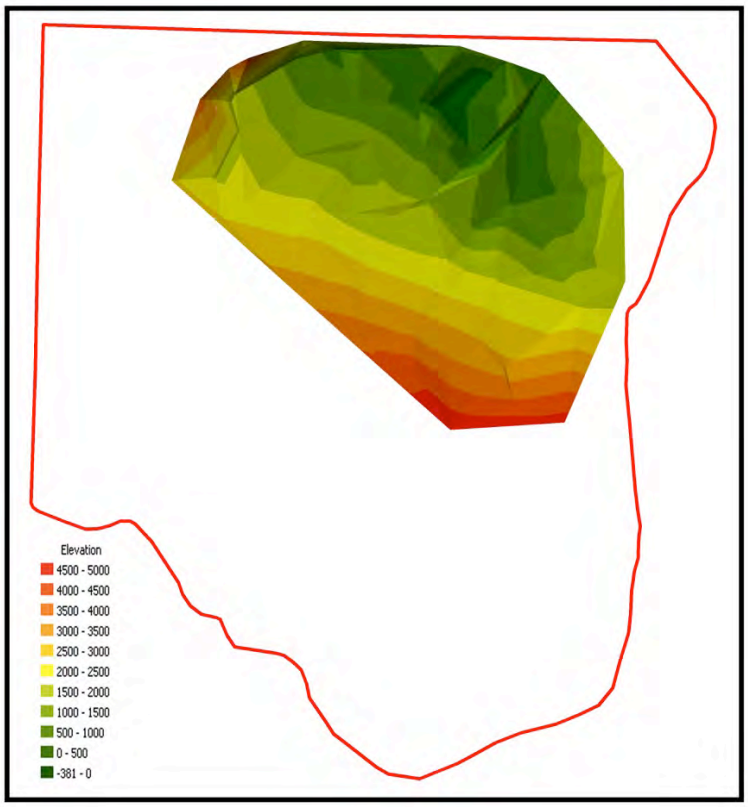

Figure 5.13. Structural map on top of the Mancos Shale (elevation = feet).

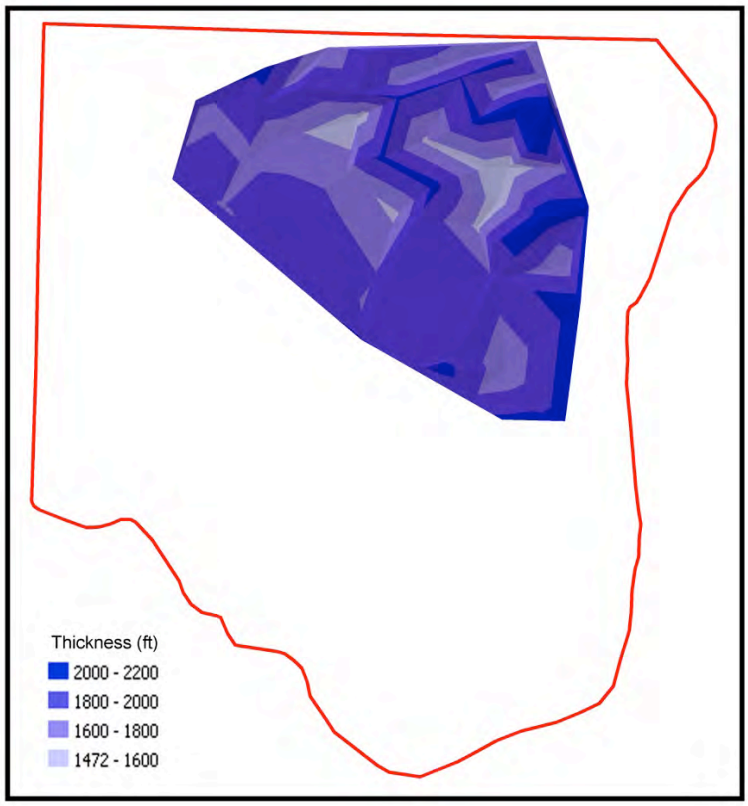

Figure 5.14. Isopachous map of the Mancos Shale (thickness = ft).

Based on foraminiferal zonation data, during Mancos deposition, the water depths within the Cretaceous Seaway may have been up to 300-400 feet deep, but this varied due to several transgressive/regressive events that occurred that period of the Cretaceous Period. The Graneros Shale Member is approximately 60 feet thick and is a transgressive shale unit. The Greenhorn Limestone Member sits on top of the Graneros Shale and is 40 to 70 feet thick. The Greenhorn Limestone Member represents the maximum transgression of the seawater into the Cretaceous Seaway of New Mexico (Molenaar, 1977). The Juana Lopez member represents the start of regressive event and consists of shallow marine fossiliferous calcarenites, sandstones and shales. The sediments that were deposited at the height of the regression and during next transgressive sequence are not well developed in the basin (McLemore et al., 1986a).

The Gallup Sandstones were deposited during the second regression and are shallow marine sediments. They are very fine to very coarse-grained sandstones with minor shales and coal that ranges from 25 to 135 feet in thickness (O'Sullivan et al., 1972). The next transgressive/ regressive/transgressive cycles resulted in deposition of Crevasse Canyon Shales. This unit contains shale, calcareous concretions and sandy zones.

The Mancos Shale ranges from being exposed on the edges of the basin to being buried by almost 8,000 ft of sediment in the "center" of the basin (Fig. 5.15).

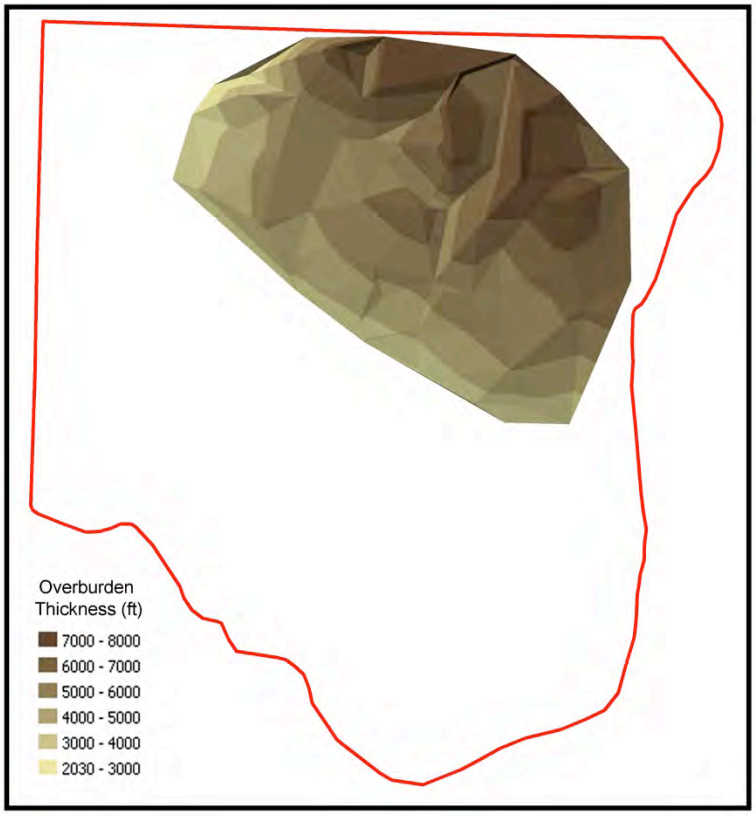

Figure 5.15. A map of the overburden (ft) on top of the Mancos Shale.

The Mancos Shale (excluding the Gallup Sandstone) has seen limited oil and gas production. Regionally, it has been considered the source rock for many of the younger Cretaceous plays. It is productive only where it is highly fractured, but in most areas, it is a seal.

The Gallup and basal Niobrara reservoirs (upper Mancos) have both oil and gas production and are stratigraphic traps with a minor structural control (McLemore et al., 1986a). The difficulty in determining production in the Mancos Shale is due to Gallup and Tocito Sandstones being misidentified by drillers, but it is likely that most of the production is from the Tocito Sandstone. The Tocito Sandstone is a super clean quartz sandstone deposited in an offshore marine bar facies. Reservoirs have net pays up to 125 feet, porosities up to 20% and permeabilities of 250 mD or less (McLemore et al., 1986a).

Summary and Recommendations:
The Mancos Shale is a potential regional seal, but it will depend on future exploration within the Mancos Shale. Areas that are currently highly fractured will most likely be a leaky seal; therefore, other seals will have to be evaluated.

5.4.3b Dakota Group

Geologic Characterization:
The first incursion of the Cretaceous Seaway into the San Juan Basin area resulted in the deposition of the Dakota Group in the San Juan Basin. The Dakota was deposited on an unconformity surface over Morrison or Burro Canyon Formations and conformably grades into the overlying Mancos Shale.

Environments range from fluvial, coastal wetlands to deltaic deposits in northwestern part of the basin to marine sandstones and shales in the southeastern part of the basin (Grant and Owen, 1974; Fassett, 1983). Deposits range from carbonaceous sandstones and siltstones, shales, coal and conglomerates. The source of the sediment appears to be from the north and consists of reworked sediments from underlying units (Burton, 1955). The Dakota Group is up to 500 ft in thickness (Figs. 5.16 and 5.17), and it varies through the basin, but there appears to be a low that trends northwest to southeast.

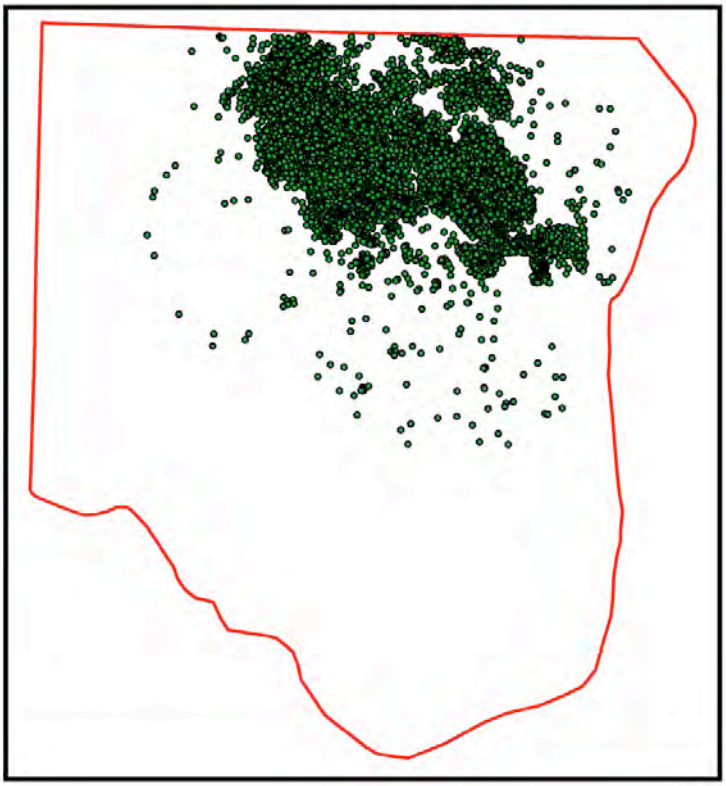

Figure 5.16. A well density map of Dakota Group wells.

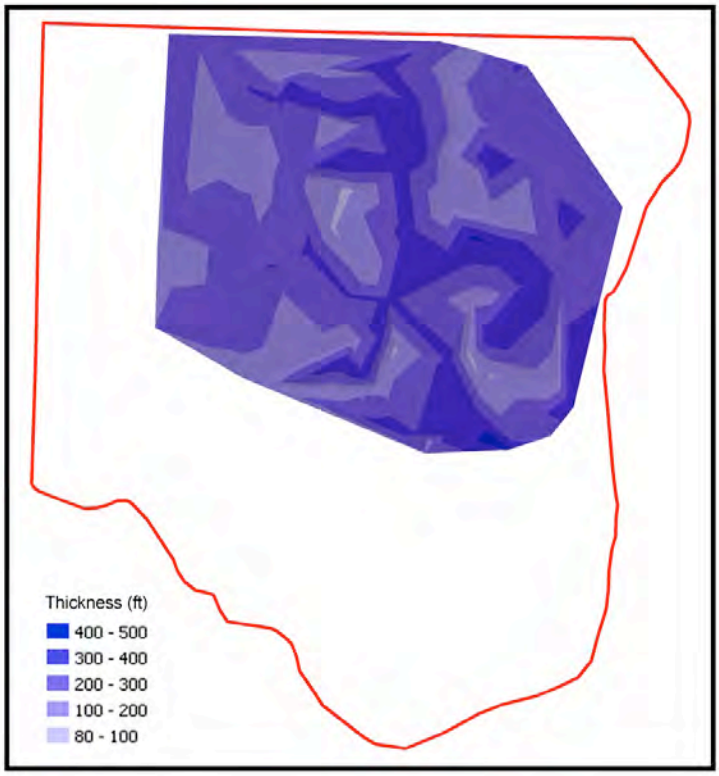

Figure 5.17. An isopachous map of the Dakota Group sediments (thickness = ft).

Gas production is not as well understood within the Dakota Group, but it probably has stratigraphic and hydrodynamic controls (McLemore et al., 1986a). The Dakota gas play has become a model for basin-centered gas (Figs. 5.18, 5.19). Oil reservoirs are a combination of structurally-controlled production along anticlines in shallower areas of the basin and fracture enhanced porosity and permeability. There may be minor stratigraphic controls on that production as well, including depositional environment and diagenetic controls. Most of the oil production in the Dakota Sandstone in the San Juan Basin occurs along the edge of the basin (Fassett, 1983). Fields trend northwest on the southwest structural axis, and most of the production is due fracturing (Fassett, 2006).

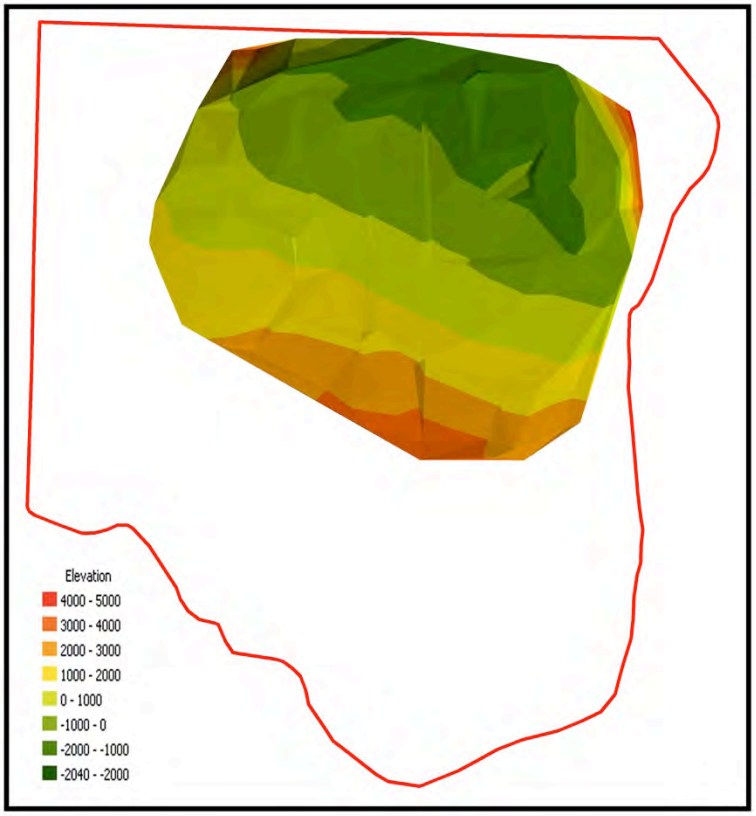

Figure 5.18. Structural map on top of the Dakota Group (elevation = feet).

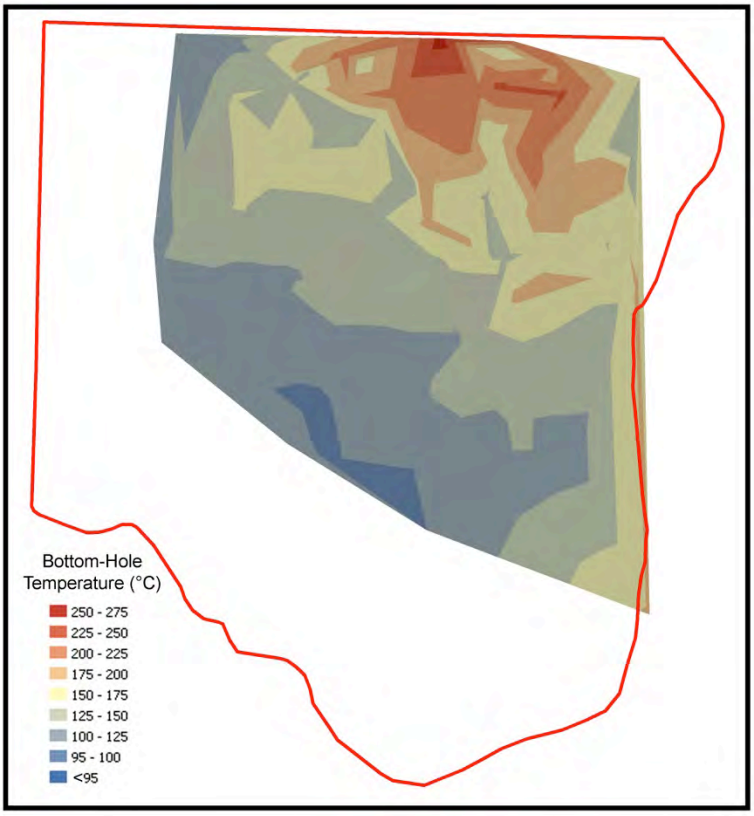

Figure 5.19. Bottom-hole temperatures for the Dakota Group. The highest temperatures are in the basin "center."

The Dakota is one of the prolific oil and gas reservoirs in the San Juan Basin (Table 5.1, Fig. 5.20). Dakota Sandstone reservoirs are within the transgressive/regressive marine littoral deposits on the western margin of the Cretaceous Seaway (Fassett, 1983). They are sourced from the Mancos Shale. Porosity within the Dakota Group is intergranular (Burton, 1955) and fracture. The "tight" sandstones have an average porosity of 7% and permeability of 0.15mD (Deischl, 1973), but they can go up to 15-20% porosity, 1,500 mD and 300 feet of pay (McLemore et al., 1986a). The core plug data within the database for the Dakota cores, this includes pay and tight zones, averages 6.7% porosity and 1.3 mD permeability. The maximum value for the porosity was 25.1%, and the maximum permeability was 715 mD.

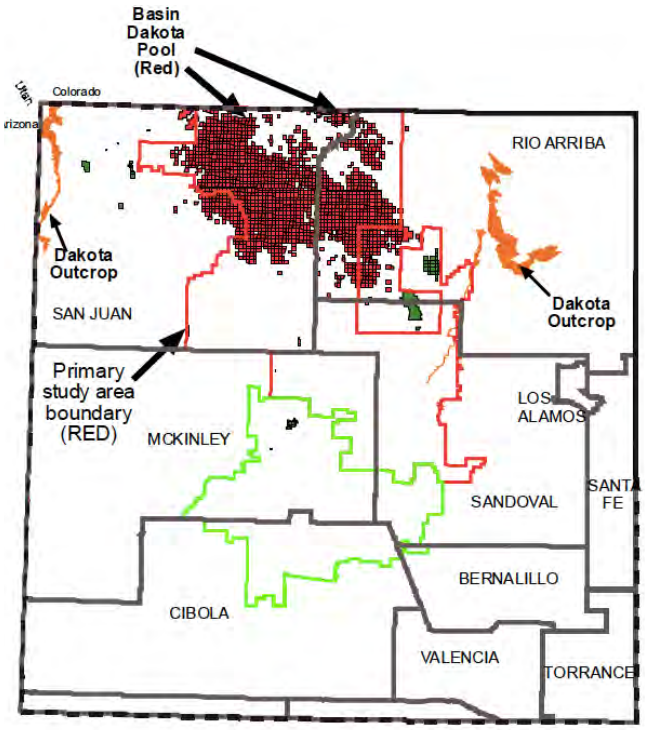

Figure 5.20. Dakota Group production in the San Juan Basin. The red areas are gas, and the green areas are oil production (from Engler et al., 2001).

CO_2 storage Capacity:

The parameters used to calculate the CO_2 storage capacity for the Dakota Group are located in Table 5.2. The basin area was determined from the overburden map (Fig. 5.21). The area is based on the 3,000 ft contour. Since the San Juan Basin has numerous completions in the Mancos Shale, the overburden map is an accurate estimate to the CO_2 reservoir size.

The thickness varies across the basin, and the data from the Dakota isopachous map was used to determine the thickness. Porosity varies greatly throughout the section from almost zero to close to 20%. Ultimately, the capacity estimates will also vary greatly from the minimum to maximum value. Possibly, a more accurate way to calculate the net capacity is to base the thickness on the net pay.

The porosity and permeability data comes from over 5,550 values from core reports within the basin. The temperature data is from well header information as well as geothermal and heatflow surveys.

The CO_2 storage capacities are presented in Table 5.3.

Table 5.2. Parameters used to calculate CO_2 storage efficiency for the Dakota Group in San Juan Basin, New Mexico.

Area (km^3)	Thickness (ft)	Porosity % (min, avg, max)	Salinity (TDS)	Permeability (mD)	Temperature (°C)	Geothermal Gradient
19,599	See Figure 5.17	2.5, 6.3, 13.2	25000	0.83	See Figure 5.19	47°C/km

Figure 5.21. A map of the overburden (ft) on top of the Dakota Group.

Table 5.3. CO_2 Storage Capacity (metric tonnes) *for the Dakota Group in San Juan Basin, New Mexico for three different efficiency factors (0.51%, 2% and 5.4%).*

Storage Efficiency Factor in Percent		
0.51%	2%	5.4%
172,502, 878 tonnes	676,481,873 tonnes	1,826,501,601 tonnes

Summary and Recommendations:
Based on the CO_2 storage capacity values, these Dakota marine to terrestrial sandstones have more limited capacity than comparable Dakota Colorado and Utah basins.

5.4.3c Entrada Sandstone

Geologic Characterization:
The Entrada Sandstone of the San Juan is part of a large aeolian dune field that covered most of the Colorado Plateau. The Entrada Sandstone unconformably overlies the Wingate Sandstone, and it is conformable with the overlying Todilto Limestone Member of the Wanakah Formation.

The Entrada Sandstones consists of fine to medium, well- to poorly-sorted, moderately well-rounded, quartz arenites of large trough, cross-bedded units. In the San Juan Basin, the Entrada Sandstone ranges from 150 to 800 feet thick (Fig. 5.22). It thickens to the northwest and thins to southeast. The upper sandstones are sometimes bleached; whereas, the lower sections are iron stained (Anderson and Lucas, 1996). The bleached zones have a different diagenetic history, and it is this zone that is usually the reservoirs. In places, they are calcite cemented which decreases the porosity and permeability of the unit. Interbedded with these sandstones are finer-grained, planar-bedded units. These have been identified as lacustrine deposits (Anderson and Lucas, 1996), but more likely these deposits represent playa lakes that were interspersed with the dune fields.

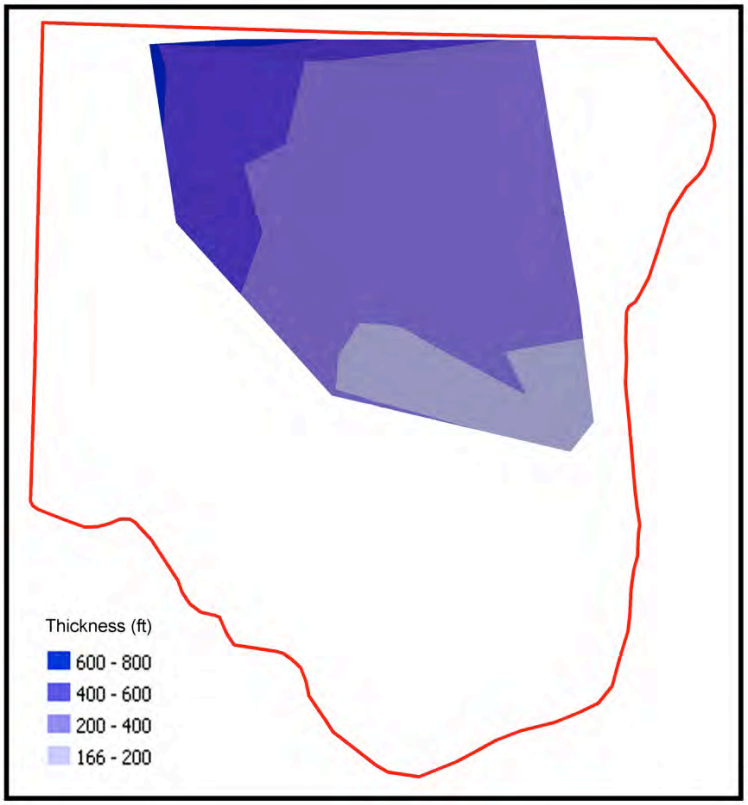

Figure 5.22. An isopachous map of the Entrada Sandstone (thickness = ft). Note that the unit thins from a thick in the northwest to a thin in the southeastern section of the San Juan Basin.

The Todilto Limestone conformably overlies the Entrada Sandstones. It consists of bedded gypsum and organic-rich, algally-laminated limestones and dolomites that were deposited in either a marginal marine or lacustrine environment (Kirkland et al., 1995; Anderson and Lucas, 1996; Lucas and Anderson, 1997; Lucas et al., 1985; Lucas et al., 2003; Ulmer-Scholle, 2005). Currently, a lacustrine environment is the favored interpretation. On outcrop, Todilto deposits can be seen filling the relief on the Entrada depositional surface.

The aeolian Entrada Sandstone's oil was probably sourced from the overlying organic-rich Todilto Limestone (Fassett, 1983). Most of the Entrada production comes from northwest Sandoval and southeast McKinley Counties, and almost all the reservoirs are stratigraphic traps. There is no gas production from the Entrada units at this time. Based on the work by Engler et al. (2001), the Entrada has future potential for both oil and gas (Fig. 5.23). Like the Dakota Group sediments, gas reservoirs should occur in areas where it is buried the deepest and has the highest temperatures (Figs. 5.24 to 5.26); and oil reservoirs will occur closer to the flanks.

Average porosity for productive Entrada units is 23% and 300 mD (Fassett, 1983), but it can be higher than 25%, have permeabilities greater than 600 mD and pay thickness of greater than 200 feet. Based on the database's measured porosity and permeability data produced for this project, the average porosity is 9.6%, and average permeability is 0.1 mD. The maximum thickness of this unit is 800 feet (Fig. 5.26). This is based on a Chinle Formation top, not the Wingate Formation. The Wingate is difficult to tell apart from the Entrada Sandstone and it is not present in large sections of the basin.

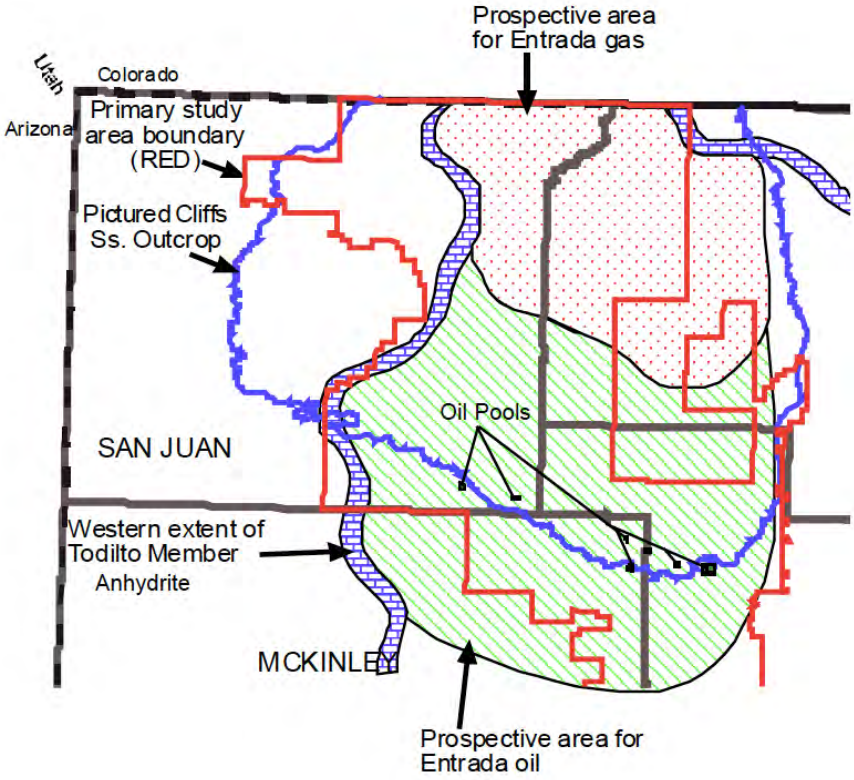

Figure 5.23. A map of prospective play areas for the Entrada Sandstone. Current production is oil and forms a linear trend on the map (from Engler et al., 2001).

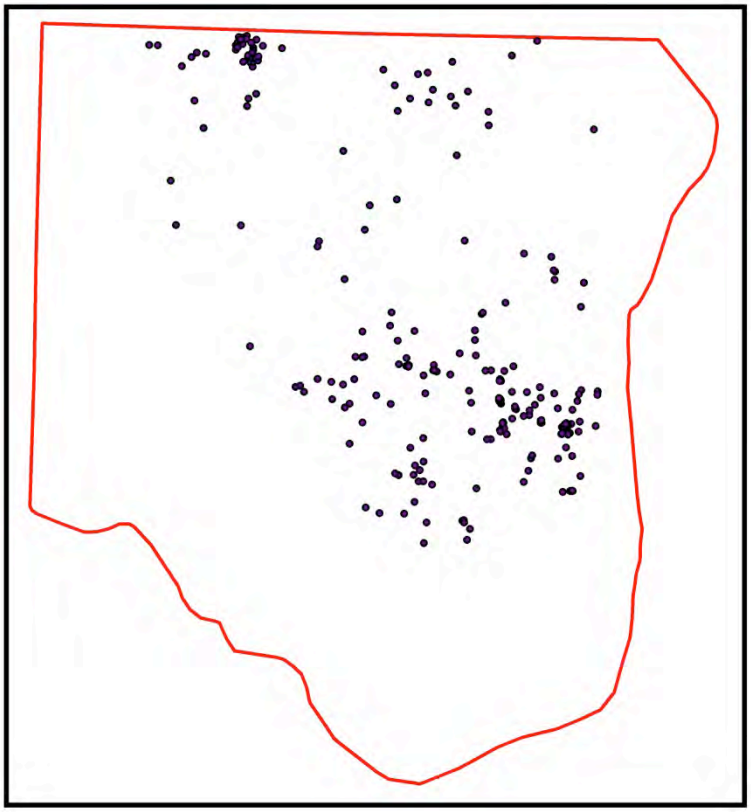

Figure 5.24. A map of the well density for the Entrada Sandstone.

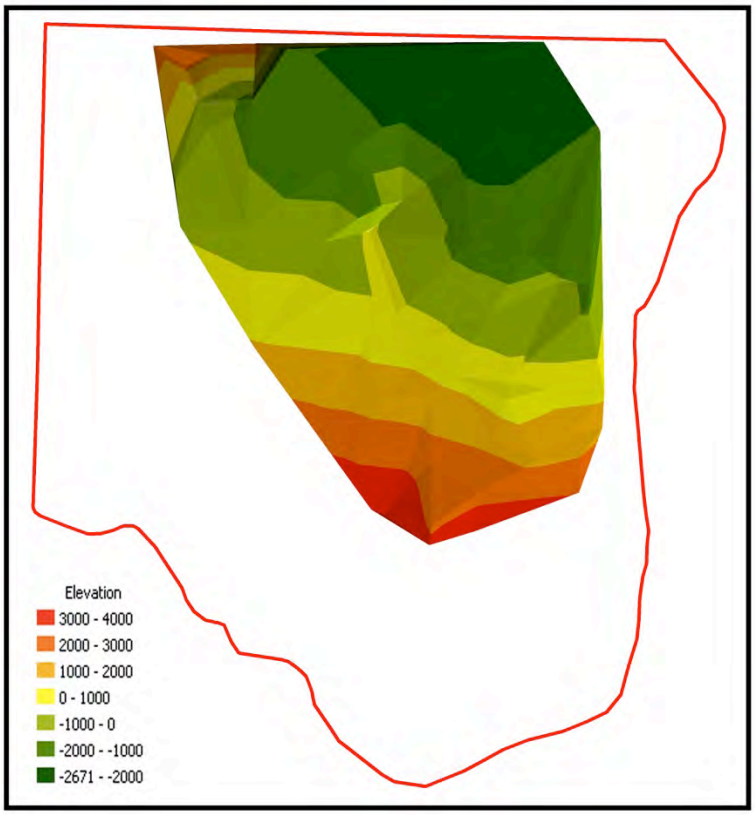

Figure 5.25. A structural map on the top of the Entrada Sandstone (elevation = feet).

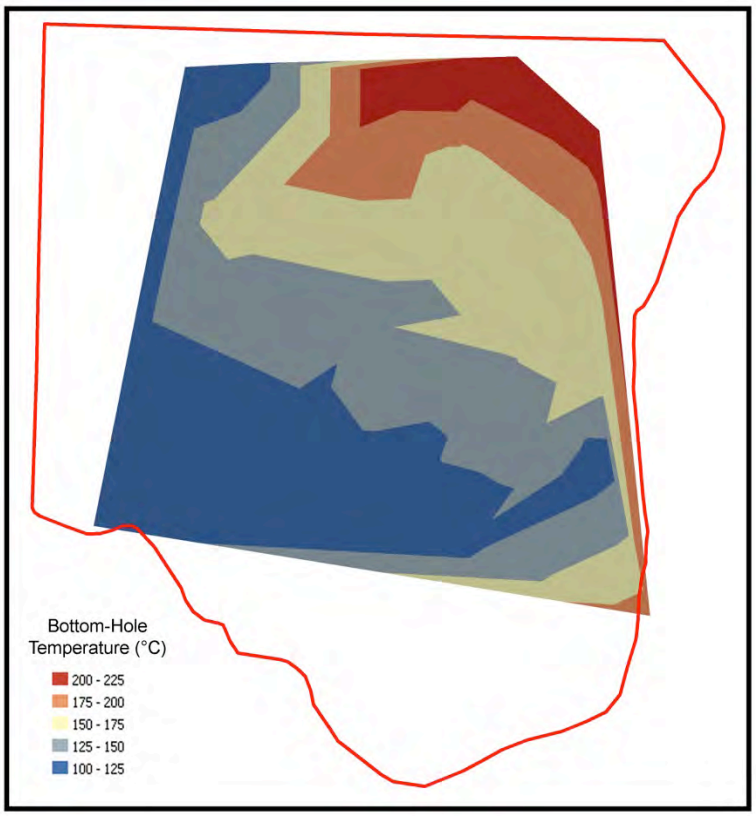

Figure 5.26. A map of the bottom-hole temperatures within the Entrada Sandstone.

CO_2 storage Capacity:

The parameters used to calculate the CO_2 storage capacity for the Entrada Sandstone are located in Table 5.4. The basin area was determined from the overburden map (Fig. 5.27). The 3,000 ft contour is the minimum depth for injection of CO_2. Due to the fact the Entrada sandstones have been drilled less extensively than the shallower horizons, the overburden map is incomplete. The extent of the Entrada sands in the San Juan Basin is probably much greater than the 16,511 km^3 calculated.

Table 5.4. Parameters used to calculate CO_2 storage efficiency for the Entrada Sandstone in San Juan Basin, New Mexico.

Area (km^3)	Thickness (ft)	Porosity % (min, avg, max)	Salinity (TDS)	Permeability (mD)	Temperature (°C)	Geothermal Gradient
16,511	See Figure 5.22	7.4, 9.6, 22.5	35000	0.09	See Figure 5.26	47°C/km

Figure 5.27. A map of the overburden (ft) over the Entrada Sandstone.

The thickness of the Entrada sands varies uniformly across the basin (Fig. 5.22), and the data from the Entrada isopachous map was used to determine the thickness. Porosity varies greatly throughout the section from almost zero to close to 25%, so the capacity estimates can also vary greatly from the minimum to maximum value.

The porosity and permeability data comes from fewer than 10 values from core reports within the basin. The temperature data is from well header information as well as geothermal and heatflow surveys.

Table 5.5 is the CO_2 storage capacity based on the data within Table 5.4.

Table 5.5. CO_2 Storage Capacity (metric tonnes) *for the Entrada Sandstone in San Juan Basin, New Mexico for three different storage efficiency factors.*

Storage Efficiency Factor in %		
0.51%	2%	5.4%
300,019,280 tonnes	1,176,546,181 tonnes	3,176,674,688 tonnes

Summary and Recommendations:

Based on the CO_2 storage capacity values, the Entrada Sandstone doesn't appear to have great potential. The storage capacity calculation is in part dependent on the area of the unit, and it is derived from the overburden map. For the Entrada Sandstone, the limited well coverage impacts this value since the true boundaries of the 3,000 ft contour could not be determined. With additional drilling, the area will increase causing the storage capacity to increase. This will make the Entrada and the overlying Todilto Limestone a much more attractive reservoir and seal.

5.4.3d Hermosa Group

Geologic Characterization:

The Hermosa Group (Pinkerton Trail, Paradox, Honaker Trail and Rico Formations) is conformable with the underlying Pennsylvanian Molas and overlying Permian Cutler Formations. The Hermosa Group was deposited on a broad shelf that was part of Paradox geosyncline and has thickness of over two thousand feet (Figs. 5.28 to 5.29).

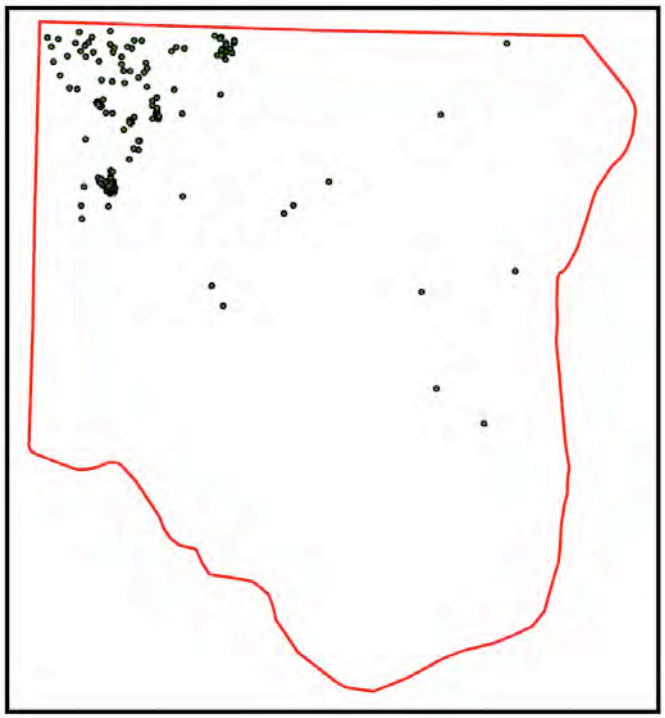

Figure 5.28. A well density map for the Hermosa Group. Most drilling has been in the northwestern corner of the state (and the basin). There are a few scattered wells elsewhere in the basin, but additional wells need to be drilled to develop future plays.

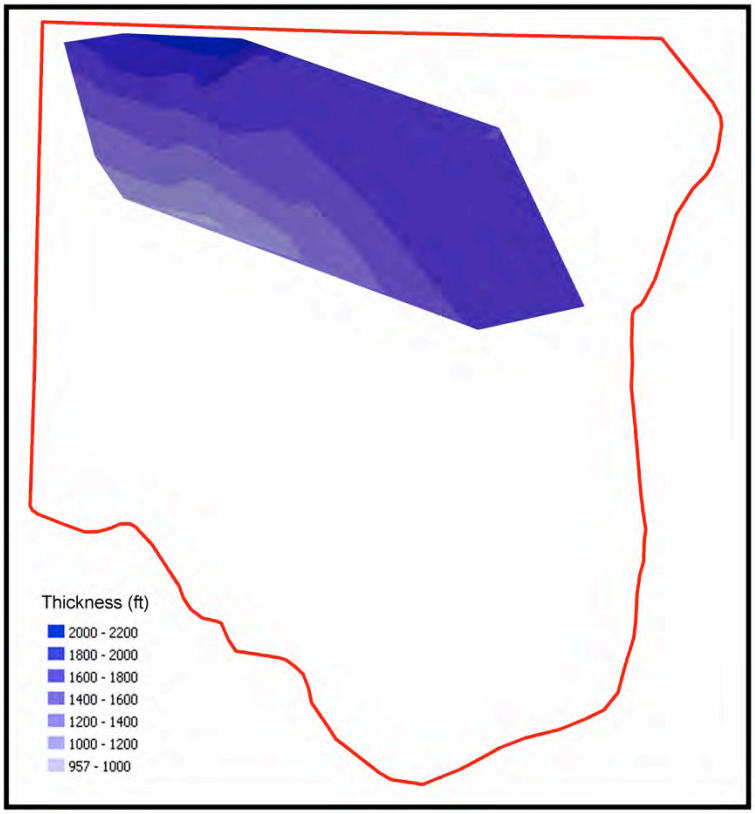

Figure 5.29. An isopachous map of the Hermosa Group. It is much more extensive in the basin, but there are too few wells to isopachous the rest of the San Juan Basin.

The Pinkerton Trail Formation is up to 200 feet thick and consists of marine, fossiliferous limestones and shales that formed during a marine transgressive event over the non-marine Molas Formation. The Paradox Formation contains algal bioherms surrounded by conglomeritic and cherty limestones, sandstones and siltstones and can reach a thickness of over 1,500 ft in the San Juan Basin (Wengard, 1959). The Honaker Trail Formation is also a marine carbonate unite with cherty, fossiliferous limestones and dolomites, sandstones, siltstones and shales. It can reach up to 1,000 feet in thickness. The Rico Formation varies from fully marine carbonates at its basin to non-marine red beds at the top. This unit represents a regressive sequence and grades into the overlying Permian Cutler Formation.

Most of the Pennsylvanian oil production is from the northwestern part of the basin from the Paradox Formation. These Paradox reservoirs are stratigraphic traps formed by phylloid algae bioherms located on paleo-structural highs. Net pay in these biohermal units can be up to 120 feet thick, 15% porosity and greater than 100 mD (McLemore et al., 1986a).

A few wells have been drilled in other parts of the basin and they show the Hermosa Group occurs throughout the San Juan Basin and that the thickness increases eastward (Fig. 5.29). The Laramide orogeny may have dissected the platform (Engler et al., 2001), but it certainly resulted in the downwarping of the present-day San Juan Basin (Fig. 5.30). The Hermosa Group sediments are now almost 5,000 feet below sea level.

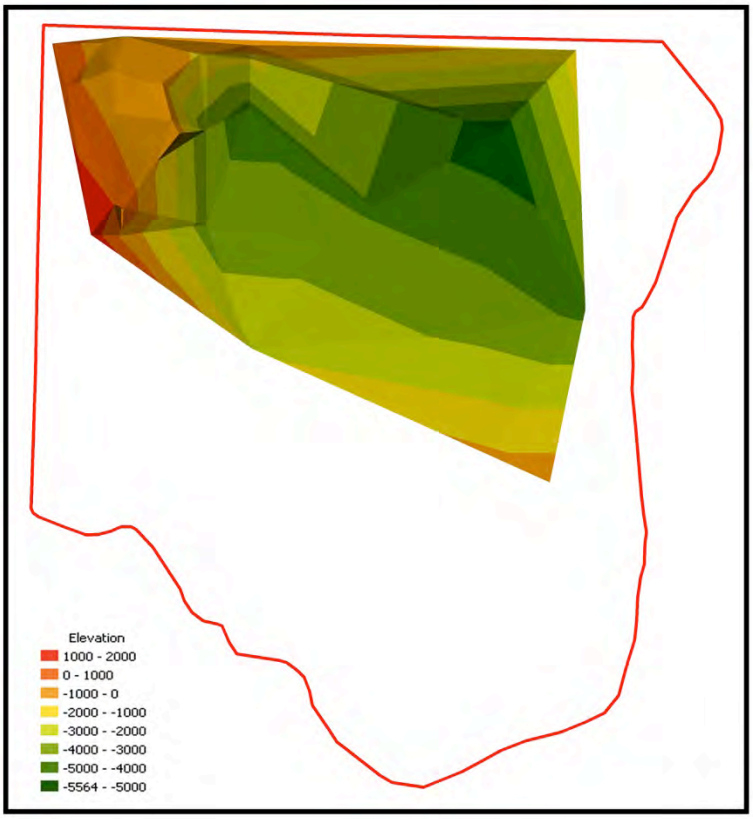

Figure 5.30. A structural map on the top of the Pennsylvanian Hermosa Group (elevation = ft).

The database produced for this project contains measured porosity and permeability from 40 plugs. The average porosity for Pennsylvanian cores is 5.1%, and the highest porosity measured is 21.4%. The average permeability is 42.6 mD, and the highest measured permeability was 1000 mD. There is little temperature data available for Pennsylvanian sediments (Fig. 5.31), but based on the underlying temperatures in the Leadville Limestone, most of the potential production in the rest of the basin is probably gas. The depth of the wells will make them expensive to drill, so any future plays will have to wait until the market drives exploration.

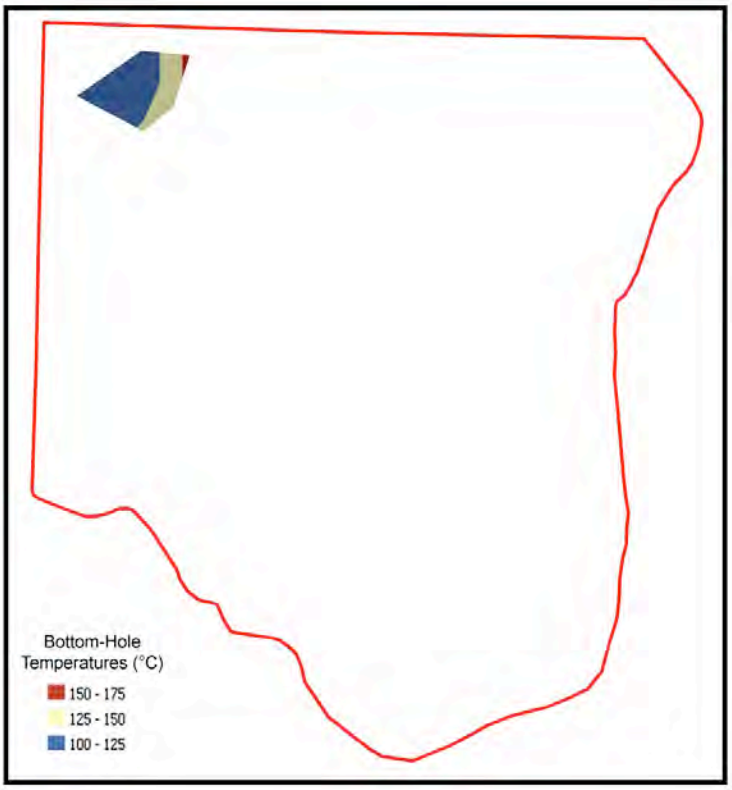

Figure 5.31. The very limited bottom-hole temperature data available for the Hermosa Group in the San Juan Basin.

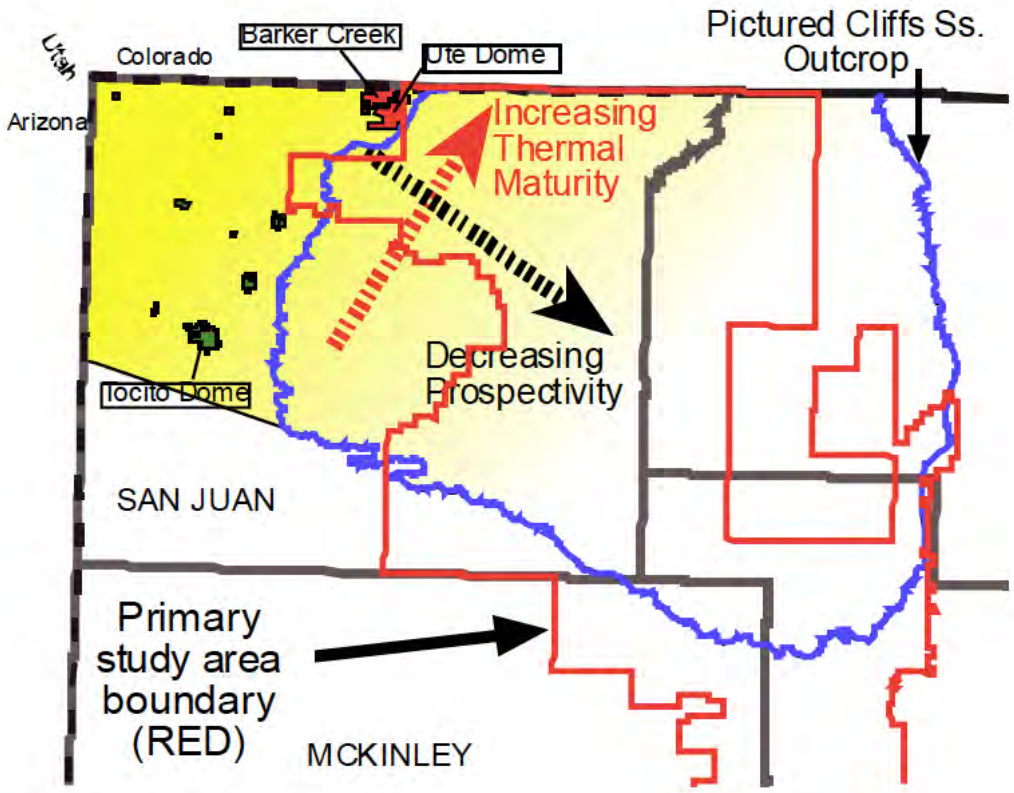

Figure 5.32. Possible future plays in the Hermosa Group. The diagram also shows where there was previous production; all the Pennsylvanian fields are now shut in (from Engler et al., 2001).

CO_2 storage Capacity:

The parameters used to calculate the CO_2 storage capacity for the Hermosa Group are located in Table 5.6. The basin area was determined from the overburden map (Fig. 5.33) by using the 3,000 ft contour as the minimum depth for injection of CO_2. The area is a minimum value since there are not enough wells to define the extent of the Hermosa sediments.

Table 5.6. Parameters used to calculate CO_2 storage efficiency for the Hermosa Group in San Juan Basin, New Mexico.

Area (km^3)	Thickness (ft)	Porosity % (min, avg, max)	Salinity (TDS)	Permeability (mD)	Temperature (°C)	Geothermal Gradient
9,444	See Figure 5. 29	3.0, 9.9, 14.2	85000	0.2	See Figure 5.31	47°C/km

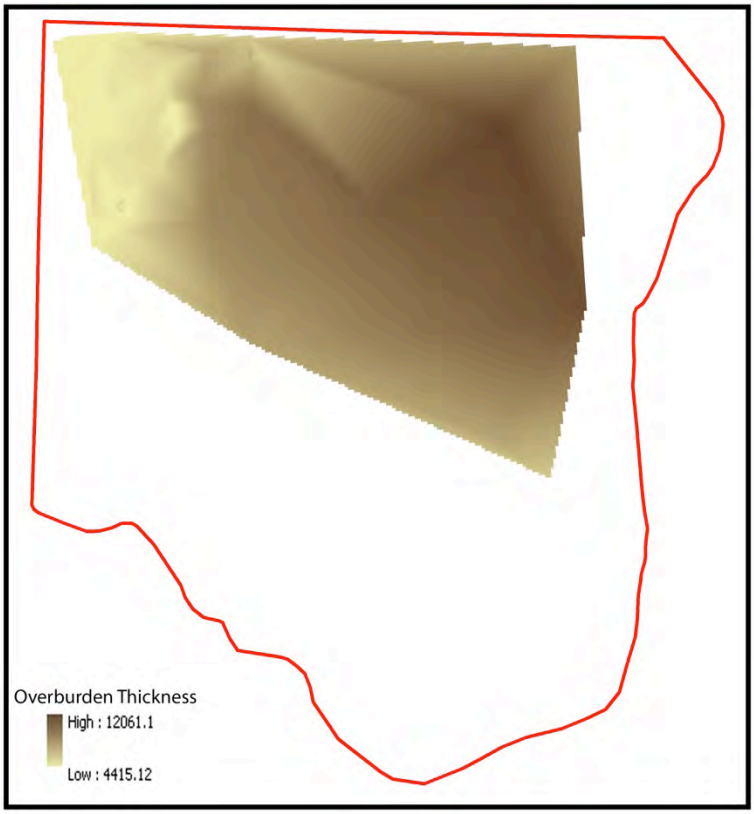

Figure 5.33. A map of overburden on the Hermosa Group.

The thickness varies uniformly across the basin, and the data from the Hermosa Group isopachous map was used to determine the thickness. Porosity varies greatly throughout the section from almost zero to close to 25%, so the capacity estimates can also vary greatly from the minimum to maximum value.

The porosity and permeability data comes from less than 10 values from core reports within the basin. Since most of the Hermosa Group wells were drilled more than 50 years ago, there are only a few bottom-hole temperatures available

Table 5.7 is the CO_2 storage capacity based on the data within Table 5.6.

Table 5.7. CO_2 Storage Capacity (metric tonnes) *for the Hermosa Group in San Juan Basin, New Mexico for three different storage efficiency factors.*

Storage Efficiency Factor in Percent		
0.51%	2%	5.4%
1,672,530,703 tonnes	6,558,943,933 tonnes	17,709,148,619 tonnes

Summary and Recommendations:

Based on the CO_2 storage capacity values, the Hermosa Group has the best potential for carbon storage. Like the Entrada Sandstone, the lack of well control in areas of the basin means that the aerial extent is underestimated. The storage capacity value can only increase making the Hermosa Group a very attractive CO_2 reservoir.

5.4.3e Leadville Limestone

Geologic Characterization:

Most of the wells that have been drilled into the Leadville Limestone are in the northwestern part of the state and the San Juan Basin (Fig. 5.34). In this area, the Leadville Limestone is relatively shallow (Fig. 5.35). Both oil and gas production within these Mississippian carbonates in the San Juan Basin occurred from a few fields (Table 5.1), but they have all been shut-in for the last 20 to 30 years. They were structural plays located on anticlines (Fassett, 1983). The reservoirs were porous limestones and dolomites, fossiliferous and oolitic limestones and solution-collapse breccias. Mississippian exploration has been limited over the years due to the expense of drilling into these deep strata.

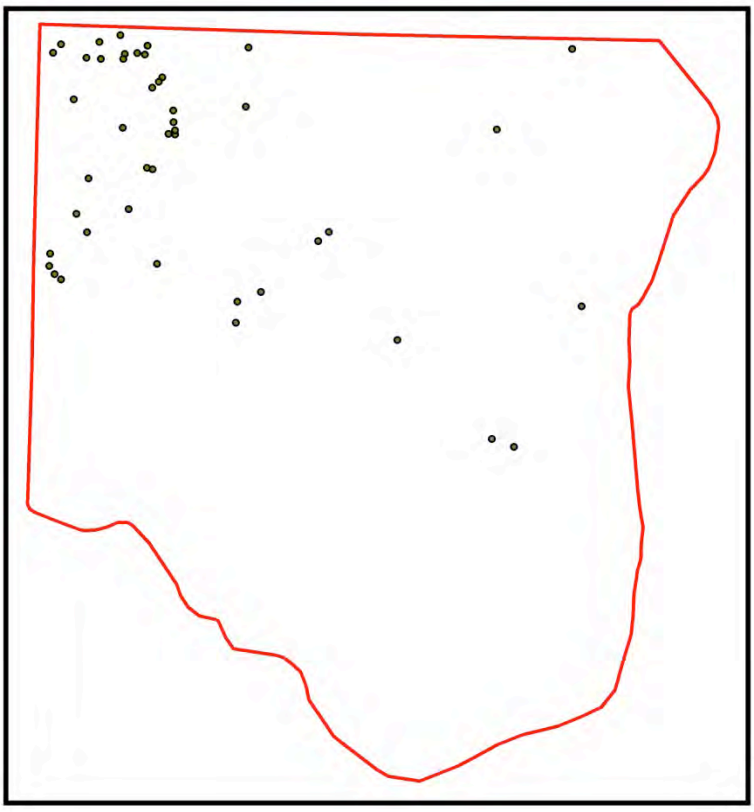

Figure 5.34. A well density map showing the scarcity of wells.

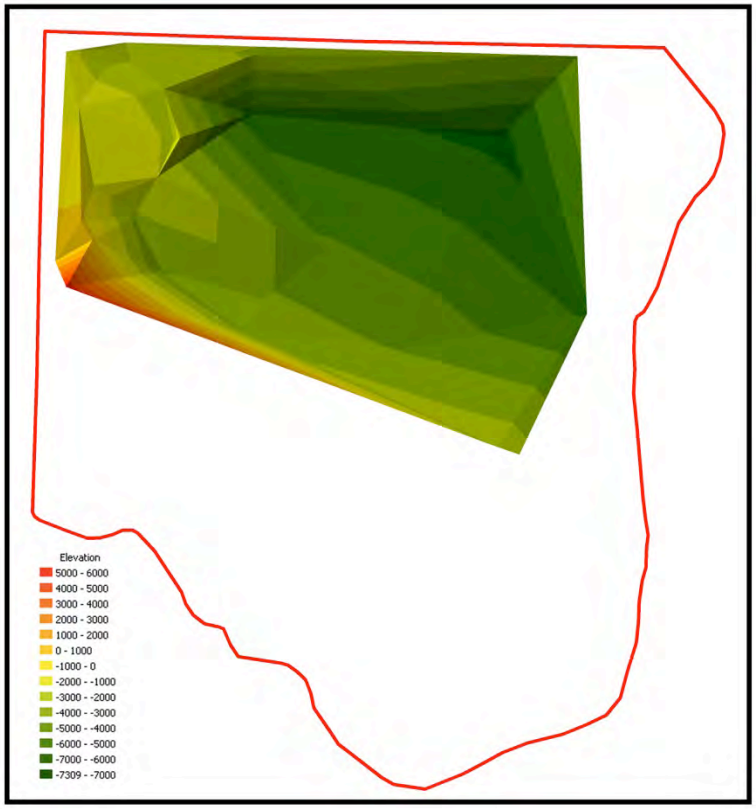

Figure 5.35. A structural map on top of the Leadville Limestone/ Arroyo Peñasco Group (elevation = ft).

The Mississippian Leadville Limestone unconformably overlies the Devonian Ouray Formation and ranges in thickness from 0 to over 300 feet thick in the San Juan Basin (Figs. 5.36 to 5.37). In the southern areas of the San Juan Basin, the Leadville is equivalent to the Arroyo Peñasco Group. In places, the Leadville Limestone/Arroyo Peñasco Group lies directly on the weathered Precambrian surface due to erosion of the underlying Cambrian and Devonian units (McLemore et al., 1986a). The Leadville Limestone consists of shallow marine, crinoid-rich limestones and dolomites (Fig. 5.38). Further to the south and east, the Arroyo Peñasco Group grades from shallow marine to supratidal carbonate and evaporite deposits. After Mississippian deposition, a major regression event resulted in an exposure that produced dissolution and brecciation within the Leadville Limestone resulting in a karst topography. Within the karstified sediments, there are porous breccia horizons that have potential as reservoirs (Armstrong and Mamet, 1977; Ulmer and Laury, 1984). The Leadville Limestone is unconformably overlain by nonmarine sediments of the Pennsylvanian Molas Formation.

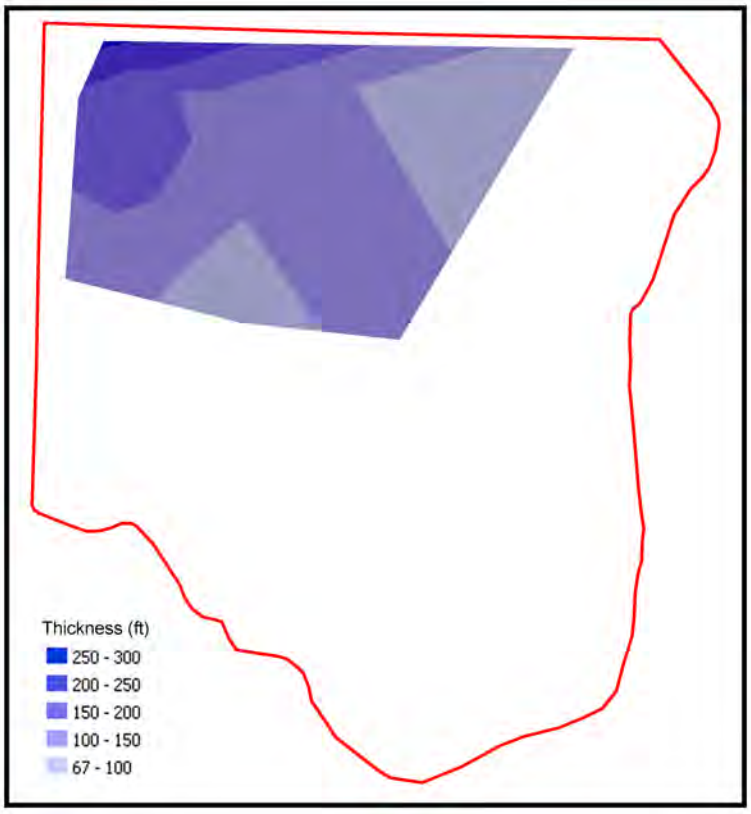

Figure 5.36. An isopachous map based on the wells within the database. The two arrows point to thin areas that are adjacent to the Peñasco Uplift and the Chaco Slope.

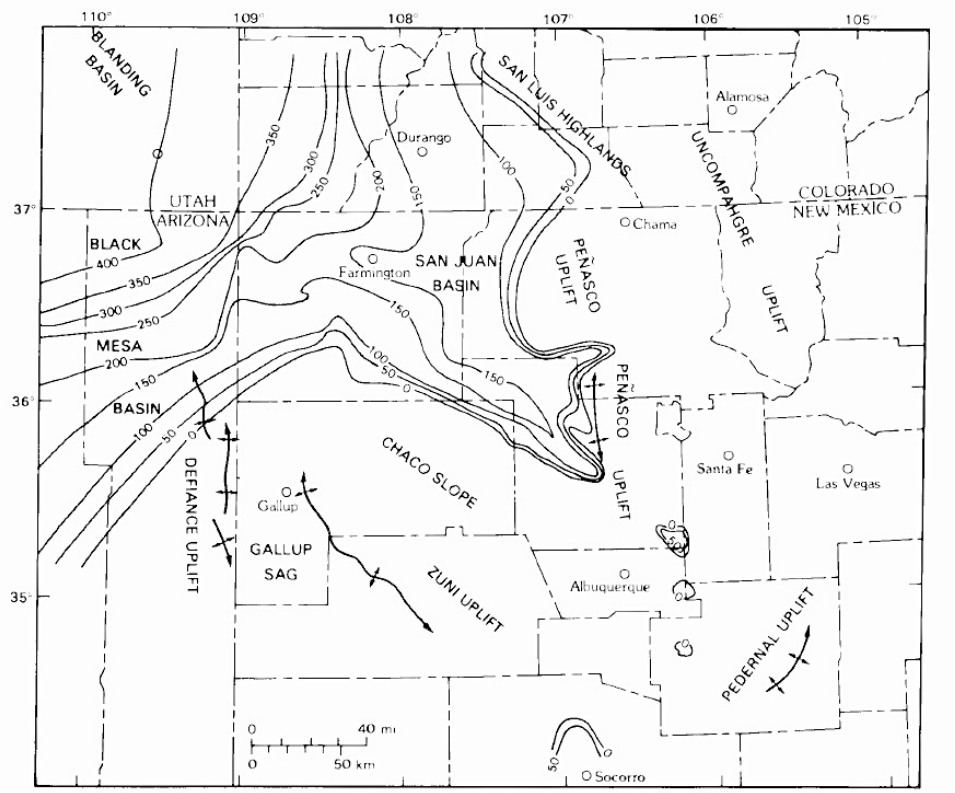

Figure 5.37. An isopachous map from Armstrong and Holcomb (1989) showing their interpretation of the distribution of Mississippian sediments in the San Juan Basin and adjacent areas based on well and outcrop data.

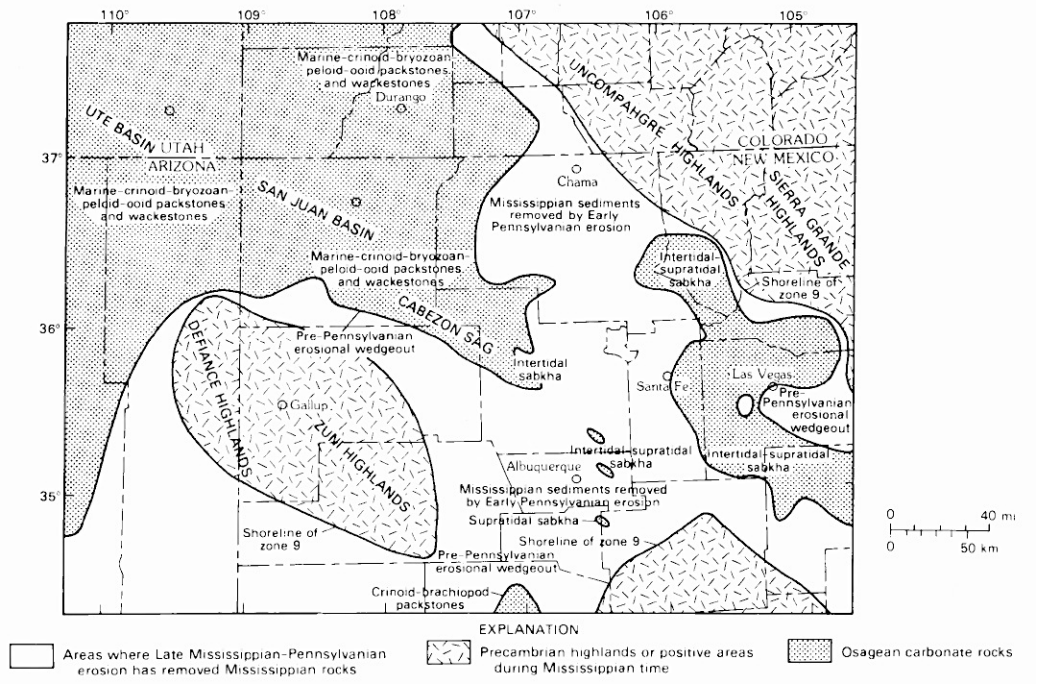

Figure 5.38. Deposition environments of the Leadville Limestone (from Armstrong and Holcomb, 1989).

CO_2 storage Capacity:

The parameters used to calculate the CO_2 storage capacity for the Leadville Limestone are located in Table 5.8. The basin area was determined from the overburden map (Fig. 5.39) by using the 3,000 ft contour as the minimum depth for injection of CO_2. The area is a minimum value since there are not enough wells to define the extent of the Leadville Limestone. On Figure 5.39, all the well data is from deeper than 3,600 feet. The actual area on the map is a small part of a possible Mississippian CO_2 reservoir.

Table 5.8. Parameters used to calculate CO_2 storage efficiency for the Leadville Limestone in San Juan Basin, New Mexico.

Area (km^3)	Thickness (ft)	Porosity % (min, avg, max)	Salinity (TDS)	Permeability (mD)	Temperature (°C)	Geothermal Gradient
12,247	See Figure 5.36	1.0, 4.0, 7.0	35000	_	See Figure 5.40	47°C/km

Figure 5.39. A map of the overburden on top of the Leadville Limestone.

The thickness varies across the basin, and it is dependent on the location of positive features on top of the Precambrian surface (Fig. 5.36). This data was used to determine the thickness used for the capacity equations. Porosity varies greatly throughout the section from 1% to close to 7%, so the capacity estimates can also vary from the minimum to maximum value.

The porosity and permeability data comes from less than 10 values from core reports within the basin. Since most of the Leadville wells were drilled more than 50 years ago, not much porosity or permeability data are available. Unlike the Hermosa Group wells, there was enough temperature data to construct a map (Fig. 5.40).

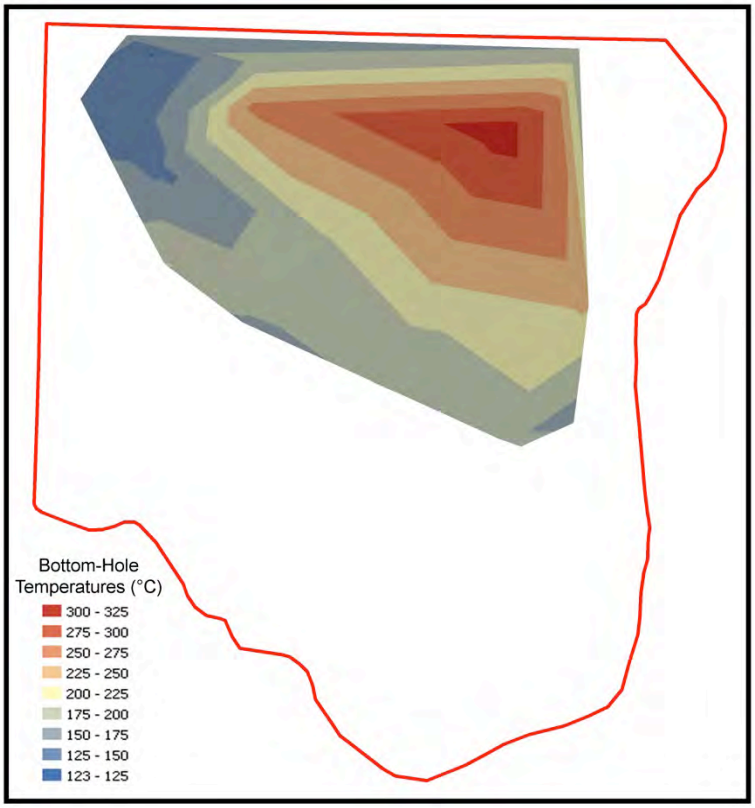

Figure 5.40. A map of the bottom-hole temperatures within the Leadville Limestone.

Table 5.9 is the CO_2 storage capacity based on the data within Table 5.8.

Table 5.9. CO_2 Storage Capacity (metric tonnes) *for the Leadville Limestone in San Juan Basin, New Mexico for three different storage efficiency factors.*

Storage Efficiency Factor in Percent		
0.51%	2%	5.4%
42,728,636 tonnes	167,563,275 tonnes	452,420,844 tonnes

Summary and Recommendations:

Based on the CO_2 storage capacity values, the Leadville Limestone, like the Entrada Sandstone, doesn't appear to have great potential for CO_2 storage. The overburden map underestimates the aerial extent of the unit because of the lack well coverage; therefore, the storage capacity calculation will increase. With additional drilling, the area will cause the storage capacity to increase as the area and thickness of the unit is better delineated. This will make the Leadville and Arroyo Peñasco Group a much more attractive reservoir.

5.5 References

Akers, J.P., M.E. Cooley, and C.A. Repenning, 1958, Moenkopi and Chinle Formations of Black Mesa basin and adjacent areas, *in* Black Mesa Basin, Northeastern Arizona: New Mexico Geological Society Guidebook 9th Field Conference, p. 88-94.

Anderson, O.J., and S.G. Lucas, 1996, Stratigraphy and depositional environments of Middle and Upper Jurassic rocks, southeastern San Juan Basin, New Mexico, *in* Jemez Mountain Region: New Mexico Geological Society Guidebook 47th Field Conference, p. 205-210.

Armstrong, A.K., and E.D. Holcomb, 1989, Stratigraphy, facies and paleotectonic history of Mississippian rocks in the San Juan Basin of northwestern New Mexico and adjacent areas, *in* Southeastern Colorado Plateau: New Mexico Geological Society Guidebook, 40th Field Conference, p. 159-166.

Armstrong, A.K., and B.L. Mamet, 1977, Biostratigraphy and paleogeography of the Mississippian system in northern New Mexico and adjacent San Juan mountains of southwestern Colorado, *in* San Juan Basin III: New Mexico Geological Society Guidebook, 28th Field Conference, p. 111-127.

Brister, B.S., and G.K. Hoffman, 2002, *in* Brister, B.S., and L.G. Price, eds., New Mexico's Energy, Present and Future: Policy, Production, Economics, and the Environment: New Mexico Bureau of Geology and Mineral Resources, Decision-Maker Field Conference 2002, p. 21-25.

Brister, B.S., and L.G. Price, eds., 2002, New Mexico's Energy, Present and Future: Policy, Production, Economics, and the Environment: New Mexico Bureau of Geology and Mineral Resources, Decision-Maker Field Conference 2002, 153 p.

Burton, G.C., Jr., 1955, Sedimentation and stratigraphy of the Dakota Group in the San Juan Basin, *in* Geology of Parts of the Paradox, Black Mesa and San Juan Basins: Four Corners Field Conference, p. 78-88.

Clarkson, G. and M. Reiter, 1988, An overview of geothermal studies in the San Juan Basin, New Mexico and Colorado, *in* Geology and Coal-Bed Methane Resources of the Northern San Juan Basin, Colorado and New Mexico: Rocky Mountain Association of Geologists, p. 285-291.

Craigg, S.D., 2001, Geologic framework of the San Juan structural basin of New Mexico, Colorado, Arizona, and Utah, with emphasis on Triassic Through Tertiary Rocks: United States Geological Survey, Professional Paper 1420, 70 p.

Deischl, D.G., 1973, The characteristics, history and development of the Basin Dakota Gas Field, San Juan Basin, New Mexico, *in* Cretaceous and Tertiary Rocks of the southern Colorado Plateau, Four Corners Geological Society Memoir, p. 168-173.

Engler, T.W., B.S. Brister, H.-Y. Chen and L.W. Teufel, 2001, A 20-year, Reasonable Foreseeable Development (RFD) Scenario Supporting the Resource Management Plan for the Farmington Field Office, Bureau of Land Management: New Mexico Bureau of Geology and Mineral Resources Open-File Report 463, 125 p.

Fassett, J.E., 1983, Stratigraphy and Oil and Gas Production of Northwest New Mexico Updated Through 1983, *in* Fassett, J. E., ed., Oil and Gas Fields of the Four Corners Area, v. III: Four Corners Geological Society, p. 849-863.

Fassett, J.E., 2006, The San Juan Basin: A complex giant gas field, New Mexico and Colorado: The Mountain Geologist, Vol. 43, No. 3, p. 225-230.

Fassett, J.E., 2010, Oil and gas resources of the San Juan Basin, New Mexico and Colorado *in* Four Corners Country: New Mexico Geological Society 61st Field Conference Guidebook, p. 181-196.

Fassett, J.E., and J.S. Hinds, 1971, Geology and fuel resources of the Fruitland Formation and Kirtland Shale of the San Juan Basin, New Mexico and Colorado: United States Geological Survey Professional Paper 676, 76 p.

Grant, K., and D.E. Owen, 1974, The Dakota Sandstone (Cretaceous) of the southern part of the Chama Basin, New Mexico—A preliminary report on its stratigraphy, paleontology, and sedimentology: New Mexico Geological Society 25th Field Conference Guidebook, p. 238-249.

Deischl, D.G., 1973, The characteristics, history and development of the Basin Dakota Gas Field, San Juan Basin, New Mexico, *in* Cretaceous and Tertiary Rocks of the southern Colorado Plateau, Four Corners Geological Society Memoir, p. 168-173.
Kirkland, D.W., R.E. Denison, and R. Evans, 1995, Middle Jurassic Todilto Formation of northern New Mexico and southwestern Colorado; marine or nonmarine?: New Mexico Bureau of Mines and Mineral Resources Bulletin 147, 39 p.

Lamb, G.M, 1978, The lower Mancos Shale in the northern San Juan Basin: Geological Society of America Bulletin, v. 89, p. 59-82.

Lucas, S.G., and Anderson, O.J., 1997, The Jurassic San Rafael Group, Four Corners region: New Mexico Geological Society, 48th Field Conference Guidebook, p. 115-132.

Lucas, S.G., K.K. Kietzke, and A.P. Hunt, 1985, The Jurassic System in east central New Mexico: New Mexico Geological Society, 36th Field Conference Guidebook, p. 213-242.

Lucas, S.G., S.C.H.A.B. Semken, W.R.H.G. Berglof, B.S.C.L.S. Kues, and J.C. Aubele, 2003, First-day road log, from Gallup to Gamerco, Yah-ta-hey, Window Rock, Fort Defiance, Navajo, Todilto Park, Crystal, Narbona Pass, Sheep Springs, Tohatchi and Gallup: New Mexico Geological Society, 54th Field Conference Guidebook, p. 1-6

McLemore, V.T., R.F. Broadhead, W.L. Chenoweth, K. Cook, J.M. Barker, G. Roybal, R.M. North, P. Copeland, J.S. Hingtgen, M.R. Bowie, and K.B. Brown, 1986a, A Preliminary Mineral-Resource Potential of San Juan County, Northwestern New Mexico: New Mexico Bureau of Mines and Mineral Resources Open-file Report 232, 258 p.

McLemore, V.T., R.F. Broadhead, G. Roybal, W.L. Chenoweth, J.M. Barker, P. Copeland, M.R. Bowie, K. Cook, J.S. Hingtgen, K. Kline, and K.B. Brown, 1986b, A Preliminary Mineral-Resouroe Potential of Western Rio Arriba County, Northwestern New Mexico: New Mexico Bureau of Mines and Mineral Resources Open-file Report 233, 157 p.

Molenaar, C.M., 1977, Stratigraphy and depositional history of Upper Cretaceous rocks of the San Juan Basin area, New Mexico and Colorado, with a note on economic resources: New Mexico Geological Society Guidebook 28th Field Conference, p. 159-166.

Molenaar, C. M., 1983, Principal reference section and correlation of Gallup Sandstone, northwestern New Mexico: Contributions to mid-Cretaceous paleontology and stratigraphy of New Mexico (Part 2): New Mexico Bureau of Mines and Mineral Resources Circular 185, p. 29-40.

Nummedal, D., and C.M. Molenaar, 1995, Sequence stratigraphy of ramp-setting strand plain successions: The Gallup Sandstone, New Mexico, *in* Van Wagoner, J.C., and G.T. Bertram, eds., Sequence Stratigraphy of Foreland Basin Deposits: AAPG Memoir 64, p. 277-310.

O'Sullivan, R. B., C.A. Repenning, E.C. Beaumont, and H.G. Page, 1972, Stratigraphy of the Cretaceous rocks and the Tertiary Ojo Alamo Sandstone, Navajo and Hopi Indian reservations, Arizona, New Mexico and Utah: U.S. Geological Survey Professional Paper 521-E, 65 p.

Reiter, M., and Clarkson, G., 1983, Relationships between heat flow, paleotemperatures, coalification, and petroleum maturation in the San Juan Basin, northwest New Mexico and southwest Colorado: Geothermics, v. 12, p. 323-339.

Repenning, C. A., Cooley, M. E., Akers, J. P., 1969, Stratigraphy of the Chinle and Moenkopi Formations, Navajo and Hopi Indian Reservations, Arizona, New Mexico, and Utah: United States Geological Survey Professional Paper 521-B, 34 p.

Simpson, J., 2006, Characterization of produced groundwater within the San Juan Basin: New Mexico Bureau of Mines and Mineral Resources Open-file Report 499, 23 p.

Stevenson, G. M., 1983, Paleozoic rocks of the San Juan Basin: an exploration frontier, *in* Fassett, J. E., ed., Oil and Gas Fields of the Four Corners Area, v. Ill: Four Corners Geological Society, p. 780-788.

Stevenson, G. M., and D.L. Baars, 1977, Pre-Carboniferous paleotectonics of the San Juan Basin: New Mexico Geological Society, Guidebook to the 28th Field Conference, p. 99-110.

Stone, W.J., F.P. Lyford, P.F. Frenzel, N.H. Mizell, and E. Padgett, 1983, Hydrogeology and water resources of the San Juan Basin, New Mexico: New Mexico Bureau of Mines and Mineral Resources Hydrogeologic Report 6, 70 p.

Tanner, W. F., 1974, Mesozoic lake history of northern New Mexico, *in* Ghost Ranch: New Mexico Geological Society 25th Field Conference Guidebook, p. 219-223.

Tweto, 0., 1975, Laramide (Late Cretaceous-Early Tertiary) orogeny in the southern Rocky Mountains, *in* Curtis, B.F., ed., Cenozoic history of the southern Rocky Mountains: Geological Society of America Memoir 144, p. 1-44.

Ulmer, D.S., and R.L. Laury, 1984, Diagenesis of the Mississippian Arroyo Peñasco Group, north-central New Mexico, *in* Rio Grande Rift: Northern New Mexico: New Mexico Geological Society Guidebook, 35th Field Conference, p. 91-100.

Ulmer-Scholle, D.S., 2005, Stromatolites in the Todilto Formation?, *in* Geology of the Chama Basin: New Mexico Geological Society, 56th Field Conference Guidebook, p. 380-388.

Wengerd, S.A., 1959 Pennsylvanian oil possibilities of San Juan Basin, Four Corners Region: American Association Petroleum Geologists Bulletin, v. 42, p. 2214-2227.

Wengerd, S.A., and M.L. Matheny, 1958, Pennsylvanian System of Four Corners region: American Association Petroleum Geologists Bulletin, v. 43, p. 2048-2106.